교육학박사 학위논문

Evaluation of suspended sediment sources in the Yeongsan River

영산강 부유토사의 기원지 평가

2016년 2월

서울대학교 대학원

사회교육과 지리전공

임 영 신

Evaluation of suspended sediment sources in the Yeongsan River

지도교수 김 종 욱

이 논문을 교육학박사 학위논문으로 제출함

2016년 2월

서울대학교 대학원

사회교육과 지리전공

임 영 신

임영신의 박사학위논문을 인준함

2016년 2월

위 원 장 _____ (인)

부위원장 _____ (인)

위 원 _____ (인)

위 원 _____ (인)

위 원 _____ (인)

Abstract

Large direct human impacts on the Yeongsan River resulting from the construction of two large weirs on the main stream and dredging of almost all sections of the main river have occurred since late 2009. Subsequent to these human impacts, some problems related to the sediment budget, such as channel changes, have occurred. To establish appropriate policies for control of sediment-associated problems, it is necessary to identify the physical and geochemical characteristics of the reservoir sediments in particulate form in the Yeongsan River. Furthermore, from a management perspective, determining sediment provenance is an essential prerequisite for handling excessive sediment problems in the source-transport-sink system. Hence, the objectives of this study were: i) to identify the physical and geochemical characteristics of the reservoir suspended sediments, ii) to evaluate promptly and quantitatively the relative contributions of slope-floor and channel-bank materials to reservoir sediment, using ^{137}Cs as a tracer, and iii) to apportion sediment sources of the reservoir sediment by applying composite fingerprinting procedures combined with a multivariate mixing model.

Time-integrated suspended sediment samplers were installed in July 2012 at the Seungchon weir (YS-S1), the Juksan weir (YS-S3), and a point halfway between the two weirs, located at the Yeongsanpo waterfront park (YS-S2). Reservoir sediment samples from three samplers were obtained at monthly intervals until October 2014. Strikingly high rates of reservoir sedimentation were recorded in summer, with increased precipitation and discharge. Medium to coarse silt-sized particles dominated the suspended sediment load, however, the proportion of the

coarser fraction increased at high flows. Concentrations of the major and trace elements of the collected sediments were analyzed and compared with the chemical composition of the underlying rocks. It was noticeable that easily mobilized elements, such as Ca, Mg, K, and Na, were considerably depleted in the suspended sediments relative to the bedrock of the river basin, indicating weak to moderate degrees of weathering. Trace elements including Ba, Co, Cr, Cu, La, Li, Mo, Nb, Ni, Pb, Rb, Sc, Sn, Sr, Ta, V, W, Y, Zn, and Zr were detected, with an abundance of several elements (e.g. Cu, W, Mo, Ba, Zn, Li, Cr, Rb, Ni, Co, and Pb) that are more likely to be affected by anthropogenic input.

For the second objective of this study, potential sources of the suspended sediment were sampled using a soil scraper on the forest floor and channel bank. Source fingerprinting was conducted using ^{137}Cs, which exhibits distinguishable characteristics between surface and subsurface (bank) materials. Probability distribution functions fit to the detected values of ^{137}Cs at the forest floor and channel bank were derived. The relative contributions of forest floor and bank materials to suspended sediments in the Yeongsan River were calculated using Monte Carlo simulation and a simple mixing model. The results indicated that the dominant source of suspended sediment was bank materials. Conveyance losses of delivered forest floor materials would be expected to occur due to various forms of impediment (e.g., hill-foot zones, alluvial fans, and agricultural dams) that act as barriers to sediment movement. Embankments largely prevent slope materials from flowing into the channel and consequently influence sediment connectivity. Dredging a riverbed and constructing river-crossing facilities can affect the channel in many ways; however, it remains unclear from this study as to how and to what

extent human impact has influenced channel erosion, due to the absence of pre-interference data.

To reduce the uncertainty and limitations of the ^{137}Cs methodology, a composite fingerprinting analysis, using fallout radionuclides, geochemical elemental concentrations, and the magnetic properties of each source material coupled with a multivariate mixing model, was conducted. Cropland topsoils, forest topsoils, and channel bank materials were selected as end-members. By applying the Kruskal–Wallis H-test and stepwise discriminant function analysis (DFA), final fingerprints were composed of different characteristics of the properties including $^{210}Pb_{ex}$, Zr, V, Pb, and Co. According to the mixing model result, channel bank materials were the dominant source of reservoir sediment during the entire monitoring period. In winter, there was a slight increase in the contribution from forest topsoils, which can be influenced by freeze–thaw actions. An examination as to whether or not incorporation of particle size and organic matter content correction factors into the mixing model was appropriate showed that there is no consistent significant correlation between element concentration and specific surface area (SSA) or organic matter content (LOI). Careful application of tracer-specific correction factors combined with uncertainty analysis is needed to better estimate source apportionment.

Keywords: Suspended sediment, Sediment source fingerprinting, Radio-nuclides, Mixing model, Human impacts, Yeongsan River

Student Number: 2012-30398

List of Contents

List of Figures

List of Tables

1. Introduction

1.1. Background

Running water on slopes and in streams is an important agent transporting materials from upper regions, and it also plays a role in eroding sediments on the sides of the channel and in the stream bed. Through the processes of erosion, transportation, and deposition, flowing water directly changes the topography of slopes and streams and also causes various changes to landforms by modifying the local base level, one criterion of geomorphological processes. While natural river changes occur as a result of interactions among the water, slopes, vegetation, and so forth at various temporal and spatial scales, direct and indirect human interference in rivers can accelerate the processes and trends of changes that occur under natural conditions and may shift the trend itself (Wolman, 1967; Schumm, 1969; Park, 1977; Petts, 1979, 1984; Schumm et al., 1984; Williams and Wolman, 1984; Brookes, 1988; Simon, 1989; Rhoads, 1991).

Recently, anthropogenic agents such as agricultural nutrient losses, the expansion of urbanized and industrialized areas and damming have altered sediment concentrations, deposition/erosion trends, and contaminant accumulation in fluvial systems (Owens et al., 2005b). Late in 2009, four main rivers in Korea began to experience large-scale direct human interference due to the Four Rivers Restoration Project (FRRP). Targeting the Han, Nakdong, Geum, and Yeongsan rivers, the main components of FRRP included dredging 460 million m^3 of riverbed, constructing 16 large weirs, reinforcing banks, and constructing a new dam and five flood-retention reservoirs (The Four Major Rivers Restoration Project

Headquarters, 2009). Human interference on such a large scale may give rise to diverse changes in the erosional and depositional processes of the rivers, material cycling, and landforms. Geomorphic and hydrologic responses to regulated weir systems would not be consistent over the entire course of the river (Phillips et al., 2005). When materials are removed by dredging sediments from riverbeds, direct degradation and headward erosion in the channel upslope can occur (Collins and Dunne, 1989; Rinaldi and Simon, 1998). Facilities constructed across a river can block flowing water and materials and, hence, cause deposition of transported sediments (aggradation) in the stagnant upper part of the facility, while degradation with respect to the sediment budget occurs in the lower part (Committee on Missouri River Recovery and Associated Sediment Management Issues, 2011), with the result that erosion accelerates in the downstream region (Chang, 1987). Especially, repeated erosion and deposition within the channel could pose serious problems for channel stability, water level maintenance, and effective reservoir management, as sediments flowing into the reservoir consistently block the flow of the river and reduce reservoir capacity (Owens et al., 2005a). To address the problems associated with the inflow of sediments, it is necessary to identify temporal variation in reservoir sedimentation and to obtain additional information about sediment sources and the relative importance of different source materials (Kim et al., 2013 and references therein).

Concerns over the effects of the FRRP on headward erosion and the stability of weirs on the Yeongsan River have been raised. Headward erosion is a phenomenon in which the base level changes through dredging or erosion in the main channel, resulting in progressive lowering of riverbeds and accelerated scouring of banks in the upstream direction; this can seriously damage the stability of the facilities in the

main channel or its tributaries (Holland and Pickup, 1976). Also, the reservoir traps sediments, aggravating the process of downstream degradation in a region that is already changing to a sediment-starved condition, and hence tends to transport more material. Under these circumstances, an understanding of sediment provenance and the relative contributions to the current river sediment load from potential sources is highly essential and urgently needed. Such an understanding is not only a prerequisite to comprehending the sediment budget but is also required for establishing suitable control strategies for channel stabilization and safe maintenance of the facilities.

Soil erosion and sediment mobilization have been recognized as major issues due to both on-site problems such as nutrient losses and a reduction in agricultural productivity, and off-site problems including reduction of water storage capacity from reservoir siltation or sedimentation (Walling, 2006). In particular, quantity and quality issues of fine-grained sediments transported to the river have been addressed in the past, as they are directly linked to increases in water turbidity, decreasing water quality, intake of river water, and quantity and quality of aquatic organism habitats (Sly and Hart, 1989; Hart and Sly, 1992). In addition, problems associated with the adsorption of various pollutants and nutrients to fine-grained particles can cause detrimental effects on human health and toxic damage to organisms, especially to benthos (Wildi et al., 2004; Tamtam et al., 2008; Devault et al., 2009; Sánchez-Chardi and López-Fuster, 2009). Excessive levels of these trace metal elements originate from either natural processes or human activities (Kabata-Pendias and Pendias, 2001). The chemical composition of the river sediment primarily depends on the geology of the catchment and weathering processes and is a key component of the water quality in source-transport-sink

pathways, through interactions between the water column and channel bed sediments and surrounding environmental conditions (Thornton, 1983).

1.2. Research trends

Traditional research on sediment sources has used intuitive and direct measurement techniques, i.e., the extent of exposed ground and materials in both eroded areas and their environs are assessed through field investigation and photographs (Wilson et al., 1993; Barker et al., 1997), or erosion pins are used to monitor potential source areas (Neller, 1988; Lawler and Leeks, 1992; Davis and Gregory, 1994). However, these methods have limitations deriving from the fact that erosion is equal to deposition and from the problems associated with temporally and spatially restricted sampling. Hence, since the early 1990s, studies of sediment sources that employ a fingerprinting approach have increased as an alternative way of connecting suspended sediment samples to potential source materials (e.g. Wallbrink et al., 1996; Wallbrink et al., 1998; Nagle et al., 2007; Kim et al., 2013).

The fingerprinting approach is based on two assumptions: i) particular potential sources can be differentiated clearly by their physical, geochemical, biogenic, or magnetic properties, and ii) the values of properties of suspended sediment can be compared with those of potential source materials so that fingerprints can be used to determine the relative importance of the potential sources (Collins and Walling, 2002). The properties used for fingerprinting (e.g., major elements, trace elements, rare earth elements, magnetic properties, radionuclides, and pollen) are varied, so researchers can select the proper properties depending on the characteristics of the

properties, the inherent differences in a study area, and the purpose of the study (Foster and Lees, 2000).

In the initial stages, fallout radionuclides, such as cesium-137 and beryllium-7, were used as single tracers to distinguish surface materials from subsurface materials and to determine the dominant erosion process (Walling and Quine, 1992; Wallbrink and Murray, 1993). Due to the unreliability of using a single diagnostic property to distinguish all potential sources, composite fingerprints are now commonly used as a powerful means of consistent and rigorous source discrimination (Walling and Woodward, 1995; Collins et al., 1997c; Bottrill et al., 2000). Various fingerprints (e.g. geochemical elements, magnetic properties, physical properties including particle color or sizes, and radionuclides) and combinations thereof have been investigated for accurately distinguishing source types, depending on the characteristics of the tracers, environmental features of the study area, and the purpose of the study (Foster and Lees, 2000). Meanwhile, composite fingerprint-based approaches have been inevitably accompanied by the development of more robust procedures both in statistical discrimination between source groups and in multivariate mixing models to estimate relative contributions from each source to high precision (Yu and Oldfield, 1989, 1993; Walling and Woodward, 1995; Collins et al., 1997b, 1998).

Because tracer properties differ in their environmental behavior, it is well established that composite fingerprints based on a wide range of different subsets are more likely to provide better discrimination (Walling et al., 1993; Walling and Woodward, 1995; Foster, 2000). Pulley et al. (2015) reported that the uncertainty incurred with the multivariate mixing model decreased when using a large number of fingerprinting properties and recommended the use of the maximum number of

tracers. However, there is no globally applicable suite of composite optimum fingerprints (Collins and Walling, 2002), because the tracer properties of each source material reflect site-specific features, including particular conditions of the catchment, geology, source types, and land use practices (Fox and Papanicolaou, 2008; Davis and Fox, 2009).

In addition to the variability of tracer properties in different locations, river sediment also varies with season or dominant contributor. Freeze–thaw actions, which cause soil fluffing, can increase the contribution of uncompacted surface materials to river sediments, and consequentially influence temporal variations in relative contribution (Bajracharya and Lal, 1992; Kim et al., 2013). Loosened materials having had experienced repeated freeze–thaw cycles showed higher erodibility and increased susceptibility to rain splash erosion and runoff (Edwards and Burney, 1989; Wang et al., 2009).

The catchment in the present study has a wide temperature range between summer and winter and tends to be fully exposed to the freeze–thaw process during cold periods. Therefore, it is necessary to identify seasonal changes in sedimentation rates and sediment sources that vary with specific site conditions or temporal variations in temperature, precipitation, and discharge. If a high suspended sediment load is observed during a particular period of time, identification of the predominant contributor in that period is key to targeting the source area effectively.

1.3. The objectives of this study

To establish appropriate policies to control sediment-associated problems, it is necessary to identify the physical and geochemical characteristics of the reservoir sediments in particulate form in the Yeongsan River. However, few attempts have been made to investigate variations in river fine suspended sediments at a high temporal resolution in Korea, and scant research has been conducted on the sediment sources and quantified contributions of each source material to the current load of river sediment. The results of this study are valuable for verifying and discussing downstream effects of fine sediment, including channel adjustments following two weir constructions, and can provide an opportunity for tracing sediment sources based on sediment geochemical properties. Furthermore, from a management perspective, determining sediment provenance is an essential prerequisite for handling excessive sediment problems in the source-transport-sink system (Collins et al., 1998; Walling and Collins, 2008). Hence, the objectives of this study were: i) to identify the physical and geochemical characteristics of the reservoir sediments in particulate form, ii) to evaluate promptly and quantitatively the relative contributions of slope-floor and channel-bank materials to reservoir sediment using ^{137}Cs as a tracer, and iii) to apportion sediment sources of the reservoir sediment by applying composite fingerprinting procedures combined with a multivariate mixing model.

Chapter 3 covers the following topics: monitoring sedimentation rates, constituent particle sizes, and chemical compositions of the suspended sediment. Three time-integrated suspended sediment samplers were installed on the upper

and middle Yeongsan River in July 2012. Reservoir sediment samples from three samplers were obtained at monthly intervals until October 2014. Seasonal trends of suspended sedimentation rates and grain size distributions were examined based on variations in precipitation and discharge fluctuations. Concentrations of the major elements of the collected suspended sediments were analyzed and compared to that of their parent rocks. Discussions on weir construction effects, variability, and abundances of the elements, and correlations between geochemical elements and affecting factors were conducted.

Chapter 4 deals with quantitative evaluation of the relative contributions of slope-floor and channel-bank materials to reservoir sediments, based on the radioactivity of ^{137}Cs in suspended sediment and possible source materials. A simple mixing model, combined with a Monte Carlo simulation, was used to calculate the relative contributions of forest-floor and bank materials and to address uncertainties in the source apportioning predicted by the mixing model through random sampling with numerous iterations. Based on the results, hillslope–channel connectivity, channel changes resulting from human interference, and uncertainty and limitations associated with the method are discussed.

In Chapter 5, to discriminate different types of land use and apportion sediment sources to reservoir sediments, composite fingerprinting procedures coupled with the multivariate mixing model, outlined by Collins et al. (2010a, 2010c), were applied. Cropland topsoils, forest topsoils, and channel bank materials were selected as end-members. Fallout radionuclides, geochemical elemental concentrations, and magnetic properties of each source material were used as diagnostic tracer properties. Relative contribution and contributions from each

source to the sedimentation rate were calculated using the numerical mixing model. An additional discussion on the incorporation of particle size and organic matter content correction factors into the mixing model is presented.

2. Study area and Methods

2.1. Study area

The Yeongsan River is located in southwestern Korea (126°26'12″–127°06'07″E, 34°40'16″–35°29'01″N). It arises in the Yongchubong, located in Yong-myeon, Damyang County, joins with many tributaries, e.g., Gwangjucheon, Hwangnyong River, Jiseokcheon, Gomakwoncheon, and Hampyeongcheon, and eventually flows into the Yellow Sea. It has a length of 135.36 km and a catchment area of about 3,470 km^2. Much of its basin lies below 100 m a.s.l. (about 61 % of the total area), but altitudes exceeding 400 m are distributed locally in the northern headwaters and in the eastern part of the basin.

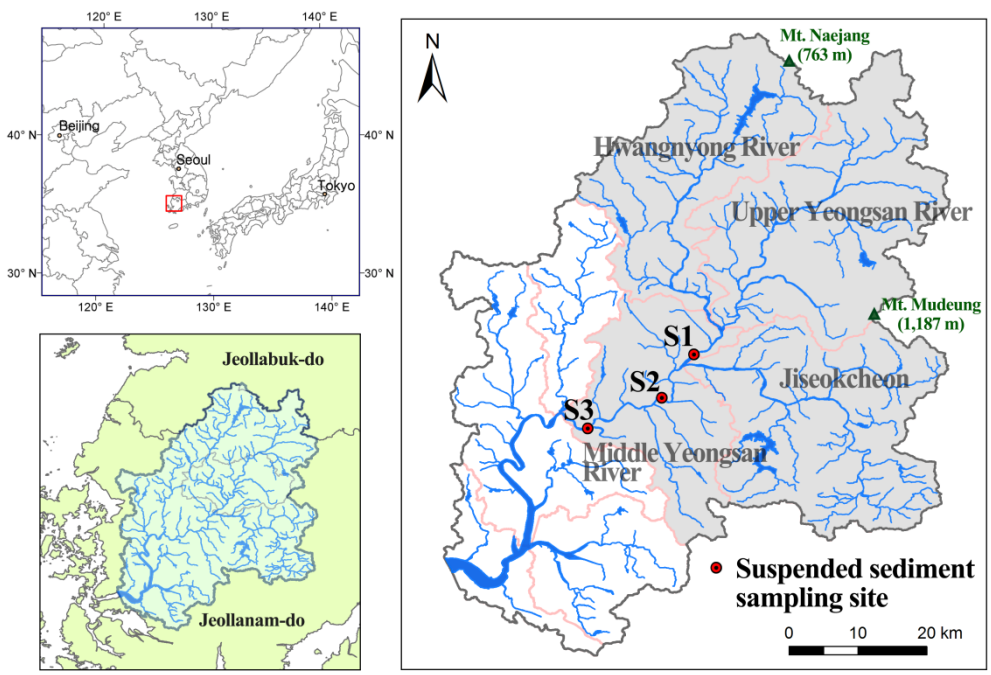

Figure 1. Location of Yeongsan River and enlarged view of sampling sites.

S1: Seungchon weir; S2: Yeongsanpo waterfront park; S3: Juksan weir.

The study area was limited to the upper catchment of the Juksan weir (S3), corresponding to the upper and middle Yeongsan River. The study catchment has an area of 2,365 km^2 and includes four subcatchments of the Hwangnyong River, Upper Yeongsan River, Jiseokcheon, and Middle Yeongsan River. Two weirs were constructed on the main stream of the Yeongsan River as part of the FRRP. The Seungchon weir (S1) is located beyond the confluence with the Hwangnyong River and before the joining with the Jiseokcheon, and the Juksan weir (S3) is located on the Middle Yeongsan River at a point before it meets the Gomakwoncheon. Time-integrated suspended sediment samplers were installed at S1, S3, and at a halfway point between the two weirs (S2), located in the Yeongsanpo waterfront park under almost stagnant conditions (Figure 1).

The mean annual temperature, measured at the Gwangju weather station (1981 to 2010; 30-year average), which is approximately in the central part of the Yeongsan River catchment (126°53'E, 35°10'N), is 13.8 °C. And the mean temperatures of the warmest and coldest months, August and January, are 26.2 °C and 0.6 °C, respectively, illustrating a wide temperature range between summer and winter. The mean annual precipitation is 1390.9 mm, and 57 % of the annual precipitation occurs during summer (June–August) (Korea Meteorological Administration, 2011). Recent records of annual precipitation for 5 years showed, in reverse order from 2012 to 2008, 1626.8, 1300.3, 1573.1, 1488.2, and 1007.2 mm, respectively, indicating that annual rates vary by about 1.6 times (Korea Meteorological Administration, 2008-2012). Annual precipitation during the monitoring period is presented in Figure 2, with a rainfall of 1626.8, 1246.4, and 1288.8 mm from 2012 to 2014. In August and September, 2012, continuous heavy

rains of more than 100 mm were recorded as a result of a series of typhoons, which was considerably above 30-year average monthly rainfall. Over the remainder, precipitation was below 30-year average, being relatively dry in September.

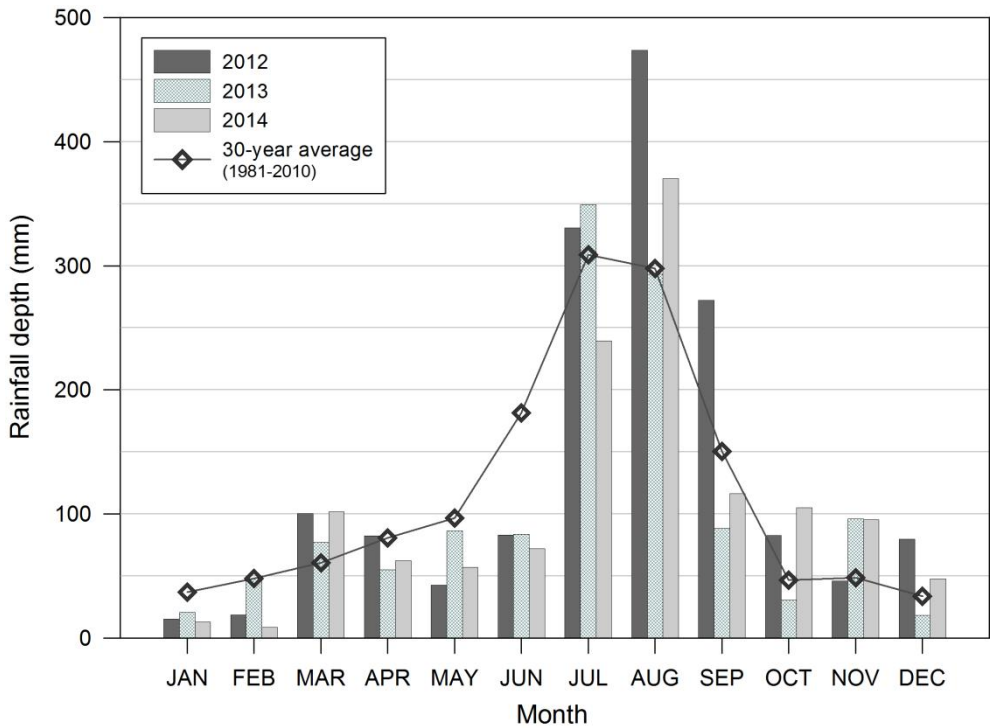

Figure 2. Monthly rainfall depth (mm) at the Gwangju weather station during the monitoring period (2012-2014), with each point of 30-year average (KMA, 1981-2010).

The underlying geology is dominated by Precambrian gneiss and includes metasedimentary rocks of the Pyongan System, gneissic granite, Silla sedimentary rocks and volcanic rocks of the Kyungsang System, Bulguksa granites, and dike rocks (Lee et al., 1997). Mesozoic Bulguksa granites are widely distributed along the main streams of the Yeongsan and Hwangnyong rivers, while high mountains, the upper part of the river, are comprised of Cretaceous volcanic rocks including rhyolite, andesite, dacite, and tuff (Figure 3).

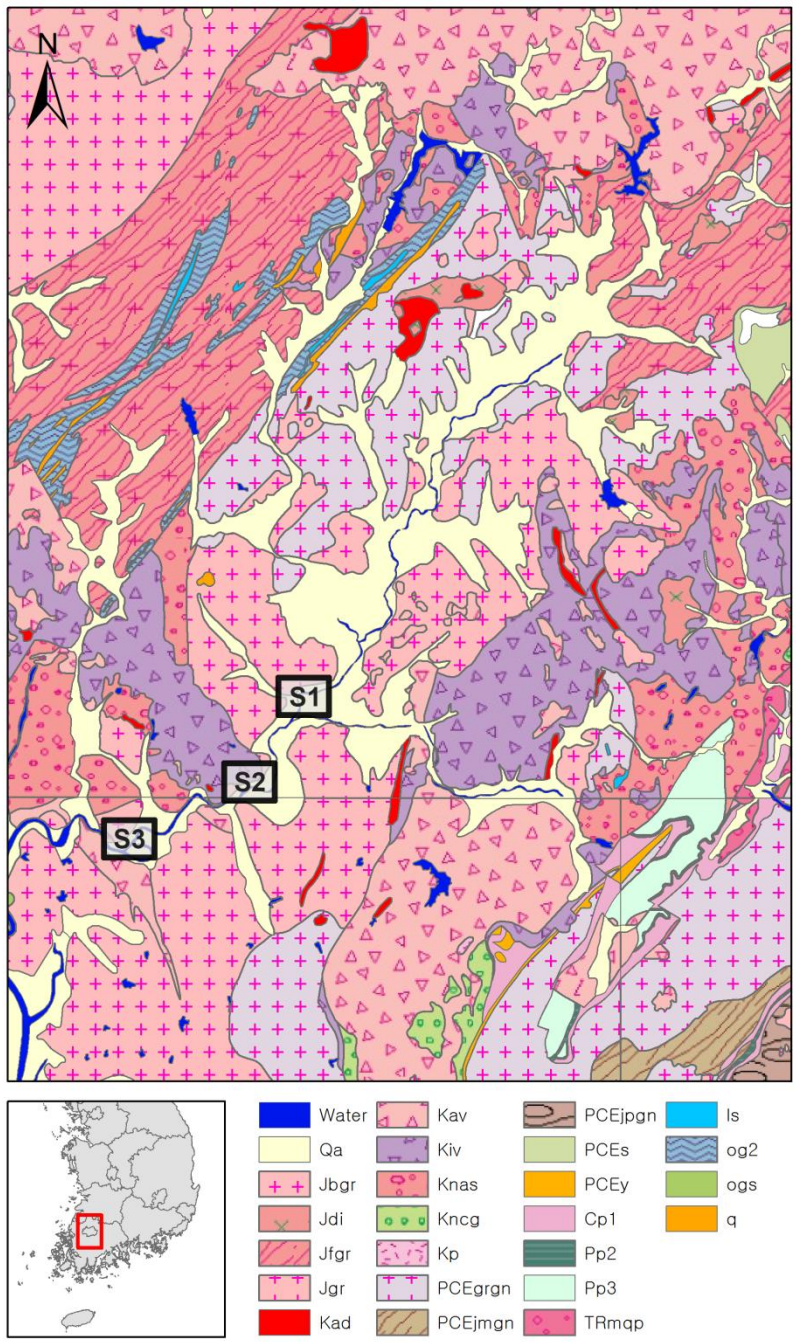

Figure 3. Geologic map (scale of 1:250,000) of the study catchment.

Abbreviations are as follows (modified from Yun et al., 2013): Qa = alluvium, Jbgr = biotite granite, Jdi = diorite, Jfgr = foliated granite, Jgr = granite, Kad = acidic dyke, Kav = acidic volcanic rocks, Kiv = neutral to alkaline volcanic rocks, Knas = sandstone and mudstone (Jinan group), Kncg = conglomerate (Jinan group), Kp = porphyry, PCEgrgn = granite gneiss, PCEjmgn = migmatitic gneiss,

PCEjpgn = porphyroblastic gneiss, PCEs = Seologri fm., PCEy = Yongamsan fm., Cp1 = lower Pyeongan group, Pp2 = middle Pyeongan group, Pp3 = upper Pyeongan group, TRmqp = meta-quartz porphyry, ls = limestone, og2 = lower phyllite zone (Ogcheon group), ogs = metapsammitic rocks, and q = quartzite.

As of 2006, the land use in the study region was dominated by forest, corresponding to 51.8 % of the total basin area, and cropland, divided into paddy and field and occupying about 33.5 % of the area (Figure 4). This basin is mostly rural, but it does include Gwangju Metropolitan City, with a population of more than 1.4 million, at the central part of the catchment. Urban areas cover 8 % of the land surface, and sparse grassland covers 2 % of the total catchment area. Wetland and bare ground are restricted to about 1 %, and areas covered by water occupy 2.5 % (WAMIS, 2013b). Rice paddy are mostly located in the floodplain which has very low slope angle, while field are located in slope-toe zones and has conventional ridge and furrow system. Generally, the ground is left bare following harvest and the arable lands are sparsely covered by crops in winter.

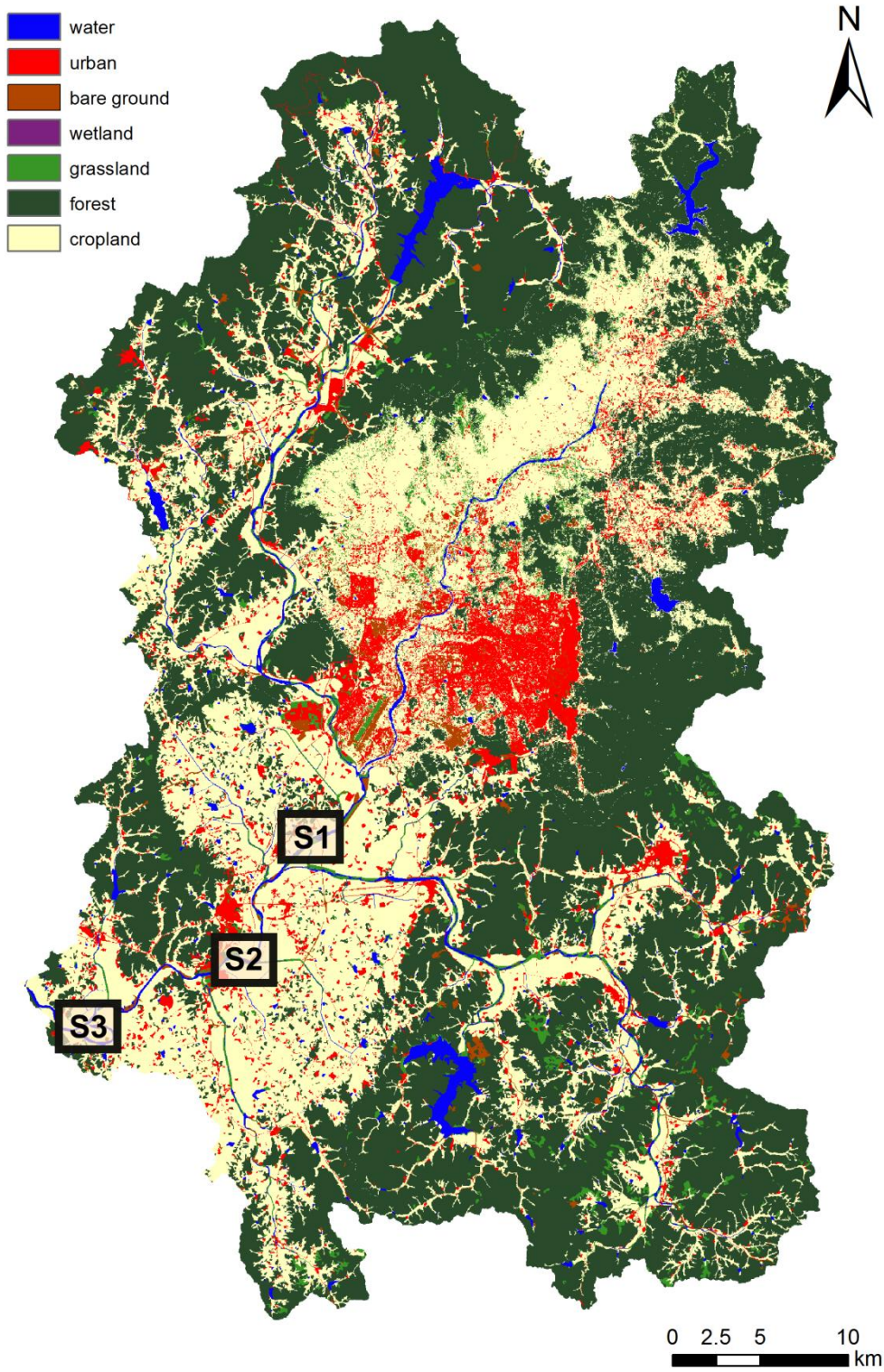

Figure 4. Land cover of the upper and middle Yeongsan River, modified from the land cover map of WAMIS for the year 2000.

2.2. Method

2.2.1. Field monitoring and suspended sediment sampling

To analyze the properties of river sediment, a sufficient amount of sample is generally required. Researchers who are interested in instantaneous river samples collect water samples during rainfall events or periods of high flow. About 100 L or more of bulk river water sample is taken using a submersible pump, and suspended sediment is extracted from each water sample by continuous-flow centrifugation (Wallbrink et al., 1998; Motha et al., 2003; Olley et al., 2012). However, a time-integrated suspended sediment sampler was designed by Phillips et al. (2000) and Russell et al. (2000) to overcome sampling difficulties and uncertainties regarding the representativeness of the overall sediment attributed to intra- and inter-event variations. The operating principles are as follows: once the cylindrical sampler is installed horizontally under a submerged condition, the inflow velocity entering a narrow inlet is reduced and this reduction of flow velocity induces sedimentation of suspended sediment particles by settling.

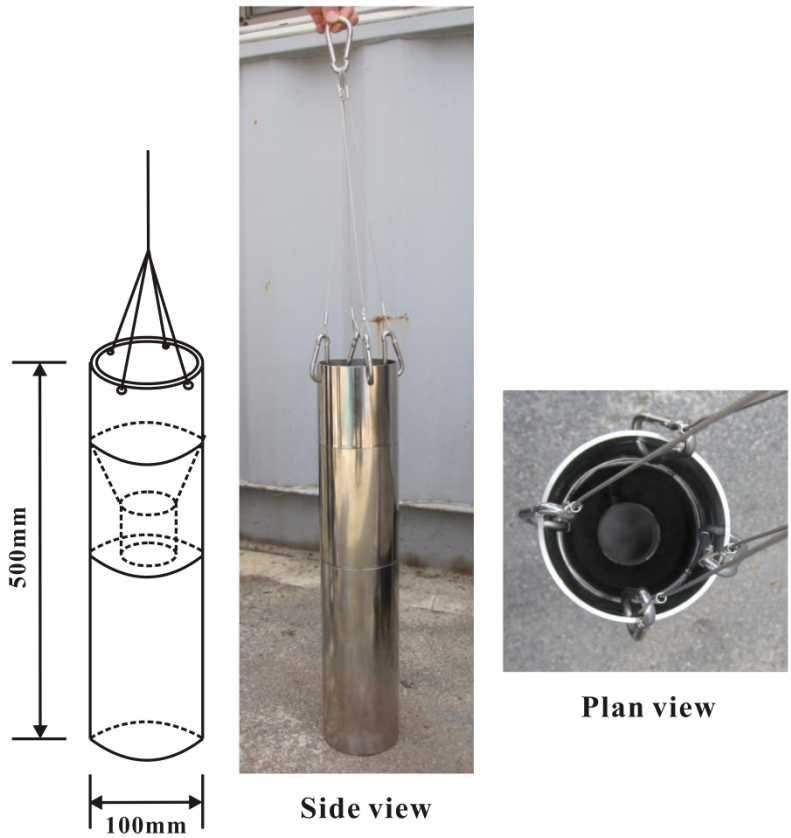

Figure 5. Time-integrated suspended sediment sampler.

However, this study site includes river flow that is almost stagnant, apparently in the same state as a typical reservoir. Considering these circumstances, a sampler was required that would be capable of collecting materials deposited vertically and that would be unaffected by a circulation current and an undercurrent occurring within the reservoir so that it would be free from loss of collected sediments. For this reason, the existing sediment trap was altered to suit this site (Lim et al., 2014); the form of this sampler is as shown in Figure 5. The time-integrated suspended sediment samplers were installed in July 2012 at the Seungchon weir (S1), the Juksan weir (S3), and a point halfway between the two weirs, located at the

Yeongsanpo waterfront park (S2) (Figure 1). Reservoir sediment samples were obtained at monthly intervals until October 2014, and 50 suspended sediment samples were collected and analyzed in this study. One sampler at the Seungchon weir (S1) was lost out on the field with the collected sediments in March 2014. All samplers took off from the sites and reinstalled in April 17 for two sites, except for the Seungchon weir (S1) in May 22. The sediments trapped in November and December were insufficient for analysis, composite samples during the two months were used to measure their geochemical, physical, and magnetic properties, and activity of radioactive isotopes.

2.2.2. Laboratory analysis

Collected suspended sediment samples and potential source materials were brought into the laboratory, and individual samples were subsequently air dried, gently disaggregated, and sieved (< 2 mm) before analysis. The screened materials were oven dried at 60 °C for 48 hours and then weighed and packed for subsequent analysis.

2.2.2.1. Geochemical analysis

The major elements (SiO_2, Al_2O_3, Fe_2O_3, CaO, MgO, K_2O, Na_2O, TiO_2, MnO, and P_2O_5) were determined by X-ray fluorescence spectrometry (XRF, MXF-2400, Shimadzu, Japan), after a fusion with lithium tetraborate ($Li_2B_4O_7$) for making glass disc. 10 oxides listed above were converted to elemental concentrations in weight percent. 29 trace elements including transition metals and several rare earth elements were measured by Inductively Coupled Plasma-Optical Emission Spectrometer (ICP-OES, Optima 5300DV, Perkin-Elmer Inc., USA) and by Atomic

Emission Spectrometer (ICP-AES, iCAP 6500 DUO, Thermo Fisher Scientific Inc., Germany). The concentration of As, Ba, Be, Bi, Cd, Co, Cr, Cu, Hf, In, La, Li, Mo, Nb, Ni, Pb, Rb, Sb, Sc, Sn, Sr, Ta, Te, Tl, V, W, Y, Zn, and Zr were determined with error less than ± 5 percent. Geochemical properties of all reservoir sediments were analyzed at the Korea Institute of Geoscience and Mineral Resources (KIGAM).

2.2.2.2. Particle size analysis

Grain size distribution of all sediments were analyzed using the laser diffraction particle size analyzer (HELOS, Sympatec GmbH, Germany) that detects particles 0.1 to 8,750 μm in diameter, at physical geography laboratory, Department of Geography Education, Seoul National University. Samples were pretreated to remove carbonates by 10 % HCl and organic materials by 35 % H_2O_2. When the reaction had completed, the samples were washed several times with distilled water. After ultrasonic dispersion procedure, grain size of the sediment samples were measured and processed by GRADISTAT program v.8 (Blott and Pye, 2001) using the method of Folk and Ward (1957). The program provides statistical analysis of particle size data, such as mean size, sorting, skewness, and kurtosis, and expressed in metric units (μm). Specific surface area ($m^2 g^{-1}$) for the individual samples was estimated from the results of grain size analysis assuming that the particles are spherical in shape.

2.2.2.3. Magnetic property and radioactivity analysis

Traditionally, mineral magnetic measurements (Oldfield et al., 1979; Caitcheon, 1993; Foster et al., 1998; Dearing, 2000) and radionuclides such as ^{137}Cs, $^{210}Pb_{ex}$, and ^{7}Be (Peart and Walling, 1986; Walling and Woodward, 1992; Wallbrink and

Murray, 1993; Wallbrink et al., 1996; Collins et al., 1998; Motha et al., 2003; Nagle et al., 2007; Blake et al., 2009; Evrard et al., 2011; Caitcheon et al., 2012; Kim et al., 2013) have been used to distinguish between surface materials and subsurface materials including gully and channel-bank deposits. Magnetic-based tracing is commonly based on the secondary magnetic enhancement, in which secondary ferrimagnetic minerals (SFMs) are developed as a result of pedogenic processes in the uppermost part of soil profiles (Dearing, 2000). However, this approach relying on the antithesis between SFM-enhanced topsoil and non-enhanced subsoil has some problems, including the fact that transformation and accumulation of SFMs are influenced by local factors and the internal response to substitution by other cations and weathering (Oldfield et al., 1979). For these reasons, quantitative assessment of sediment sources using magnetic properties as a single tracer seems impracticable.

Many studies have attempted to use radionuclide concentrations to trace sediment sources or investigate soil erosion processes. Some previous studies such as Wallbrink et al. (1996), Wallbrink et al. (1998), Nagle et al. (2007), and Kim et al. (2013) applied ^{137}Cs alone as a tracer to distinguish source types between surface and subsurface sources (bank/gully walls). The method was based on the previous finding that ^{137}Cs concentrations generally decrease to half the surface activity at a depth between 30 and 50 mm (Wallbrink and Murray, 1993). Because fallout radionuclides that arrive at the earth's surface are commonly quickly adsorbed by surficial materials and then accumulate, concentrations near the surface are relatively high in undisturbed soils. Unlike geochemical properties, radiometric properties have the virtue of conserving concentrations from the genesis of sediment through transportation to deposition in a channel or reservoir

(Motha et al., 2003), so it is possible to evaluate quantitatively the contributions of the various sediment sources.

The penetration-depth characteristics of nuclides allow us to distinguish surface from subsurface materials and thus trace sediment sources (Walling and Woodward, 1992); respectable amounts of ^{137}Cs activity were observed within 30 mm. And the naturally occurring radionuclide ^{210}Pb distributes within 50 mm, whereas the penetration profile of the cosmogenic radionuclide ^{7}Be shows a distribution at smaller penetration depths near the surface (Walling and Quine, 1992; Walling and Woodward, 1992; Wallbrink and Murray, 1993). The proper timescale of erosion events depends on the half-life and the different characteristics of the penetration depth of the radionuclide, e.g., ^{7}Be is useful for evaluating a single rainfall event occurring within a few days, whereas ^{137}Cs and ^{210}Pb are widely used to evaluate the history of erosion from several decades to 100 years. In this study, ^{137}Cs and ^{210}Pb were selected as a tracer taking account of the fallout of radionuclides and erosion processes.

For radionuclide analysis, all samples were packed and sealed in containers and left for at least three weeks, the time to achieve secular equilibrium between ^{226}Ra and its short-lived progeny, ^{222}Rn, (about five times the half-life of ^{222}Rn) prior to counting (Murray et al., 1987; Mizugaki et al., 2008). Since then, fallout and lithogenic radionuclides were measured in the reservoir sediment and possible source materials using a gamma detector (BEGe 5030-ULB, Canberra, Inc., USA) for 86,400 s at the Korea Basic Science Institute (KBSI). Radioactivity of some of the samples was measured at the Korea Institute of Geoscience and Mineral Resources (KIGAM) using REGe (Reverse-Electrode Coaxial Ge) type gamma detector (Model Number GR10026, Canberra). Energy and efficiency calibrations

for the gamma detector were carried out using a standard sample which includes ^{210}Pb (peak at 46.5 keV), ^{137}Cs (661.6 keV), ^{40}K (1460.8 keV).

^{210}Pb, a naturally occurring radioisotope of the ^{238}U decay series (half-life 22.2 years), is derived from the intermediate decay of ^{226}Ra (half-life 1622 years) to gaseous ^{222}Rn (half-life 3.8 days). Background or 'supported' ^{210}Pb contained in soils and rocks is derived via in situ decay of ^{226}Ra, and assumed to be in equilibrium with its parent isotope. Other than in situ production, additional atmospheric supply of ^{210}Pb is termed 'excess' ^{210}Pb, that washed out of gaseous ^{222}Rn by precipitation and subsequent sorption into surface material. Determination of ^{226}Ra radioactivity in samples was made indirectly by averaging gamma emissions from radon daughter lines, ^{214}Pb photopeaks at 295 keV and 352 keV and ^{214}Bi at 609 keV (Jia and Jia, 2012, and references therein). Direct measurement of ^{226}Ra activity from 186.1 keV is not very sensitive due to its low γ-ray probability and the interference of the 185.74 keV γ-rays emitted from ^{235}U (Murray et al., 1987). And excess ^{210}Pb was calculated by subtraction of ^{226}Ra radioactivity (i.e. proxy of supported ^{210}Pb activity) from total ^{210}Pb, which was measured at 46.5 keV.

Magnetic susceptibility was measured using MS2 magnetic susceptibility meter (Bartington Instruments Ltd., UK) with a resolution of 10^{-5} SI units.

2.2.3. Hydrological data acquisition

After the completion of reservoir construction, Korea Water Resources Corporation (K-water) has provided autonomous-measuring hydrologic data at the Seungchon weir and the Juksan weir from 27 August 2012. Only for a period of

time without on-site data, rainfall amount (mm) data based on the daily observation record from the Gwangju weather station was used. And the discharge (m^3/sec) was obtained from daily data at the Bondong (126°46′30″E, 35°04′08″N) which is approximately 1 km upstream from Seungchon weir (S1) and Hoejin gauge stations (126°40′25″E, 34°59′47″N), located at the halfway point between the Yeongsanpo waterfront park (S2) and the Juksan weir (S3), provided by the Water Management Information System (WAMIS). As to the Yeongsanpo waterfront park (S2), data of the closest stations, the Gwangju weather station and the Hoejin gauge station, was used for all monitoring period. But there can be differences between on-site actual values and referenced data used.

3. The physical and geochemical properties of suspended sediments in the Yeongsan River

3.1. Temporal variation in physical characteristics

Figure 6 represents the temporal variation in sedimentation rate (kg/m^2) and mean grain size (μm) at three sampling sites with the fluctuation of the daily rainfall and discharge. First of all, precipitation is concentrated in summer from June to September, and the fluctuation range of discharge was extremely big at the daily rainfall greater than 100 mm. Remarkably high rates of reservoir sedimentation were recorded in this period with increased precipitation and discharge. Temporal variations in precipitation and discharge are relatively small in other seasons (except summer), and therefore sedimentation rate during these seasons are less than 5 kg/m^2 at all sites.

The highest rates of reservoir sedimentation occurred at YS-S3 during June 26 to July 22 2013, and the next highest point was recorded at YS-S1 in first sampling period. Sedimentation rates greater than 100 kg/m^2 at all sites occurred only during second sampling period. In this period from August 21 to September 25 2012, 18 days with precipitation and continuous heavy rains of more than 100 mm were recorded as a result of a series of typhoons (15^{th} Bolaven on 28 AUG -14^{th} Tembin on 30 AUG - 16^{th} Sanba on 17 SEP).

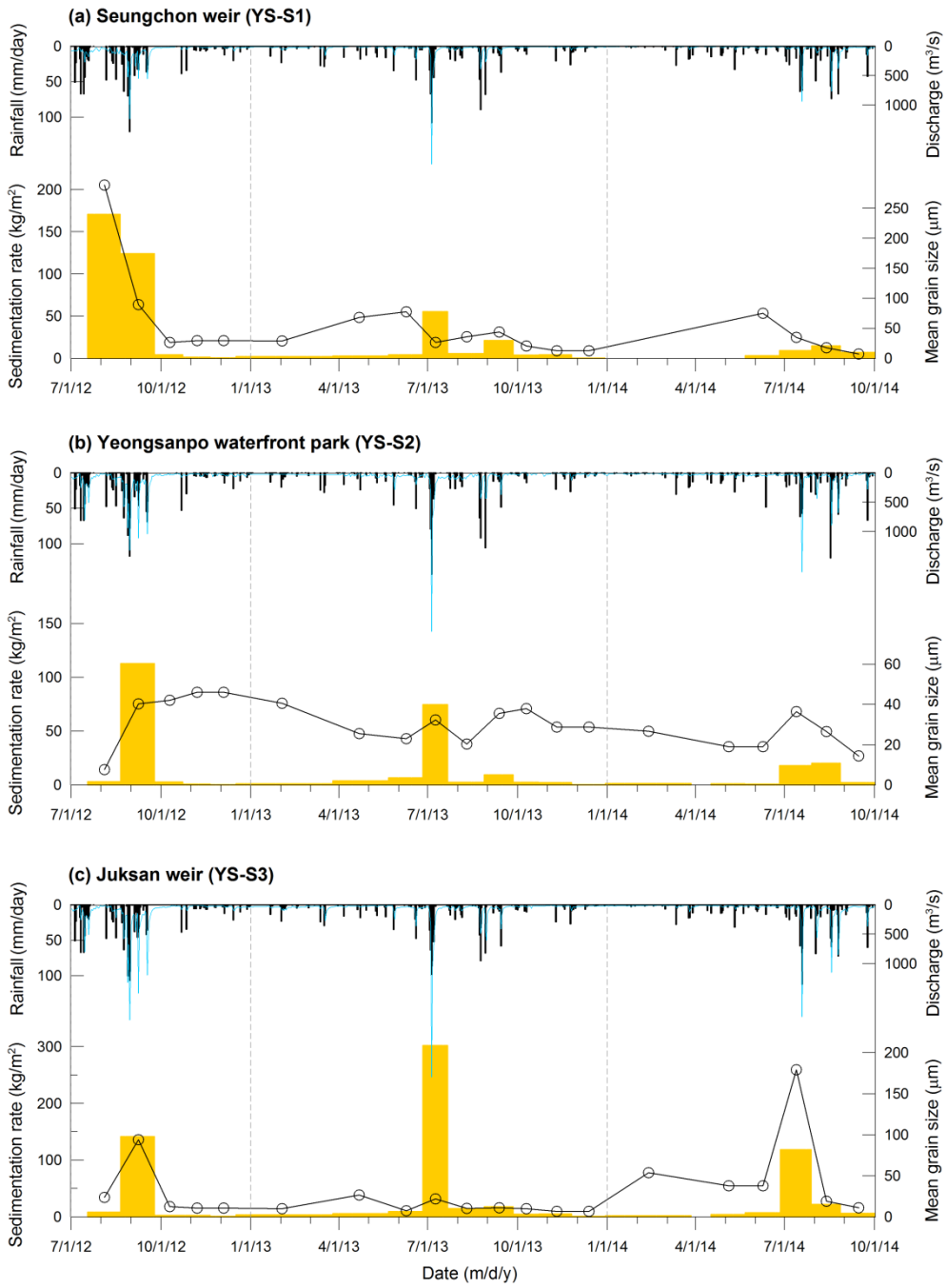

Figure 6. Variations in reservoir sedimentation rate and mean grain size of the sediment at (a) Seungchon weir, (b) Yeongsanpo waterfront park, and (c) Juksan weir. Hydrograph including daily rainfall amount (mm) and discharge (m^3/s) data is plotted upside down.

The total amount of precipitation in summer 2013 (June to September) was about 86 percent of the 30-year average value, but cumulative rainfall amount more than 250 mm was concentrated on five days from July 3rd to 7th under the influence of summer monsoon. Daily rainfall of 143 mm was recorded on July 5, and annual peak discharges also occurred on the same day (YS-S1, S2, and S3; 2004.2 m^3/s, 2693.4 m^3/s, and 2925.6 m^3/s respectively). In 2014, high rate of reservoir sedimentation at YS-S3 is noticeable during June 27 to July 29, and it can be explained by the locally concentrated rainfall almost 2 times more than other regions. On July 19 2014, daily rainfall amount of 112.3mm was recorded at the Juksan weir (YS-S3), while 57.5 mm and 62.5mm for the Seungchon weir (S1) and Gwangju weather station (applied at S2), respectively. It is expected that there were frequent erosion events as a result of cumulative antecedent rainfall from July 17 plus concentrated heavy rain around the Juksan weir, and it is reflected in high sedimentation rate and mean grain size of the reservoir sediments larger than 170 μm.

The relationship between cumulative rainfall during sampling period and peak discharge (Figure 7a) and between peak discharge and sedimentation rate (Figure 7b) showed demonstrable seasonality. Each individual data points at monthly sampling intervals were grouped into two seasons: summer (June to October) and winter (November to May). There is a positive correlation between cumulative rainfall and peak discharge for summer, though there are very slight variations in peak discharge with relatively broad range of cumulative rainfall for winter. During the winter, rainfall amounts for each rainfall event are generally small, and continuous precipitation enough to influence discharge increase occurs very seldom. Different response of discharge to similar amount of rainfall originated with spatial difference in three sampling sites. Figure 7 (b) exhibited exponential increase of

reservoir sediments with increase in discharge. It seems obvious that sedimentation rates during the winter were very low, whereas both discharge and sedimentation rate for summer are beyond compare.

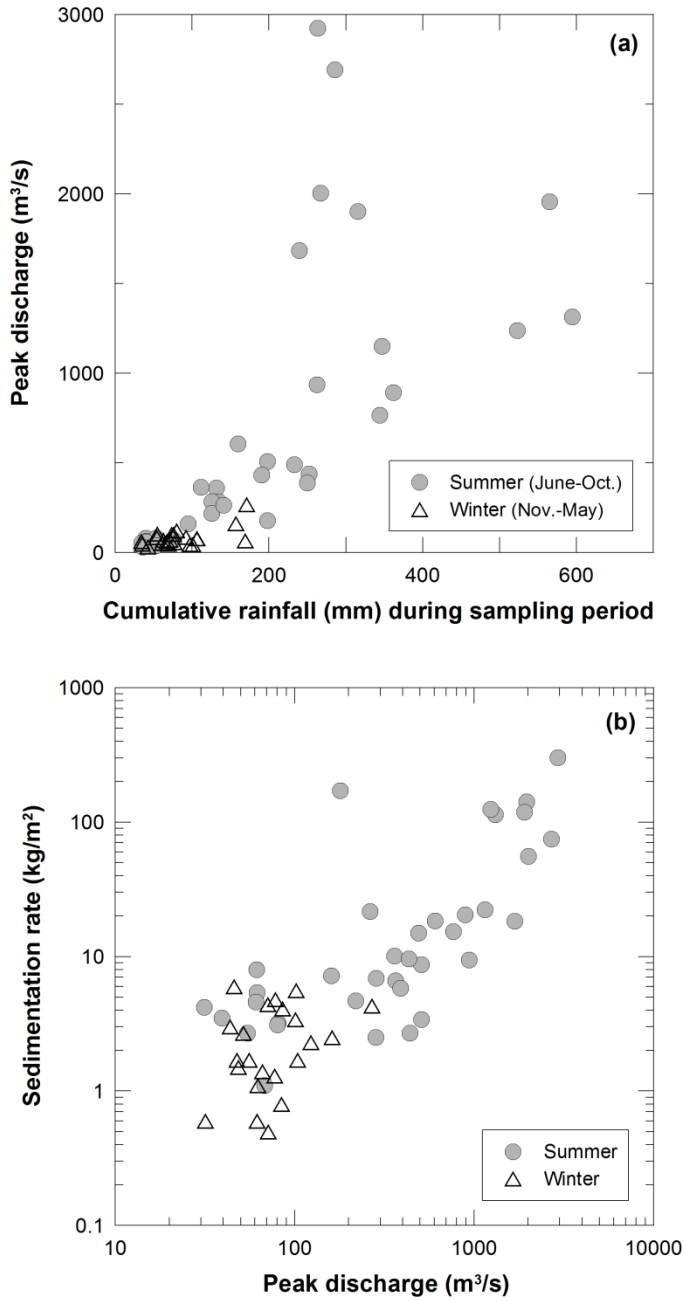

Figure 7. The relationship between (a) cumulative rainfall during sampling period and peak discharge, and (b) peak discharge and sedimentation rate.

By comparing grain size distributions at the two weirs with distance of about 20 km, there is a downstream fining trend, though fluctuated with temporal variations. Figure 8 shows the proportions of sand, silt and clay of the three sites sediments for monitoring periods. Each size fractions are as follows; sand for 2000 μm ~ 63 μm, silt for 63 μm ~ 2 μm, and clay for particles less than 2 μm. Silt and clay sizes occupied most of sediments at Juksan weir, except for some summer samples, while the relatively large proportion of sand size appeared at Seungchon weir. Because reservoir samples are time-integrated sediments, representative values such as mean grain size or sand-silt-clay percentage are insufficient to express the temporal variation reflecting multiple factors, e.g. precipitation, discharge, catchment condition and so on.

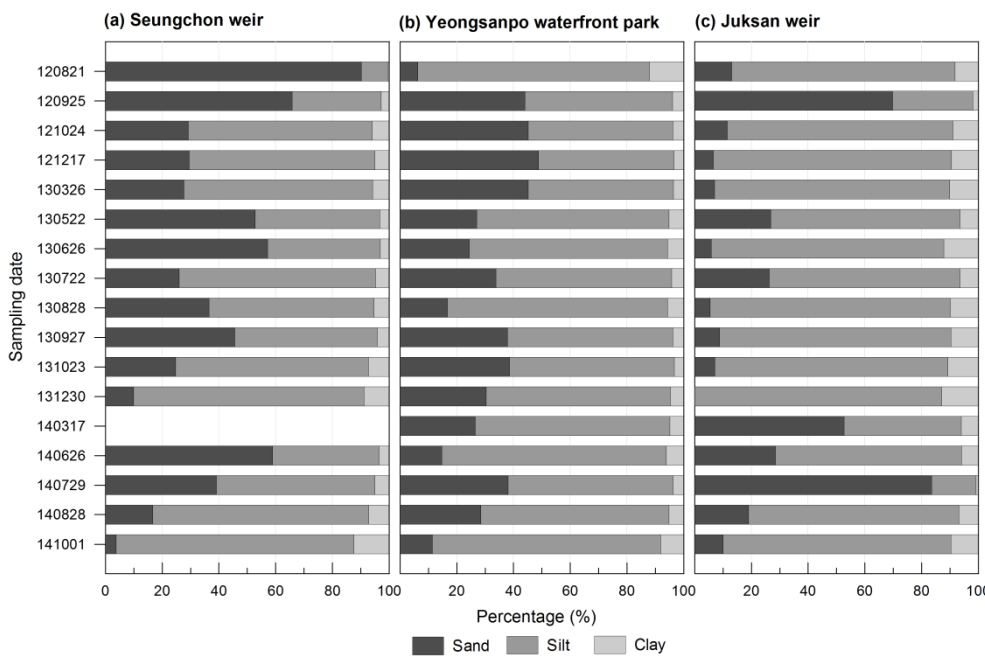

Figure 8. Proportions of sand, silt and clay present in the sediments at (a) Seungchon weir, (b) Yeongsanpo waterfront park, and (c) Juksan weir.

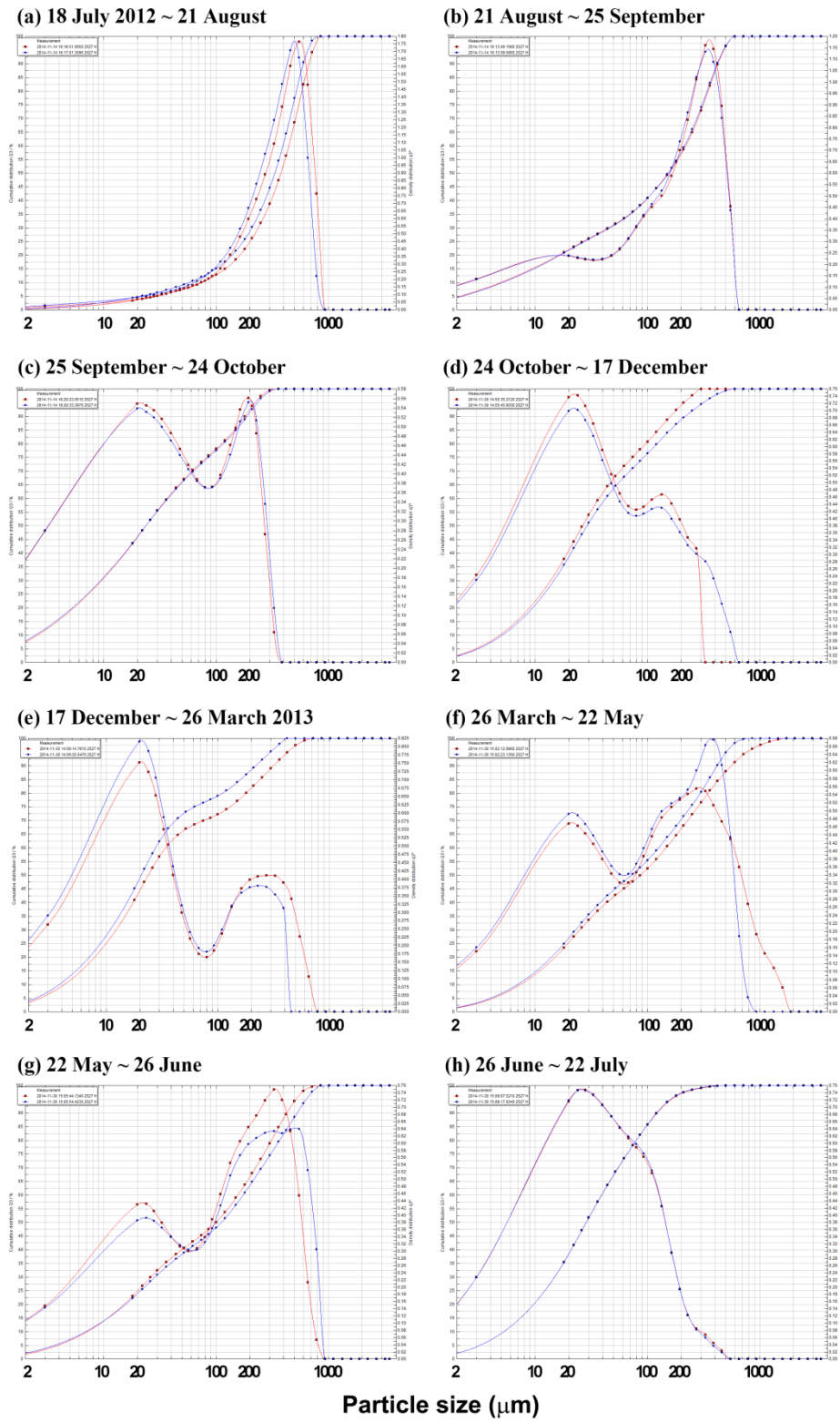

Figure 9. Particle size distribution of the suspended sediments at Seungchon weir during the first one year of sampling (July 2012 to July 2013)

Figure 9 directly show how the particle size distribution varies with time, representing time series of size distribution at Seungchon weir during the first one year of sampling. At the YS-S1, proportions of the clay were less than 10 % during most of the time (Figure 8), and coarse silt (< 31 μm) and very fine sand (< 125 μm) were predominant. The first sampling period exceptionally exhibited a unimodal distribution with a dominant peak in the 500 - 550 μm range (Figure 9a). The next period has a bimodal distribution with major mode centered between 300 - 400 μm and minor mode centered at 10 - 20 μm (Figure 9b). Third sample containing changes toward reducing rainfall and discharge is characterized by a bimodal distribution with a large increase in the fraction less than 20 μm and the other peak 200 μm (Figure 9c). And that of November and December (composite sample) shows dominant peak centered between 20 - 30 μm and the minor mode between 100 and 200 μm (Figure 9d). In other words, negative skewness (the tail on the left side of the probability density distribution) in summer shifts to positive skewness (the tail on the right side) in winter as finer fraction around 20 μm increases. Conversely, as spring changed into summer, a distribution skewed toward the coarse fraction between 300 and 400 μm in reverse order (positive to negative skewness), shown in Figure 9 (e) through 9 (h).

In case of the Juksan weir located in downstream, reservoir sediments most often fall within the medium silt size (< 16 μm). Silt and clay-sized particles dominated the suspended sediment load, however, proportion of the coarser fraction increases during the period of high discharge (Figure 8). Similar to the Seungchon weir, the unimodal distribution with 200 μm mode in summer changed to a distribution skewed toward the finer fraction (< 8 μm) in winter season, passing through

transitional phase which is gradually increasing the other peak less than 10 μm.

At the Yeongsanpo waterfront park, a halfway point between the two weirs, silt-sized particles account for around 50 % of the sediments and coarse particles greater than 200 μm occur very seldom. Clay fraction ranges between 3.4 and 12.1 percent, and mean grain sizes of the sediment fall between 8 and 46 μm during all monitoring periods. Particle size composition which is relatively less sensitive to season changes, compared to the two weirs. It is obvious that intra- and inter-seasonal variations in grain size distributions were less than those in the sedimentation rate at YS-S2. For example, differences between grain size of winter to early spring and that of summer were less by generally no more than a factor of two, while rate of reservoir sedimentation more than 10-fold greater occurred during the high flows (Figure 6).

In short, at the YS-S1, coarse silt (< 31 μm) with medium sand-sized peak under high flows appeared. At the halfway point between the two weirs (YS-S2), medium to coarse silt-sized particles accounted for 50 % of the sediments, regardless of season. At the downstream YS-S3, most sediments fell within the medium silt size (< 16 μm) with an increase in the coarser fraction with high flows.

3.2. Geochemical characteristics of suspended sediments

3.2.1. Major elements

Table 1 represents major element concentration of the suspended sediments for the three sampling sites (YS-S1, S2, and S3). Concentrations of the major elements in the reservoir sediments of the study area range as follows; Si 21.47 ~ 36.44, Al 5.93 ~ 10.40, Fe 1.16 ~ 4.72, Ca 0.62 ~ 3.85, Mg 0.16 ~ 0.85, K 2.02 ~ 3.49, Na 0.61 ~ 2.58, Ti 0.15 ~ 0.51, Mn 0.02 ~ 0.47, and P 0.03 ~ 0.83 in weight percent (Table 1).

The Seungchon weir (YS-S1) shows higher potassium (K) and phosphorus (P) concentrations with very low iron (Fe) and magnesium (Mg) contents of the sediments. At YS-S2 site, concentrations of most of the major elements including Al, Fe, Mg, Na, and Ti are higher than the other sites, while mean value of silicon (Si) contents is very low (< 25.7 wt. %). And the Juksan weir (YS-S3) has highest Si content on average (> 28 wt. %) with high calcium (Ca) and manganese (Mn) concentrations and low organic matter contents, compared to two sites.

For comparison with the chemical composition of the underlying rocks, existing data on bedrock geochemistry of the study catchment area was used; Park et al. (1995) that covered granitoid rocks such as biotite granite, hornblende-biotite granodiorite, and two-mica granite in the Gwangju-Naju area, Kim et al. (1998) that analyzed precambrian granite gneiss, Jurassic gabbro-diorite, biotite granodiorite, porphyritic granite, and leucogranite in eastern region of the Jangsung area, and Park (2003) that focused the volcanic rocks including Hwasun andesite, Changdong formation (tuff), Togok rhyolite, and Mudeungsan dacite in the Mt. Mudeung area. And element concentrations of the river bed materials in the

Gwangju and Naju areas researched by Kim and Park (2005) and Park et al. (2006) were examined also. In these studies, river bed materials, especially the undersized materials that passing through the 150 μm sieve, in 1:50,000 geomorphological map of Gwangju and Naju sheets were collected and analyzed by geological groups such as precambrian granitic gneiss, schist, Jurassic granite, arenaceous rock, tuff, andesite, and rhyolite (Kim and Park, 2005; Park et al., 2006). Since a part of the samples in the Naju sheet was beyond the area bounds, elemental concentrations of the schist were excluded from the comparison. Using these data, average concentrations of the bedrock of the river basin and of the river bed materials for each element were calculated, respectively (Table 1).

It is noticeable that the easily mobilized elements, such as Ca, Mg, K, and Na, are considerably depleted in the suspended sediments relative to the bedrock of the river basin (Table 1). Al, Fe, Ti, Mn, and P contents of the suspended sediments are higher than the average value of underlying rocks. On the contrary, there is a very close correspondence between element concentrations of the suspended sediments and of the river bed materials.

Chemical Index of Alteration (CIA) values suggested by Nesbitt and Young (1982) were calculated from the molecular proportions of oxides in order to address the difference between geochemical composition of the parent rock and the suspended sediments, and to quantify the extent of their weathering. Ternary diagrams of A–CN–K (Al_2O_3, CaO + Na_2O, and K_2O) and A–CNK–FM (Al_2O_3, CaO + Na_2O + K_2O, and Fe_2O_3 + MgO) after Nesbitt and Young (1984, 1989, 1996) and Nesbitt et al. (1996) were also used to deduce weathering trends (Figure 10).

		LOI	Si	Al	Fe	Ca	Mg	K	Na	Ti	Mn	P
YS-S1	**Min.**	1.82	21.47	5.93	1.16	0.78	0.16	2.02	0.69	0.15	0.02	0.03
	Max.	19.36	36.44	10.06	4.67	1.75	0.77	3.49	1.42	0.48	0.43	0.83
	Mean	11.64	27.88	8.19	3.25	1.12	0.56	2.46	0.99	0.33	0.14	0.23
	Std.	4.48	3.65	1.13	0.89	0.29	0.16	0.39	0.20	0.09	0.09	0.18
YS-S2	**Min.**	4.52	23.60	7.41	2.22	0.68	0.36	2.11	0.90	0.26	0.05	0.06
	Max.	16.83	32.80	10.40	4.72	1.73	0.85	3.13	2.58	0.49	0.26	0.25
	Mean	12.14	25.67	9.52	4.05	1.00	0.70	2.36	1.54	0.44	0.16	0.16
	Std.	2.74	2.02	0.85	0.54	0.28	0.10	0.21	0.62	0.06	0.06	0.04
YS-S3	**Min.**	3.62	25.36	5.81	1.76	0.62	0.30	2.08	0.61	0.22	0.05	0.05
	Max.	16.34	35.36	9.67	4.36	3.85	0.80	2.78	1.16	0.51	0.47	0.42
	Mean	10.99	28.30	8.03	3.43	1.27	0.61	2.28	0.85	0.37	0.19	0.17
	Std.	3.72	2.92	1.07	0.69	0.76	0.14	0.22	0.15	0.07	0.11	0.09
ALL	**Mean**	11.59	27.27	8.59	3.58	1.13	0.62	2.36	1.13	0.38	0.16	0.19
	Std.	3.65	3.09	1.21	0.79	0.50	0.14	0.29	0.48	0.08	0.09	0.12
Underlying rocks *			32.89	7.74	1.45	1.83	0.80	3.12	2.31	0.24	0.05	0.05
River bed materials **			28.56	8.38	3.83	0.75	0.69	2.58	0.85	0.53	0.09	0.07

Table 1. Major elements concentrations of the reservoir suspended sediments in study area (wt. %).

Average concentrations of the underlying rocks of the river basin (*) and of the river bed materials (**) for each element were calculated by using values of Park et al. (1995), Kim et al. (1998), and Park (2003), and values of Kim and Park (2005) and Park et al. (2006), respectively.

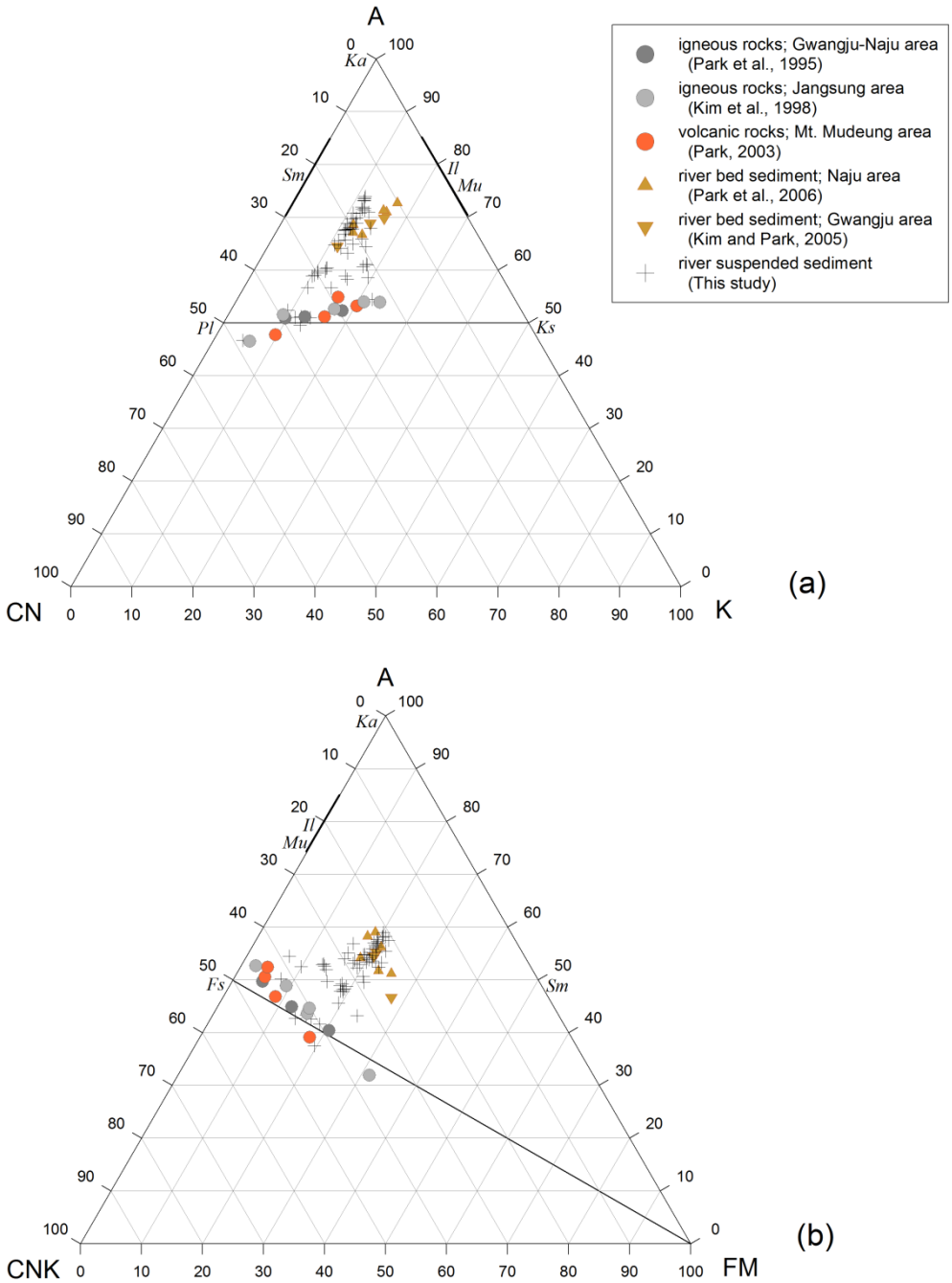

Figure 10. Ternary diagrams of (a) A–CN–K (Al_2O_3, CaO + Na_2O, and K_2O), and (b) A–CNK–FM (Al_2O_3, CaO + Na_2O + K_2O, and Fe_2O_3 + MgO) after Nesbitt and Young (1984, 1989, 1996) and Nesbitt et al. (1996).

Idealized compositions of minerals were labelled as *Pl* = plagioclase; *Ks* = K-feldspars; *Il* = illite; *Mu* = muscovite; *Sm* = smectite; *Ka* = kaolinite; and *Fs* = feldspars (plagioclase and K-feldspar).

On the ternary plot of A–CN–K (Figure 10a), various igneous rocks which are represented by filled circles are plotted close to the plagioclase–K feldspar tieline, at 50 % Al_2O_3 on the left and right-hand boundaries, respectively. As chemical weathering progresses, preferential leaching of sodium and calcium from plagioclase with the retention of potassium produced general chemical weathering trends parallel to the A–CN line; at a more advanced stage of weathering, losses of potassium in K-feldspars shift the weathering trend towards the Al_2O_3 apex (Nesbitt and Young, 1984, 1989). River suspended sediments are distributed in parallel lines of A–CN, showing relatively weak to moderate degrees of weathering. It indicates that the weathering of the suspended sediments in Yeongsan River has not yet reached the advanced stage. CIA values for the suspended sediments ranged from 61.5 to 79.5 with a mean value of 72.9, whereas CIA values for the underlying rocks are distributed within narrow ranges (from 58.9 to 62.8) with a mean value of 60.8.

Figure 10 (b) shows the molar proportions of Al_2O_3, $CaO + Na_2O + K_2O$, and $Fe_2O_3 + MgO$. Plagioclase and K-feldspar which are denoted by *Fs* of the figure is plotted on the left-hand boundary at 50 % Al_2O_3. A variety of igneous rocks which are represented by filled circles are distributed within one-third of the *Fs*–FM tieline, indicating variations in mafic minerals with the relatively high content of feldspars. In common with the A–CN–K diagram (Figure 10a), river suspended sediments experiencing the release of alkali and alkaline earth elements show weathering trends parallel to the A–CNK line. There is no clear evidence of intense weathering of the river suspended sediments that has lost Fe and Mg.

It is noted that river bed materials in study catchment represented by triangle and inverted triangle (Kim and Park, 2005; Park et al., 2006) are plotted on both the A–

CN–K and the A–CNK–FM diagrams similar to the suspended sediments. River bed materials are not only weathering products of underlying rocks but also potential source of downstream suspended sediments through resuspension.

3.2.2 . Trace elements

Concentrations of the trace elements in the reservoir suspended sediments range as follows; Ba 517 ~ 14,000 mg/kg, Co 0 ~ 25.4 mg/kg, Cr 0 ~ 438 mg/kg, Cu 0 ~ 3,483 mg/kg, La 11.9 ~ 53.9 mg/kg, Li 12.9 ~ 57.9 mg/kg, Mo 11.0 ~ 56.8 mg/kg, Nb 0 ~ 40.7 mg/kg, Ni 0 ~ 246 mg/kg, Pb 13.7 ~ 49.2 mg/kg, Rb 164 ~ 293 mg/kg, Sc 0 ~ 13.9 mg/kg, Sn 0 ~ 124 mg/kg, Sr 110 ~ 220 mg/kg, Ta 0 ~ 22.3 mg/kg, V 15.0 ~ 83.9 mg/kg, W 0 ~ 43.8 mg/kg, Y 0 ~ 22.7 mg/kg, Zn 38.2 ~ 347.0 mg/kg, Zr 28.3 ~ 218.0 mg/kg (Table 2). As, Be, Bi, Cd, Hf, In, Sb, Te, and Tl were at lower concentrations than the detection limit. Most of the reservoir samples exhibit the tantalum (Ta) and stannum (Sn) value below 10 mg/kg (detectability limit), so average values of these elements determined by specific cases.

Mean concentrations of most of the trace metal elements including zirconium (Zr), niobium (Nb), barium (Ba), cobalt (Co), copper (Cu), lithium (Li), nickel (Ni), lead (Pb), rubidium (Rb), vanadium (V), and zinc (Zn) are much higher than the average concentrations of the bedrock of the river basin (Park et al., 1995; Kim et al., 1998; Park, 2003). Elemental concentrations of lanthanum (La), scandium (Sc), yttrium (Y), chromium (Cr), and strontium (Sr) are lower than those of underlying rocks.

Tungsten (W) and molybdenum (Mo), members of the Group 6 transition metals, have the pronounced higher values than average concentration in the suspended

sediment of World rivers (Viers et al., 2009). Detected tungsten concentration was 23.6 mg/kg on average, and the maximum value of 43.80 mg/kg. Also molybdenum concentrations were very high with an average of 15.7 mg/kg and maximum value of 56.80 mg/kg. In both cases, highest mean and maximum values were observed at the Yeongsanpo waterfront park.

Barium (Ba) concentrations in 2012 show unusual higher values over 10,000 mg/kg (up to 14,000 mg/kg), and it is more than 10-fold compared to the next monitoring period. Excluding these distinctive observed values in 2012, Ba concentrations ranged from 517 to 802 mg/kg with an average of 617.2 mg/kg. Copper (Cu) abundances in the time when heavy rainfall events were infrequent and discharge was relatively less fluctuated are noticeable. Observed Cu concentration was 392.8 mg/kg on average, and the maximum value of 3,483 mg/kg. The strong enrichment about or more than 2,000 mg/kg of Cu concentration was common all over the sampling point during winter and early spring seasons (January to May).

Average concentrations of Nb, Sc, and V are slightly lower than those of the river bed materials. Other trace elements in suspended sediments, such as Zr, Ba, Cr, and Cu, have higher concentrations compared to the river bed materials.

		Ta	W	Mo	Zr	Nb	La	Sc	Y	Sn	Ba	Co	Cr	Cu	Li	Ni	Pb	Rb	Sr	V	Zn
YS-S1	Min.	0	0	11.0	28.3	0	11.9	0	0	0	534	0	0	0	12.9	0	13.7	169.0	118.0	15.0	38.2
	Max.	22.3	36.4	28.5	193.0	40.7	53.9	13.8	22.5	124.0	12400	19.3	199.1	2720.0	50.7	89.8	49.2	282.0	220.0	78.4	347.0
	Mean	3.6	21.8	14.5	123.4	23.3	39.0	4.9	15.9	9.5	2727.1	12.6	67.4	529.0	38.4	31.3	30.8	204.2	155.8	60.3	175.0
	Std.	6.8	13.2	4.0	44.6	14.1	11.0	5.8	5.3	30.9	4464.2	6.6	44.8	781.5	10.6	22.7	8.7	31.7	28.9	17.6	77.5
YS-S2	Min.	0	0	12.1	47.8	0	25.9	0	10.0	0	517	0	15.1	18.5	25.1	0	16.5	190.0	117.0	31.1	61.9
	Max.	14.1	43.8	56.8	208.0	31.9	51.9	11.9	22.0	100.0	14000	25.4	438.0	845.0	52.8	246.0	40.9	293.0	199.0	80.7	264.0
	Mean	2.2	26.7	19.1	146.6	23.9	43.1	7.3	18.1	7.3	3141.6	18.3	93.1	190.5	44.9	43.7	30.5	219.9	165.0	67.6	190.8
	Std.	4.9	12.0	10.6	50.3	12.4	6.2	5.6	2.9	24.6	4786.1	6.3	115.9	217.3	7.0	56.6	6.0	26.0	22.1	12.2	47.3
YS-S3	Min.	0	0	11.4	63.1	0	32.2	0	10.0	0	528	0	18.3	11.5	24.9	0	16.7	164.0	110.0	35.6	47.0
	Max.	12.8	33.1	16.0	218.0	36.1	51.9	13.9	22.7	0	13300	21.7	138.0	3483.0	57.9	56.1	40.0	276.0	172.0	83.9	281.0
	Mean	2.8	22.3	13.6	137.4	24.7	41.8	6.8	18.1	0	3110.5	15.9	57.0	466.8	44.6	25.8	29.1	207.8	132.5	69.3	157.6
	Std.	5.3	12.8	1.4	40.1	12.9	5.7	5.9	3.0	0	4698.8	5.1	27.7	830.3	8.7	11.6	6.4	30.0	19.1	12.2	61.4
ALL	Mean	2.8	23.6	15.7	136.0	24.0	41.4	6.4	17.4	5.5	2998.4	15.6	72.6	392.8	42.7	33.6	30.1	210.8	151.0	65.8	174.4
	Std.	5.6	12.6	7.0	45.3	12.9	7.9	5.7	3.9	22.5	4563.5	6.4	74.1	670.6	9.2	36.1	7.0	29.5	27.0	14.4	63.2
Upper crust		2.2	-	-	190	25	30	-	22	5.5	550	10	35	25	-	20	20	112	350	60	71
Underlying rocks *		-	-	-	57.0	14.3	47.4	8.1	20.8	-	687.1	8.1	180.7	11.8	28.0	15.3	16.4	156.0	306.4	50.9	51.4
River bed materials **		-	-	-	116.8	29.9	-	11.0	-	-	1379.8	10.1	50.3	24.8	37.3	22.0	22.6	125.8	131.9	78.3	115.4

Table 2. Concentrations of the trace elements for the reservoir suspended sediments in study area (mg/kg).

Average concentrations of the underlying rocks of the river basin (*) and of the river bed materials (**) for each element were calculated in the same way as was done in Table 1.

3.3. Discussion and summary

3.3.1. Weir construction effects on fluvial system

The Yeongsanpo waterfront park (YS-S2), located in 10 kilometers downstream from the Seungchon weir (YS-S1) and 10 kilometers upstream from the Juksan weir (YS-S3), exhibited the physical characteristics of sediments with distinctly different from two weirs (Figure 6 and Figure 8). First, the sedimentation rates of the YS-S2 were commonly lower than those of the Seungchon weir for most of the sampling period, although Jiseokcheon which is the biggest tributary in study area joins with main stream of the Yeongsan River at between two sampling sites (YS-S1 and S2). Secondly, narrow ranges of intra- and inter-seasonal variations were found for grain size distributions, while grain size distributions for the two weirs showed obvious temporal variations that coarser fraction increases under high flows and gradually skewed toward the finer fraction in winter season (Figure 9).

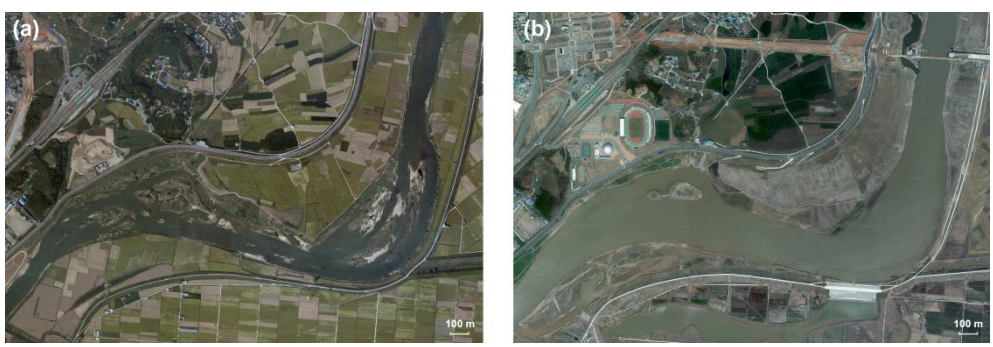

Figure 11. Aerial photo taken in 2008 (a), and in 2012 (b) showing the geomorphic changes in middle Yeongsan river.

Source: Daum map (http://map.daum.net).

There is a possibility that locational and geomorphic characteristic of sampling point (the Yeongsanpo waterfront park) could cause aforementioned two physical characteristics of sediments. During unregulated period (before the 1930s), the Yeongsan river free-meanders across its wide floodplains that lies on the left side of the river, especially in the middle course (confluence of Gwangjucheon and Yeongsan river ~ Yeongsan Bridge) (Iksan Regional Construction and Management Administration, 1998). As stream's velocity decreases, transported sediments are deposited on the inside bank of a meander bend or in mid-channel. There were a lot of large point bar and vegetated mid-channel bar with trees and grass (Figure 11a, aerial photo taken in 2008), and size of the accumulated area naturally increased or decreased depending on the hydrological regime. In a recent photo, most of fluvial landforms disappeared or reduced, as dredging a riverbed and maintaining consistent water level. Besides, newly created artificial wetland on either side of the river has provided accommodation spaces for sedimentation temporarily or permanently. It seems relatively stagnant environment enough to settle the suspended sediments when flow velocity decreases, as for the mainstream course of YS-S1 and YS-S2. Under lake-like condition of YS-S2, the result implies 1) the decrease in sediment supply from upper stream, particularly for coarse suspended sediments greater than 200 μm, or 2) delivered sediments as before the pre-weir construction were deposited on another place and additional sediment supply from the tributaries was restricted by some factors, e.g. reduced hydraulic gradient and the consequential reduction of energy, and rising water level of mainstream.

As many studies pointed out effects of dam construction, downstream channel scouring, widening, and coarsening of channel bed materials, or opposing patterns have been generally predicted and observed (Petts, 1979, 1984; Williams and

Wolman, 1984; Simon, 1994; Church, 1995; Friedman et al., 1998; Brandt, 2000; Petts and Gurnell, 2005; Yang et al., 2005; Yang et al., 2007; Committee on Missouri River Recovery and Associated Sediment Management Issues, 2011; Yang et al., 2011). Phillips et al. (2005) showed that there is no consistent channel geomorphic response to post-dam changes, and other controls such as sea level rise and backwater effects are more influential to the lower reaches of the river located near or below sea level. Howard and Dolan (1981) adopted a careful approach which was separating two processes influencing scour and fill as “short-term local processes” and “long-term general processes”. After construction of the Glen Canyon Dam, reduced transport capacity by flow regulation and subsequently weakened flood peak couldn't flush the sediments from the tributary Paria River, and eventually caused the aggradation (increase of bed elevation).

The Seungchon weir is composed of two fixed weir parts on both sides of middle movable weir applying Truss type lift gate. The movable gate is controlled by the flow regime, and it can be expected that delivered sediments can be trapped primarily into the reservoir at ordinary flows, and flowing water which is partly including suspended sediments is temporarily released to downstream through the lifted gate under high flows. High runoff enough to entrain coarser materials over a dam wall would be restricted to summer season, especially one or two months in a year. Particle size distributions of the YS-S2 sediments showing less temporal variation can be interpreted as combination of limited supply of coarser materials and deposition within a short distance. Relatively finer fraction of sediments (< 16 μm, smaller than medium silt size) which can be transported further distances without settling even at the low velocities mainly deposited at YS-S2 site.

Meanwhile, the formation of a lake-like condition by the obstruction from the

two weirs upstream and downstream makes the hydraulic gradient reduce, and consequently decrease sediment transport capacity. Jiseokcheon, which has a catchment area of 664 km^2 and transports mostly sand, gravel, and boulder in the steep upper part of the catchment and sand and gravel in the lower part based on the channel beds materials (Iksan Regional Construction and Management Administration, 1998), joins with main stream of the Yeongsan River between YS-S1 and S2 sites. Inflowing coarser sediments from the Jiseokcheon can't be removed effectively, and deposited at around a confluence. And then, particle size distributions of the YS-S3 sediments reflecting hydrological variation implied additional sediment inflow from the other tributaries or sediment sources from river bank that has less opportunity for conveyance losses.

Contrary to conventional prediction such as Williams and Wolman (1984), however, it is particularly difficult to ascertain if degradation (erosion) trend that both based on the sediment supply, and channel bed elevation change dominated downstream due to the lack of long-term monitoring data regarding fluvial responses after weir construction. Fluvial responses to weir construction would be different depending on where detailed locations are, which geomorphic and hydrologic features appeared around, and how much sediment contribution from tributaries is made (Graf, 2006). With regard to the YS-S2 sediments, it seems best explained by that reduced hydraulic gradient which was made by two weirs upstream and downstream, decreased complexity of landforms and reduced turbulence flow cause less variable environment .

3.3.2. Seasonal changes of the geochemical properties

3.3.2.1. Variability of the major and trace elements

Dispersion of the concentrations of major and trace elements was examined as the seasons change. The coefficient of variation, ratio of the standard deviation to the mean, which is commonly expressed in percent is used due to its advantage of independence of measuring units or the extent of the data. Figure 12 shows various magnitudes of change arranged in ascending order of percent, from lower variability (i.e. Si) to highly variable elements (i.e. Ta and Sn). CV values depicted in Figure 12 were derived from average for three sampling sites.

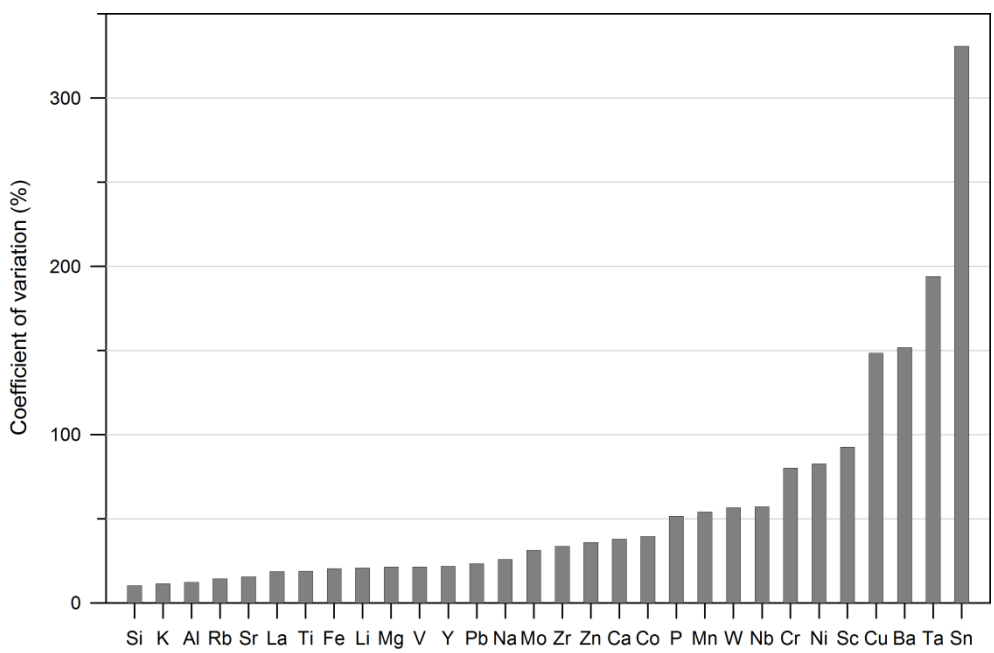

Figure 12. Coefficient of variation (CV, %) of the geochemical element concentrations. CV values are derived from the average for three sampling site values.

The concentration of Ta and Sn in the reservoir sediments are almost below 10 mg/kg (detectability limit), so the difference between the (null) values less than

detection limit and several detected cases makes these highly variability. Thirteen elements (silicon to lead) remained below 25 percent on the coefficient of variation. Variability of the trace elements is generally greater than that of the major element excepting cases of element Na, Ca, P, and Mn (> 25%). Sodium and calcium which are in the list of macronutrients needed by plants are known for being extracted from the granite during the initial stages of weathering (Nesbitt and Young, 1984), and likely to be transported in dissolved form in river (Dupré et al., 1996; Dekov et al., 1997). Similarly, in case of the phosphorus, numerous transformations between the particulate (suspended sediments) and dissolved phase occur during the migration processes, undergoing interactive reactions with water column and channel bed sediments (Förstner and Wittmann, 1983; Mainstone and Parr, 2002). Heavy metals such as Cu, Ni, and Cr which are both originated from natural and anthropogenic sources show very high variability. The behavior of these variable elements can be influenced by natural factor (e.g. discharge increase, changes of pH in river water, and surrounding biota) and human activities related both to the diffuse source (applying fertilizer or pesticides, livestock waste) and to the point source (sewage effluent from populated areas) (Lee et al., 2003; Jarvie et al., 2006).

To estimate the anthropogenic impact on sediments, an enrichment factor (EF) was calculated for each element using Al as the reference element. Al is considered as conservative element since it is of terrestrial sources, so does not vary with time or geographical location relatively. The EF was calculated using the following equation (Zoller et al., 1974):

$$\mathrm{EF} = \frac{(\mathrm{X}/\mathrm{Al})_{\mathrm{sample}}}{(\mathrm{X}/\mathrm{Al})_{\mathrm{upper\ crust}}} \qquad \text{(Eq. 1)}$$

where $(X/Al)_{sample}$ represents the ratio of given element X concentration to Al concentration in observed suspended sediment, and it is divided by the average upper crust values of these elements. Elemental concentrations in the upper continental crust suggested by Taylor and McLennan (1985) were used.

If EF for element X is close to 1, this element may have a terrigenous source, while high EF greater than 1 can be attributed to anthropogenic input. But high value of EF can be originated with characteristic geology of the sampling site, not from the anthropogenic interference. In other words, concentrations of the reference element are quite heterogeneous from region to region. Though there are many papers pointing out inherent flaws of the enrichment factor (e.g. Reimann and de Caritat, 2000; 2005), Figure 13 can provide approximate tendency to be enriched or depleted compared to the average upper crust, along with issues regarding anthropogenic excess.

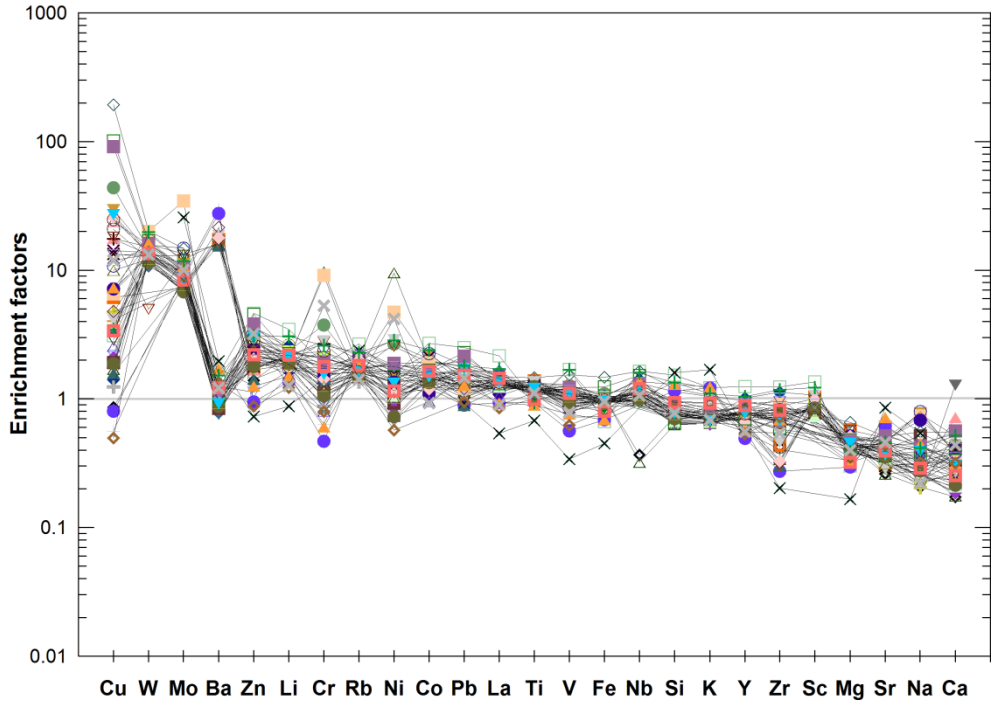

Figure 13. Enrichment factors for the geochemical data, in decreasing order of average EF. Each point represents the monthly geochemical data for reservoir sediments from three sampling sites.

Monthly geochemical data for reservoir sediments was plotted as each point, and EFs for the each element presented in decreasing order of average enrichment factor (Figure 13). Most of the major elements are located at right side of the figure. Though there is variation within the element, enrichment factors of Ti, Fe, Si, and K fall close to unity and Mg, Na, and Ca are below 1. Mg, Sr, Na, and Ca occupying the lowest parts of the EFs are related with high ionic potential of elements during chemical weathering. These highly mobile elements are depleted in suspended sediments (Figure 13), but likely to be enriched in dissolved phase (Dupré et al., 1996).

Previous findings pointed out that the variability of the major elements (Al, Fe,

Mg, Ca, Na, Si, Ti) can be explained by the climatic features which are influencing the intensity of the weathering (Martin and Meybeck, 1979; Meybeck, 2003; Viers et al., 2009). It is well known that alkali metals (Group 1 of the periodic table; Na, K, Rb, Cs), and alkaline earth elements (Group 2; Mg, Ca, Sr, Ba) tend to be strongly removed and easily transported in the dissolved form, while the larger cations (e.g. Rb, Cs, and Ba) are generally retained adsorbed on secondary clays during chemical weathering processes (Nesbitt and Markovics, 1980). Furthermore, Canfield (1997) grouped major elements into three categories by the element chemical behavior on weathering; refractory elements retained in particulate form during weathering such as Al, Fe, and Mn / SiO_2 showing low element mobility / labile elements including remaining major elements which are more easily lost (weathered) to solution than SiO_2 such as Ca, Na, Mg, and K. In this study, geochemical composition of the suspended sediments showed relatively weak to moderate degrees of weathering that has lost Ca and Na from plagioclase with the retention of K (Figure 10).

However this study covers present-transported river sediment which is under relatively homogeneous climate condition throughout all sampling sites, while the studies focusing on relationship between variability of the elements and the weathering condition was on a world or continental scale. It is very difficult to determine that temperature, runoff, and the consequential weathering intensity and element mobility changed significantly in the monitoring period. Instead it would be obvious that variations in weather condition such as precipitation and discharge can affect ability of the river to erode deeper part of the soil surface and to transport pre-weathered coarser particles.

3.3.2.2. Abundances of trace elements by anthropogenic activities

Predominant origin of the trace metals in river sediments can be largely categorized as lithogenic or anthropogenic. Whereas metals such as Zr, Rb, and Sr are derived from weathering and sequential diagenesis of parent rock materials, enrichments of metals including Cr, Co, Ni, Cu, Zn, Cd, and Pb are involved in human activities (Förstner and Salomons, 1980; Grousset et al., 1995).

Gaillardet et al. (2003) classified sources of trace elements in aquatic systems as rock weathering, atmosphere, or other anthropogenic contributions. Enrichment of elements can be primarily attributed to their abundance in source rocks and the weathering style. In addition, atmospheric input of trace elements into river includes both via direct release of particles (volcanic products, ashes from forest fires, sea salts) and through rainwater-dissolved phase. Lantzy and Mackenzie (1979) emphasized that anthropogenic influxes through the rainout of elements such as Cu, Cd, Zn, As, Sb, Mo, and Pb based on fossil-fuel burning and industrial emissions. Besides, various man-made contributions of commercial exploitation of ore deposits, treated sewage effluent, and widespread application of fertilizer and pesticides into fluvial system have been reported (Chester and Stoner, 1973; Logan et al., 1979; Logan, 1987; Neal et al., 1997; Neal et al., 2000; Schäfer and Blanc, 2002; Devault et al., 2009; N'guessan et al., 2009).

As to the result in 3.3.2.1 (Figure 13), EF of Cu ranges up to 192.76 (average value is 16.18), followed by W (~20.20, mean value 11.17), Mo (~34.57, 10.03), Ba (~29.37, 5.15), Zn (~4.64, 2.31), Li (~3.46, 2.01), Cr (~9.72, 1.91), Rb (~2.67, 1.79), Ni (~9.56, 1.54), Co (~2.71, 1.45), and Pb (~2.50, 1.42). It is commonly accepted that EF for a given element below 2 can be caused by intrinsic mineralogical composition of the sampling site (Sutherland, 2000; Hernandez et al.,

2003), a significant enrichment is suspected to have been affected by anthropogenic input regarding more than 2. Excess of these elements beyond acceptable concentrations can cause impairment of water quality and consequential effects on ecosystems (Owens et al., 2005b; Sánchez-Chardi and López-Fuster, 2009).

These strongly enriched trace elements may be explained by anthropogenic activities, as pointed out by Oh et al. (2003) that examined geochemical concentrations of channel bed materials from mainstream of the Yeongsan river, Hwangnyong River, and Gwangjucheon. In their result, contamination level around confluence of Gwangjucheon and Yeongsan river was remarkable, since Gwangjucheon pass through many industrial complex inside or around the Gwangju Metropolitan City. Furthermore, this study area was traditionally dominated by agricultural land uses including rice cultivation on the floodplain and fruit orchard (pears and grapes).

If these metal elements were derived from the diffuse sources such as phosphate fertilizer or fuel combustion, it is expected that pollutants influxes by surface runoff and interflow may be concentrated in summer. However, copper contents more than 500 mg/kg were appeared during winter to early spring samples for three sites. It implies the point source ingress that cannot be explained by the fluctuations of the concentration with runoff regime. Other factors such as runoff characteristics, conveyance losses of these elements, or affinity of these trace elements for oxides should be investigated in order to decipher sources of metal elements abundances.

3.3.3. Correlation between geochemical elements and affecting factors

Possible association between the geochemical elements or between elements and controlling variables (e.g. discharge, particle size, or organic matter contents) was examined, and correlation matrix for the variables presented in Table 3. Most elements are correlated with the peak discharge and the organic matter contents assessed by loss on ignition (statistically significant at the $p < 0.01$;** and $p < 0.05$;*). It is well established that high concentrations of major and trace (metal) elements are associated with fine-grained sediments due to their high specific surface area (e.g. Horowitz, 1985; Rubio et al., 2000; Bouchez et al., 2011). At YS-S2 site showing smaller mean grain size and less seasonal variability in particle size, concentrations of Al, Fe, Mg, Ti and most of trace elements are higher than the other two sites. However, no significant correlations were observed between elemental concentrations and variables associated with particle size such as sand, silt, clay percentages or absolute value of grain size.

The most noticeable correlations were between organic contents and peak discharge (negative) and between Si, K and peak discharge (positive). Increased stream power generally caused by increase of discharge is able to erode and carry even larger materials from river banks or deeper part of the soil layer, while ordinary water flow can remove near-surface humus layer. As discharge increases along with sandy component, proportion of quartz and K-feldspar in particulate form is expected to increase due to sufficient ability of the stream to carry coarser sediments (Schäfer and Blanc, 2002). It is noted that most of the elements are negatively correlated with Si, and it can be attributed to the dilution effect by quartz. Bouchez et al. (2011) suggested that low concentration of most other

elements can be explained by the increase of Si that contained relatively coarse quartz grains distributed near the channel bed. It is in a different context from the grain-size fraction (e.g. Taylor and McLennan, 1985), which demonstrates that chemical composition of the sediments can be explained by the concentration of clay minerals accompanied by chemical weathering of quartz and feldspar. Since reservoir sediments are the result of a complex combination of various types of weathered rocks within a catchment and of erosion and (re)mobilization processes, relative proportions of organic matter contents and concentrations of Si and K can be discussed in terms of ability to erode or transport capacity of river flows rather than change in the weathering regime releasing secondary clay mineral. Other major elements commonly have negative or non-significant correlation with the discharge.

Whereas there are no significant correlations between elemental concentrations and particle size, organic matter contents are strongly correlated with most of the elements, such as Mn, P, W, Nb, Y, Co, Cu, Li, Pb, V, and Zn. Phosphorus adsorption onto organic matter and binding of Cd, Cu, Pb and Zn to soil humic materials has already been demonstrated (Irving and Williams, 1948). Phosphorus positively correlated with organic contents (r=0.72), Mn (r=0.7), Cu (r=0.68), Zn (r=0.65), Pb (r=0.58), Fe (r=0.39), V (r=0.38), and Nb (r=0.37) while displaying a negative correlation with peak discharge (r=-0.34) and with sedimentation rate (r=-0.31). Concentrations of the sediment-associated phosphorus generally increase under high flows, since phosphorus absorbs strongly on the soil particles, as opposed to the result of this study. According to Mainstone and Parr (2002), most of the phosphorus load from diffuse source inflows the river at higher runoff events, and much of this load would be likely to be immediately flushed out of the fluvial

system while accumulation of the phosphorus in the river occurs under lower flows.

As to the non-point source related to the agricultural practices, it can be interpreted in terms of the restricted phosphorus losses in eroding agricultural cropland during summer cultivation period. Kim et al. (2006) showed that total phosphorus concentrations are not correlated with discharge under water-ponded conditions in rice paddy, contrary to strong positive correlation under non-ponded conditions. And agricultural land that sparsely covered by crops can be easily exposed to soil erosion and phosphorus loss even at lower rainfall intensities (Jarvie et al., 2008; Walling et al., 2008b). Actually correlation analysis for winter samples, corresponding to drained and bare soil period after harvesting, exhibited positive correlation between peak discharge and phosphorus concentration ($r=0.51$).

Although there are variations of elemental concentrations in site-to-site, in discharge regime or seasons, or in grain size compositions of the sample, the samples are basically time-integrated collected by settling down of the suspended sediments for about a month. Increase of phosphorus concentration in river water with simultaneous sediment release under high storm flows may not be reflected in these time-integrated reservoir samples due to the flushing-out. On the other hand, phosphorus-rich soil particles from cultivated area can be retained within the river system during winter season because of low transport capacity which is insufficient to resuspend or remobilize the bottom sediments.

Meanwhile, trace metals, such as Cu, Ni, Co, Zn, Pb and various rare earth elements, tend to coprecipitate with or adsorb onto Fe and Mn hydrous oxides (Robinson, 1981; Stumm, 1987). In this study, Fe and Mn oxides in reservoir sediments are positively correlated with the concentrations of trace metal elements such as Cu, Co, Zn, and Pb. Although correlation between elemental concentrations

exhibited strong positive relationship each other, determining if adsorption or coprecipitation with other trace metal elements is the dominant mechanism releasing manganese deserves to be considered with care. Adsorption or desorption of trace metals can be affected by surrounding water pH, concentration of the suspended sediment, and sediment surfaces conditions (mineral pH) occurring competition with protons and other cations in aquatic system (Bourg, 1983). Other potential factors such as releasing from Mn-bearing minerals, Fe–Mn solid solution, or synthetic detergents in river and sewage water can contribute to Mn concentration (Lee et al., 2003).

	Ta	**W**	**Mo**	**Zr**	**Nb**	**La**	**Sc**	**Y**	**Sn**	**Ba**	**Co**	**Cr**	**Cu**	**Li**	**Ni**	**Pb**	**Rb**	**Sr**	**V**	**Zn**
Peak discharge	-0.03	0.03	-0.08	0.13	0.06	0.11	0.08	0.06	0.18	-0.05	-0.12	-0.07	-0.30*	-0.07	-0.04	-0.08	0.05	-0.03	-0.14	-0.22
Sedimen-tation rate	0.34*	-0.20	0.11	-0.06	-0.23	-0.01	0.10	-0.11	-0.01	0.19	-0.04	0.12	-0.22	-0.08	0.15	-0.27	0.25	-0.09	-0.14	-0.30
Particle size	0.27	-0.25	0.00	-0.12	-0.24	0.00	0.19	-0.07	-0.05	0.22	0.08	0.02	-0.01	0.09	0.09	-0.07	0.34*	-0.03	0.04	-0.03
LOI	-0.16	0.40**	0.10	0.24	0.36**	0.32*	0.00	0.43**	-0.08	-0.25	0.53**	0.28	0.53**	0.43**	0.29*	0.59**	-0.10	-0.25	0.57**	0.68**
Si	0.09	-0.37**	-0.14	-0.28*	-0.30*	-0.49**	-0.18	-0.54**	0.02	0.16	-0.64**	-0.32*	-0.32*	-0.55**	-0.34*	-0.58**	-0.10	0.20	-0.62**	-0.66**
Al	0.05	0.14	0.04	0.28	0.08	0.63**	0.51**	0.56**	0.09	0.04	0.52**	0.25	-0.28*	0.56**	0.27	0.34*	0.43**	-0.14	0.45**	0.33*
Fe	0.06	0.22	0.07	0.25	0.14	0.63**	0.45**	0.61**	0.00	0.03	0.68**	0.33*	0.16	0.66**	0.37**	0.47**	0.36**	-0.34*	0.64**	0.51**
Ca	-0.03	0.09	0.02	-0.08	0.09	-0.11	-0.25	-0.07	-0.04	-0.09	0.00	-0.02	0.17	-0.06	-0.04	0.05	-0.26	-0.01	0.02	-0.03
Mg	0.22	0.04	0.07	0.13	-0.03	0.57**	0.42**	0.54**	0.01	0.17	0.66**	0.28	0.14	0.61**	0.31*	0.31*	0.40**	-0.29*	0.56**	0.39**
K	0.24	-0.43**	0.06	-0.44**	-0.41**	-0.51**	-0.21	-0.68**	0.15	0.28*	-0.61**	-0.23	-0.18	-0.57**	-0.25	-0.51**	0.10	0.48**	-0.72**	-0.53**
Na	0.06	0.07	0.52**	0.01	-0.08	-0.08	-0.18	-0.12	-0.06	0.02	0.23	0.17	0.09	0.00	0.11	-0.09	0.08	0.51**	-0.04	0.12
Ti	0.10	0.10	0.01	0.26	0.05	0.64**	0.52**	0.61**	-0.01	0.09	0.60**	0.25	-0.12	0.63**	0.29*	0.33*	0.43**	-0.33*	0.55**	0.33*
Mn	-0.12	0.31*	0.14	0.18	0.28*	0.19	-0.01	0.29*	-0.10	-0.16	0.46**	0.15	0.55**	0.36*	0.17	0.38**	-0.06	-0.12	0.45**	0.49**
P	-0.18	0.34*	0.03	0.08	0.37**	0.11	-0.13	0.18	-0.01	-0.24	0.27	0.15	0.68**	0.24	0.16	0.58**	-0.17	-0.18	0.38**	0.65**
Ta	1.00	-0.77**	-0.02	-0.71**	-0.88**	-0.03	0.36*	-0.32*	0.09	0.83**	-0.07	0.15	-0.11	-0.09	0.24	-0.44**	0.71**	-0.08	-0.27	-0.37**
W	-0.77**	1.00	0.29*	0.74**	0.90**	0.24	-0.21	0.47**	-0.18	-0.81**	0.40**	0.34*	0.18	0.32*	0.29*	0.59**	-0.49**	-0.04	0.52**	0.57**
Mo	-0.02	0.29*	1.00	0.09	0.04	-0.13	-0.17	-0.13	-0.11	-0.12	0.20	0.63**	-0.02	0.00	0.45**	-0.11	0.05	0.33*	0.07	0.13

Table 3. Pearson's correlation coefficient between the geochemical elements or between the elements and controlling variables (e.g. peak discharge, particle size, or organic matter contents), with a significance level of 0.05 (*) and 0.01 (**), respectively.

	Ta	W	Mo	Zr	Nb	La	Sc	Y	Sn	Ba	Co	Cr	Cu	Li	Ni	Pb	Rb	Sr	V	Zn
Zr	-0.71**	0.74**	0.09	1.00	0.81**	0.54**	0.14	0.73**	-0.14	-0.73**	0.48**	-0.01	-0.12	0.53**	-0.08	0.53**	-0.32*	-0.10	0.61**	0.47**
Nb	-0.88**	0.90**	0.04	0.81**	1.00	0.23	-0.23	0.50**	-0.18	-0.91**	0.29*	-0.02	0.20	0.30*	-0.08	0.64**	-0.64**	-0.08	0.50**	0.54**
La	-0.03	0.24	-0.13	0.54**	0.23	1.00	0.66**	0.91**	0.09	-0.03	0.75**	0.14	-0.12	0.86**	0.18	0.60**	0.43**	-0.41**	0.79**	0.53**
Sc	0.36*	-0.21	-0.17	0.14	-0.23	0.66**	1.00	0.51**	0.10	0.28*	0.50**	0.08	-0.29*	0.64**	0.16	0.15	0.65**	-0.29*	0.46**	0.16
Y	-0.32*	0.47**	-0.13	0.73**	0.50**	0.91**	0.51**	1.00	-0.05	-0.30*	0.76**	0.12	-0.04	0.87**	0.14	0.68**	0.16	-0.44**	0.88**	0.60**
Sn	0.09	-0.18	-0.11	-0.14	-0.18	0.09	0.10	-0.05	1.00	0.22	-0.08	-0.07	-0.03	-0.09	-0.07	-0.05	0.10	0.08	-0.14	-0.03
Ba	0.83**	-0.81**	-0.12	-0.73**	-0.91**	-0.03	0.28*	-0.30*	0.22	1.00	-0.16	0.12	-0.16	-0.11	0.19	-0.51**	0.74**	-0.07	-0.31*	-0.43**
Co	-0.07	0.40**	0.20	0.48**	0.29*	0.75**	0.50**	0.76**	-0.08	-0.16	1.00	0.39**	0.09	0.90**	0.43**	0.54**	0.36**	-0.34*	0.89**	0.65**
Cr	0.15	0.34*	0.63**	-0.01	-0.02	0.14	0.08	0.12	-0.07	0.12	0.39**	1.00	0.00	0.23	0.95**	0.08	0.30*	-0.12	0.30*	0.28*
Cu	-0.11	0.18	-0.02	-0.12	0.20	-0.12	-0.29*	-0.04	-0.03	-0.16	0.09	0.00	1.00	0.01	0.02	0.34*	-0.29*	-0.14	0.16	0.38**
Li	-0.09	0.32*	0.00	0.53**	0.30*	0.86**	0.64**	0.87**	-0.09	-0.11	0.90**	0.23	0.01	1.00	0.27	0.60**	0.44**	-0.45**	0.93**	0.60**
Ni	0.24	0.29*	0.45**	-0.08	-0.08	0.18	0.16	0.14	-0.07	0.19	0.43**	0.95**	0.02	0.27	1.00	0.11	0.39**	-0.20	0.31*	0.28*
Pb	-0.44**	0.59**	-0.11	0.53**	0.64**	0.60**	0.15	0.68**	-0.05	-0.51**	0.54**	0.08	0.34*	0.60**	0.11	1.00	-0.10	-0.18	0.69**	0.89**
Rb	0.71**	-0.49**	0.05	-0.32*	-0.64**	0.43**	0.65**	0.16	0.10	0.74**	0.36**	0.30*	-0.29*	0.44**	0.39**	-0.10	1.00	-0.12	0.19	-0.03
Sr	-0.08	-0.04	0.33*	-0.10	-0.08	-0.41**	-0.29*	-0.44**	0.08	-0.07	-0.34*	-0.12	-0.14	-0.45**	-0.20	-0.18	-0.12	1.00	-0.52**	-0.09
V	-0.27	0.52**	0.07	0.61**	0.50**	0.79**	0.46**	0.88**	-0.14	-0.31*	0.89**	0.30*	0.16	0.93**	0.31*	0.69**	0.19	-0.52**	1.00	0.70**
Zn	-0.37**	0.57**	0.13	0.47**	0.54**	0.53**	0.16	0.60**	-0.03	-0.43**	0.65**	0.28*	0.38**	0.60**	0.28*	0.89**	-0.03	-0.09	0.70**	1.00

Table 3. *(continued)* Pearson's correlation coefficient between the geochemical elements or between the elements and controlling variables (e.g. peak discharge, particle size, or organic matter contents), with a significance level of 0.05 (*) and 0.01 (**), respectively.

3.3.4. Summary

To investigate the temporal variations both in physical and geochemical properties of the reservoir sediments, three time-integrated suspended sediment samplers were installed on the upper and middle Yeongsan River (YS-S1, S2, and S3) in July 2012. Reservoir suspended sediment samples were obtained from three samplers at monthly intervals until October 2014. Seasonal trends of suspended sedimentation rates and grain size distributions were examined based on variations in precipitation and discharge fluctuations. Remarkably high rates of reservoir sedimentation were recorded in summer, especially in the period from August 21 to September 25 of 2012, with increased precipitation and discharge. The relationships between cumulative rainfall during sampling period and peak discharge, and between peak discharge and sedimentation rate showed demonstrable seasonality, respectively. As to the particle sizes of the reservoir suspended sediments in three sites, i) coarse silt (< 31 μm) with medium sand-sized peaks under high flows appeared at the YS-S1, ii) at the halfway point between the two weirs (YS-S2), medium to coarse silt-sized particles accounted for 50 % of the sediments regardless of season, iii) at the downstream YS-S3, most of the sediments fell within the medium silt size (< 16 μm) with an increase in the coarser fraction at high flows.

Concentrations of the major and trace elements of the collected sediments were analyzed and compared with the chemical composition of the underlying rocks. It was noticeable that easily mobilized elements, such as Ca, Mg, K, and Na, were considerably depleted in the suspended sediments relative to the bedrock of the river basin, indicating weak to moderate degrees of weathering. Trace elements

including Ba, Co, Cr, Cu, La, Li, Mo, Nb, Ni, Pb, Rb, Sc, Sn, Sr, Ta, V, W, Y, Zn, and Zr were detected, with an abundance of several elements (e.g. Cu, W, Mo, Ba, Zn, Li, Cr, Rb, Ni, Co, and Pb) that are more likely to be affected by anthropogenic input. This information is valuable for verifying and discussing downstream effects of fine sediment, including channel adjustments following two weir constructions, and can provide an opportunity for tracing sediment sources based on sediment geochemical properties.

4. Evaluation of suspended sediment sources in the Yeongsan River using Cs-137 after major human impacts

4.1. Temporal variation in discharge and reservoir sedimentation

Reservoir sediment samples were obtained at monthly intervals until December 2012, and 15 suspended sediment samples were collected and analyzed in this study, i.e., five samples from each site. Because the sediments trapped in November and December were insufficient for analysis, composite samples during the two months were used for the analysis.

Figure 14 shows the (a) rainfall amount, (b) discharge, and (c) rate of reservoir sedimentation obtained from the suspended sediment samplers after drying in chronological order from installation of the samplers (along the *X*-axis). The total period studied was divided into five periods, Period 1–5, based on sampling time. During Period 1, most of the recorded daily rainfall amounts were about 20 mm, but daily precipitation amounts of about 50 mm were recorded on two occasions. This period showed relatively limited variation, but the sampled reservoir sedimentation at S1 was about 170 kg/m^2, which may be interpreted as a peculiarly large amount. In Period 2, 18 days with rainfall were recorded, and daily rainfall amounts of around 90 mm were recorded twice as a result of the influence of typhoons occurring one after another. Discharge fluctuations at the Hoejin gauging station were greater than those at the Bondong station during this time, and peak discharges at the Bondong station had conspicuously lower values than those at the

Hoejin station. It may be that the Bondong station near the Seungchon weir, where discharges fluctuated only slightly, was directly affected by the water-level control system. On the other hand, the Hoejin station, located between Yeongsanpo (S2) and the Juksan weir (S3), may have been relatively less affected by the weir's control. Also, the confluence of the Yeongsan River with the Jiseokcheon, the largest sub-catchment of the Yeongsan River basin, occurs downstream of the Seungchon weir (S1). The sampled reservoir sedimentation at each site during this period was a large amount, more than 110 kg/m^2, a result of frequent erosion events and abundant precipitation. Records for Periods 3, 4, and 5 primarily indicated daily precipitation of about 5 mm, with the exception of the rainfall events around mid- and late October. Discharge fluctuated within a narrow range, and sampled reservoir sedimentation at all sites was less than 5 kg/m^2.

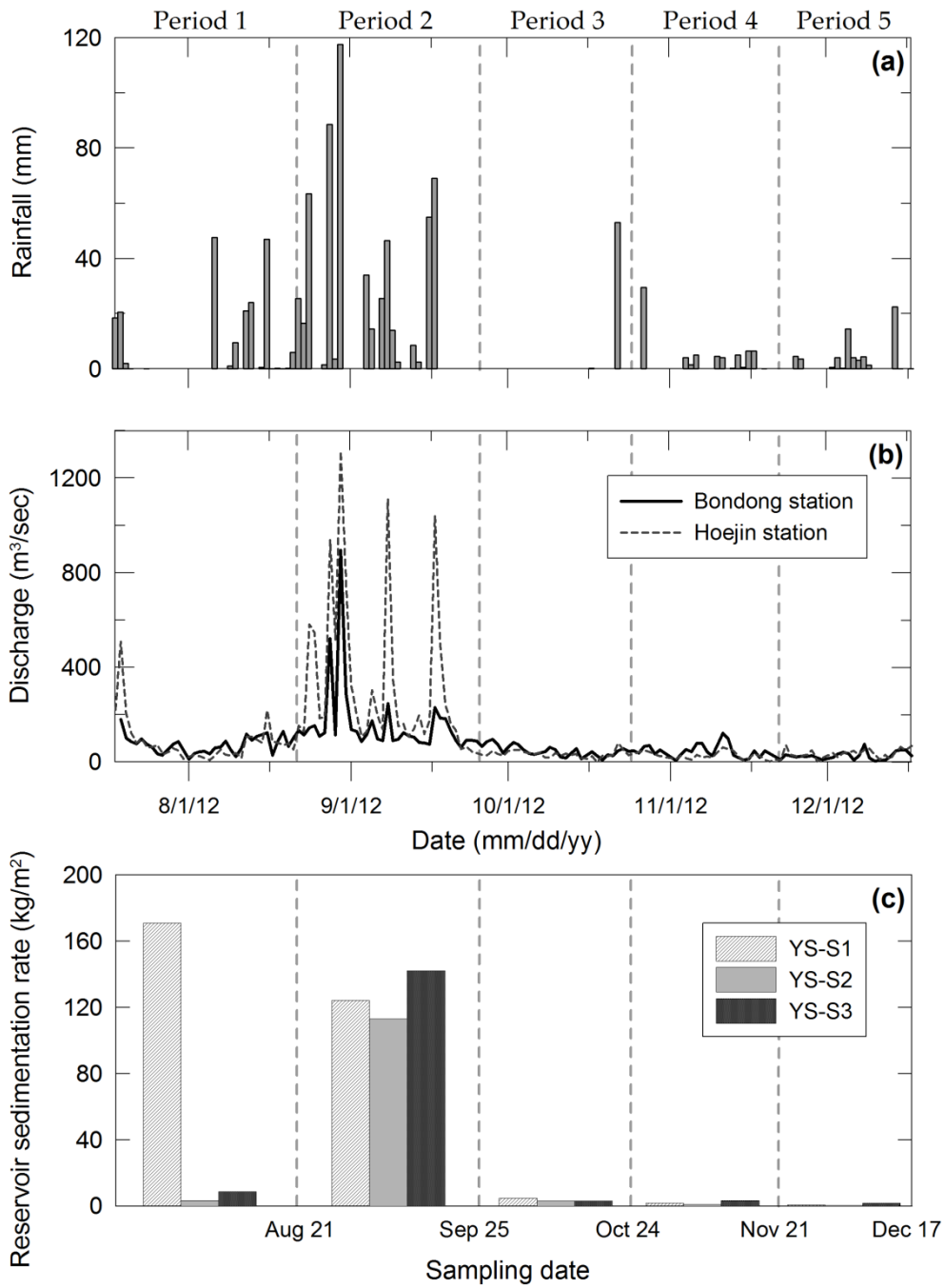

Figure 14. (a) Rainfall amount, (b) discharge, and (c) reservoir sedimentation rate from suspended sediment samplers after drying and weighing in the Yeongsan River.

4.2. ^{137}Cs measurement and construction of a probability density function

Because the purpose of this study was to identify types of sediment sources and not to focus on the spatial locations of primary sources, potential sediment provenances were divided according to source type into slope (forest floor) and channel-bank sources, which are representative of surface soil and subsurface material, respectively. Bank materials were sampled by targeting the face that is relatively erodible through channel change, that is, the lower surface of the riverbank on undercut slopes.

Generally, surface-soil samples must be taken with consideration of the spatial distribution of geological zones or land use (e.g., cultivated land, grassland, or pasture) and field conditions so as to address the spatial provenance of sediment sources. However, in this study, ^{137}Cs radioactivity was used as a single diagnostic property rather than using a composite fingerprinting approach with properties capable of characterizing potential sediment sources due to the necessity of promptly investigating sediment provenance in terms of source type. For this reason, source types of suspended sediment were divided mainly into two erosional processes (i.e., whether sediments are derived from surface erosion or from subsurface erosion), and surface soil samples were restricted to forest slope materials receiving little human interference (e.g., cultivation or tilling).

In total, 22 probable sources of reservoir sediment were taken (0–2-cm depth), considering the spatial distribution of the Yeongsan River catchment, by using a soil scraper: 10 from the forest floor and 12 from the channel bank. These source material samples were subsequently air dried, gently disaggregated, and passed

through a 2-mm sieve. After discarding the >2 mm fraction, the screened materials were oven dried at 60 °C for 48 h and then weighed and sealed in containers for radionuclide analysis. After leaving samples for at least 3 weeks, the ^{137}Cs radioactivity of the reservoir sediment and possible source materials was measured using a gamma detector (BEGe 5030-ULB, Canberra, Inc., USA) for 86,400 s at the Korea Basic Science Institute (KBSI). The detection limit of the equipment for ^{137}Cs was 1.3 Bq/kg, within two standard deviations (2δ).

4.2.1. ^{137}Cs activities in potential source materials and suspended sediments

Table 4 shows the statistics of ^{137}Cs distribution at the forest floor and channel bank. Probable source materials from the forest floor were sampled 10 times, and the values of ^{137}Cs concentration ranged between 2.6 and 40.6 Bq/kg, with a mean value of 13.5 Bq/kg. The standard deviation was 11.4, and the median value was 9.7 Bq/kg. The number of channel bank samples taken was 12, and the ^{137}Cs activity ranged from 0 to 6.9 Bq/kg. The mean value of channel-bank samples was smaller than that of forest-floor samples, and the median value approached zero. The standard deviation was relatively small.

Statistic	**Forest floor**	**Channel bank**
Sample size	10	12
Range	38	6.89
Mean	13.51	2.24
Std. deviation	11.392	2.682
Std. error	3.603	0.774

Table 4. Descriptive statistics of ^{137}Cs distribution on forest floor and channel bank.

The collection of suspended sediment samples and analysis of ^{137}Cs concentration revealed a very small or scarcely detectable amount of ^{137}Cs at all sampling points at each monitoring time (Table 5). It may be that extremely small amounts, near the detection limit of the gamma detector, existed in the samples. However, one exception was a trace amount of ^{137}Cs of about 2.1 Bq/kg detected in the reservoir sediment sample on 25 September at the S2 site.

Date	Sampler	Cs-137 (Bq/kg)
2012-08-21	S1	0
	S2	0
	S3	0
2012-09-25	S1	0
	S2	2.1
	S3	0
2012-10-24	S1	0
	S2	0
	S3	0
2012-11-21 and 2012-12-17 (composite sample)	S1	0
	S2	0
	S3	0

Table 5. ^{137}Cs distribution of suspended sediments.

4.2.2. Comparison of ^{137}Cs distribution in forest floor with ^{137}Cs in the channel bank

^{137}Cs concentrations on the forest floor were greater than those on the channel bank (Table 4), which seems consistent with earlier studies (Wallbrink et al., 1996; 1998) showing that ^{137}Cs concentrations decrease exponentially to half the surface activity at a depth between 30 and 50 mm and that there is little or no ^{137}Cs at

depths greater than 50 mm. Because ^{137}Cs release and distribution are fundamentally based on the radionuclide's penetrating quickly into soil. After fallout from atmospheric nuclear weapons testing or accidents, most of the radionuclide was absorbed in the uppermost part of the soil profile.

Riverbanks were less likely to be exposed at the earth's surface during the highest ^{137}Cs release around 1960, and the present geomorphic forms are products of continuous active erosion since that time; hence, ^{137}Cs concentrations on channel bank were expected to be comparatively low. However, in the case of the forest floor, ^{137}Cs of more than 30 Bq/kg remained in some relatively undisturbed soils, although ^{137}Cs redistribution has occurred due to surface erosion and transfer of the eroded materials. Exceptionally low concentrations of ^{137}Cs, similar to the ^{137}Cs concentrations on the channel bank, occurred on forest floor where severe erosion or disturbance had occurred.

To use the ^{137}Cs concentration on the forest floor and channel bank as a diagnostic property capable of distinguishing potential sources, it was necessary to confirm that the ^{137}Cs concentration of these two groups could be discriminated statistically. An independent-sample *t*-test was conducted to determine whether the two sets of ^{137}Cs values were significantly different from each other. According to Levene's test for equality of variances, this case was one in which equal variances were not assumed ($F = 6.31$, $p = 0.02 < \alpha = 0.05$). To overcome the violation of the assumption of homogeneity, the degrees of freedom were adjusted ($df = 9.83$), resulting in a statistically significant difference in ^{137}Cs concentrations between forest floor and channel bank according to the *t*-test ($t = 3.06$, $p = 0.01$ (2-tailed) < $\alpha = 0.05$).

4.2.3. Probability distribution of ^{137}Cs of the source materials

Based on the fact that source materials do not have constant ^{137}Cs values close to the average value but that a probability distribution exists, probability distribution functions, fit to the detected values of ^{137}Cs at the forest floor and channel bank, respectively, were derived instead of calculating mixing model by using average values of ^{137}Cs in source materials. This method was expected to address differences within a potential source group without assuming a normal distribution or single mean value and therefore to accurately estimate the contribution of each source material to the reservoir sediments. The best-fit probability distribution functions for the forest floor and channel bank were selected through three goodness-of-fit tests (Kolmogorov–Smirnov, Anderson–Darling, and chi-squared).

The four-parameter Burr distribution was most suitable for the probability density function fit to the detected values of ^{137}Cs at the forest floor. According to all three tests of distributional form, the values of ^{137}Cs at the forest floor followed the Burr distribution at a significance level of α = 0.01. The four-parameter Burr distribution function is as follows (Eq. 2), where k = 0.32932, α = 7.6121, β = 12.642, and γ = -6.3821.

$$f(x) = \frac{\alpha k \left(\frac{x-\gamma}{\beta}\right)^{\alpha-1}}{\beta\left(1+\left(\frac{x-\gamma}{\beta}\right)^{\alpha}\right)^{k+1}} \quad \text{(Eq. 2)}$$

In the case of the probability density function for the channel bank, the five-parameter Wakeby distribution defined by the quantile function was selected. At a significance level of α = 0.01, the data followed the Wakeby distribution well according to all three goodness-of-fit tests. The Wakeby distribution function, fit to

the detected values of ^{137}Cs at the channel bank, is as follows (Eq. 3), with parameter values of α = 3.0234, β = 0.00863, γ = 0, δ = 0, and ξ = -0.75674.

$$x(F) = \xi + \frac{\alpha}{\beta}\left(1 - (1 - F)^{\beta}\right) - \frac{\gamma}{\delta}\left(1 - (1 - F)^{-\delta}\right) \qquad \text{(Eq. 3)}$$

4.3. Contributions of forest floor and channel bank to suspended sediments

4.3.1. Simple mixing model and Monte Carlo simulation

Numerous studies estimating relative contributions based on ^{137}Cs concentrations of eroded sediments from surface erosion and those from subsurface erosion have been carried out (Wallbrink et al., 1996; Wallbrink et al., 1998; Nagle et al., 2007; Kim et al., 2013), and a typical mixing model can be described as follows (Wallbrink et al., 1996; 1998):

$$C_s = \frac{P_r - P_b}{P_s - P_b} \times 100 \quad \text{(Eq. 4)}$$

where C_s (in %) is the contribution from forest-floor surface sources, P_r is the ^{137}Cs value for reservoir sediment, P_s is the ^{137}Cs value for forest-floor soil that moves as a result of sheet or rill erosion, and P_b is the ^{137}Cs value for bank material, related to channel or gully erosion.

Significant progress has been made over the past decade in fingerprinting techniques that incorporate quantitative uncertainty analysis. If just one ^{137}Cs value for a source material was selected to calculate Eq. 4, the calculated contribution of each source material could be erroneous because the ^{137}Cs value of each source material is not constant but has a probability distribution. To handle the uncertainty in the mixing model and that from the use of a single property, ^{137}Cs, a Monte Carlo simulation was applied. This study found the relative contribution of forest floor (C_s) materials to reservoir sediment with the highest occurrence probability

through repeated random sampling of the ^{137}Cs values from each derived probability distribution function and calculated Eq. 4 with 100,000 iterations by applying the Monte Carlo simulation. All 100,000 possible outcomes for the predicted contribution of the forest floor were presented as a statistical distribution of values. The 50th percentile (Q2) for the distribution of predicted C_s values, as the median, constituted the highest occurrence probability, and the other quartiles, i.e., the 25th percentile (Q1) and the 75th percentile (Q3), were used to better understand the dispersion of the predicted values (Nagle et al., 2007).

4.3.2. Relative contributions to suspended sediments

The relative contributions of forest-floor and channel-bank materials to reservoir sediments were estimated (Table 6). The contributions of forest-floor surface materials to reservoir sediments were virtually zero for most of the observation period, which indicates that the dominant source of suspended sediments in the Yeongsan River is channel-bank materials that are eroded, stored, and remobilized within the channel. For the contribution on 25 September at site S2, there was an exceptional likelihood of a contribution from the forest floor to reservoir sediments, with a median value of 8.9 %.

Even though the dominance of bank materials is obvious, this result does not mean that channel erosion accelerated under the influence of riverbed dredging or construction of the river-crossing facility. The effect of human impacts on channel erosion remains unclear from the results of this study alone due to the absence of pre-interference data. Thus, a consideration of the (dis)connectivity between the hillslope and channel could be helpful for assessing this result and for further discussion.

Date	Sampler	Contribution of forest floor (%)			Contribution of bank materials (%)
		25^{th} low	50^{th} median	75^{th} high	50^{th} median
2012-08-21	S1	0.0	0.0	0.9	100.0
	S2	0.0	0.0	0.9	100.0
	S3	0.0	0.0	0.9	100.0
2012-09-25	S1	0.0	0.0	0.9	100.0
	S2	0.0	8.9	23.5	91.1
	S3	0.0	0.0	0.9	100.0
2012-10-24	S1	0.0	0.0	0.9	100.0
	S2	0.0	0.0	0.9	100.0
	S3	0.0	0.0	0.9	100.0
2012-11-21 and 2012-12-17 (composite sample)	S1	0.0	0.0	0.9	100.0
	S2	0.0	0.0	0.9	100.0
	S3	0.0	0.0	0.9	100.0

Table 6. Relative contributions of forest floor and channel bank to suspended sediments.

4.4. Discussion and summary

4.4.1. Hillslope–channel connectivity

This study indicated that the dominant source of suspended sediments in the Yeongsan River is channel-bank materials, and this result can be better understood by considering the (dis)connectivity between the hillslope and channel. Because numerous variables are involved in the sediment-delivery processes, ranging from transfer to temporary storage and remobilization of the eroded materials through the systems (Fryirs and Brierley, 2001), the contribution of materials originating from the hillslope to the values at downstream sampling sites could be slight for sediment load generated at individual slope sites. Various conditions, e.g., topography, soil, underlying rock, land use, and vegetation, can cause complex spatial and temporal patterns with regard to sediment connectivity (Fitzjohn et al., 1998; Ludwig et al., 1999; Bracken and Croke, 2007).

Sediment connectivity is defined as the physical linkage of sediment transport from an on-site location to another off-site location through a fluvial system (Hooke, 2003). And this construct has been addressed by the sediment delivery ratio in terms of the efficiency of material conveyance (Walling, 1983; de Vente et al., 2007). According to Harvey (2002), breaks in the continuity of sediment transmission may be influenced by two factors: the morphology of the valley and channel and the characteristics of sediment input and transmission from reach to reach. In other words, the presence and locations of geomorphic features that act as impediments to sediment movement, such as bars, alluvial fans, terraces, bedrock steps, and sediment slugs, and that provide space for sediment stores and sinks can be taken into account in terms of spatial lumping (Fryirs et al., 2007). Additionally,

seasonal or annual patterns of precipitation and runoff that control sediment availability can be considered in terms of temporal lumping (Walling, 1983).

In the case of this study area, such conveyance losses would be expected to occur due to various forms of impediment, e.g., hill-foot zones, alluvial fans, and dams, which can disrupt the movement of sediments and can trap sediments and eventually cause long-term or temporary storage. According to the study by Kim et al. (2013), conducted in a small mountainous catchment in Korea, subsurface material such as that from banks and forest roads made up about 96 % of the reservoir sediment, whereas forest floor material contributed less than 5 % of the total sediment for the whole study period. In this study area, after passing through the delivery processes, most of the materials from the forest floor might have difficulty connecting with the channel network. This is because a total of 664 agricultural dams designed for storing runoff water and providing for agriculture are distributed over the study area (WAMIS, 2013a) and act as barriers to sediment movement. In addition to the dam effect, embankments artificially constructed along the sides of streams to control the flow of running water and prevent floods largely prevent slope materials from flowing into the channel and consequently influence sediment connectivity (Callow and Smettem, 2009). On the other hand, channel bank materials can be eroded within the channel and delivered directly to the flowing water.

The exceptional result showing that forest-floor materials contributed 8.9 % (median) at site S2 between the first and second sampling (Table 6) can be interpreted as reflecting temporal discontinuity in sediment delivery. Period 2, from 21 August to 25 September, included many precipitation days, with rainfall amounts of about 90 mm recorded twice under the influence of typhoons that

occurred one after the other, and discharge fluctuated more than in any other period (Figure 14). Based on the 48-hour accumulated precipitation using the general extreme value (GEV) distribution selected from records of the last 61 years, the storm corresponds to a 3-year return period probability (Ministry of Construction and Transportation, 2000). Because slope erosion processes depend highly on rainfall energy related to rainfall intensity, rainfall amount, and rainfall duration (Cerdà, 1997; Jayawardena and Rezaur, 2000), it is expected that more slope materials were generated by active erosion during these storms than during other observation periods. Additionally, along with increasing discharge, forest roads play the role of conduits between hillslope and channel (Sidle et al., 2004; Mizugaki et al., 2008; Kim et al., 2013), and this condition may have improved sediment connectivity. Thus, an inflow of slope materials resulting from the higher conveyance efficiency could have resulted in the increased relative contribution of the forest floor to the river.

Another reason for the higher relative contribution from the forest floor to suspended sediment at site S2 could be the proximity of the Jiseokcheon basin. S2 is located between S1 (Seungchon weir) and S3 (Juksan weir) and beyond the joining with inflow from the Jiseokcheon basin. This basin has 422 km^2 of forest cover, corresponding to approximately 64 % of the subcatchment area, and is also the largest of the four subcatchments in the study area. It would be overreaching to conclude that the large proportion of sediment derived from forest topsoil is directly related to a high sediment yield from the forest floor; however, the high percentage of forest cover in the Jiseokcheon subcatchment and close proximity of this basin to site S2 might be reflected in the exceptional relative contribution. In a study by Owens et al. (2000), a relatively high contribution from channel banks

(about 40 %) arose from well-developed banks throughout the whole basin area and the ease of delivery of eroded materials. These researchers emphasized proximity to the sampling site and the channel network because a long travel distance from the source area results in increased opportunities for conveyance losses.

Furthermore, the slope samples of this study were restricted to comparatively undisturbed forest floor topsoil due to the use of the single diagnostic property (^{137}Cs). But surface soils from various patterns of land use, such as arable land (paddy, field), grassland, and bare ground, can reflect the characteristics of each source area. In the case of paddy land, which occupies about 20 % of this study basin, drastic erosion and transport would be difficult due to the very low slope angle, the cohesion of wetted fine particles (clay and silt), and the cropping system, which demands a ponded condition that hinders the movement of water and suspended sediment. In contrast, on field and bare ground, it is possible that large-scale erosion may occur and that gulleys may develop during storms (Jung et al., 2005; Kim et al., 2009; Kim, 2009). By observations, most of the fields in study basin are located in slope-toe zones or are surrounded by paddy lands (Figure 15); thus, connectivity to channel networks is poor. The sediment connectivity of bare ground is also expected to be low because grasslands form on the bare ground during the summer season when most of the precipitation occurs. Exceptions for bare ground include several construction sites, but engineered features (e.g., settling ponds) are usually installed downstream of construction sites to prevent eroded sediments from flowing out.

In short, the factors causing the dominant contribution from the channel bank may be summarized as follows. Aside from the on-site sediment yield, most of the

sediments generated from upstream hillslopes are temporarily stored and trapped in hill-foot zones or agricultural dams, whereas the channel bank materials have efficient delivery. These conveyance losses, combined with the effect of embankments that prevent additional inflow of slope materials, resulted in the dominance of in-channel suspended sediments (those that are eroded, stored, and remobilized within the channel) at the sampling sites. The possibility that contributions from the slope floor were underestimated due to the connectivity problem arising from the impediments to sediment movement cannot be excluded.

Figure 15. Typical paddy lands (left) and fields (right) in the study area.

Paddy lands which have the very low slope angle demand a water-ponded condition that hinders the movement of water and suspended sediment. And most of the fields are located in slope-toe zones or are surrounded by paddy lands.

4.4.2. Channel changes resulting from human interference

Changes to the channel in the natural state occur at various temporal and spatial scales by the processes of erosion, transportation, and deposition and by the response to running water (runoff), along with interactions with the slopes and vegetation around the river. However, when human-induced impacts, such as aggregate extraction (mining), levee building, river straightening, construction of channel-crossing facilities, land-use changes, and urbanization, are exerted directly and indirectly on the natural channel, the processes and trends of changes expected to occur in the natural state can accelerate or be altered in tendency (Wolman, 1967; Schumm, 1969; Park, 1977; Petts, 1979, 1984; Schumm et al., 1984; Williams and Wolman, 1984; Brookes, 1988; Simon, 1989; Rhoads, 1991). River adjustment to such changes varies depending on the magnitude and extent of the imposed disturbance (Simon, 1994).

The policy keynote of FRRP is proactive flood protection through dredging riverbeds, lowering the water level, and expanding flood-control capacity. In the interest of these objectives, 5.3 million m^3 in the section from Seungchon weir to Gwangjucheon and 11.3 million m^3 in the section from Juksan weir to Seungchon weir were dredged (The Four Major Rivers Restoration Project Headquarters, 2009). Such extensive dredging of deposited sediments in the main stream beds and the removal of the materials causes degradation, which implies a lower base level of erosion (Collins and Dunne, 1989; Rinaldi and Simon, 1998). According to Chang (1987), who simulated channel changes in response to aggregate mining in streambeds by applying a mathematical model at San Juan Creek, California, headward erosion, downstream scouring, and gravel pit deposition were induced by

aggregate mining. These adjustments of the stream may be interpreted as a system for recovering the missing sediments of the channel bed, accomplished by substantial channel incision upstream and an attempt to deposit eroded materials in the lowered riverbed. The recovery will be finished when the river establishes a new gradient fitted to the lowered base level and reaches equilibrium.

The large weirs constructed across the Yeongsan main river can affect both the upper and downstream areas of the channel by obstructing the flow of water and trapping sediments. Upstream of the weir, because the river-crossing facility reduces flow velocity, transported materials are deposited where the river enters the slack water of the reservoir, resulting in aggradation of the riverbed. Under the continuous inflow of sediments from upstream to the reservoir, maintaining the water level and safe management of the weir are possible only through constant dredging. Downstream of the weir, degradation of the riverbed occurs due to sediment-budget imbalances resulting from the sediment-poor condition, which means that more sediment flows downstream than is delivered to the region from the upper channel (Committee on Missouri River Recovery and Associated Sediment Management Issues, 2011).

This study identified that peak discharges at the Bondong station located near the Seungchon weir were conspicuously lower than those at the Hoejin station, which is relatively less affected by the weir's control (Figure 14). The reduction of peak flood discharge has been documented as a major downstream effect resulting from the construction of a large dam and reservoir (Williams and Wolman, 1984; Friedman et al., 1998; Committee on Missouri River Recovery and Associated Sediment Management Issues, 2011). Dredging a riverbed and constructing river-crossing facilities also commonly affect the channel in many ways, e.g.,

downstream channel erosion may be accelerated. However, although the results indicated that the dominant source of reservoir sediment is the channel bank and implied the prominence of in-channel suspended sediments from channel erosion, it is impossible to determine the degree to which the human impacts influenced channel erosion due to the lack of pre-construction data.

4.4.3. Uncertainty and limitations of the methodology for using ^{137}Cs

The evaluation of soil erosion using the ^{137}Cs method fundamentally postulates that atmospheric fallout and transfer of radionuclides to the soil are spatially uniform. Because conservative radionuclide concentrations maintain the amount of the element present after fallout and quickly infiltrate the soil, the penetration profile of ^{137}Cs at the earth's surface shows a spatially uniform distribution. Under these assumptions, measured inventories of reference sites and other sites are compared, and ^{137}Cs values are converted into soil-erosion rates using a conversion model. However, Parsons and Foster (2011) suggested that the assumptions include a fatal flaw, namely the problem of spatial uniformity of ^{137}Cs fallout, and insisted that diversely distributed ^{137}Cs on surface soil cannot provide reliable information about soil erosion.

Fingerprinting approaches, nonetheless, can be unrestricted by the uniformity problem by recognizing differences in ^{137}Cs inventories of soil samples and by using these differences for classification of potential source materials, as documented by Kim et al. (2013). Furthermore, by applying derived probability distribution functions fitted to the detected values of ^{137}Cs at the forest floor and channel bank, as done in this study, it is possible to address the differences within a

potential source group without assuming a normal distribution or single mean value. Whereas the method of calculating using average values of ^{137}Cs in source materials could introduce errors by ignoring the probability that the values of ^{137}Cs inventories within the source group are not equal and may distribute far from the average. This study found the relative contribution of each source material to reservoir sediment with the highest occurrence probability by randomly extracting values of ^{137}Cs from each derived probability distribution function and calculating with numerous iterations by applying a Monte Carlo simulation.

However, the limitation remains that identifying the spatial distribution of the main sediment sources and distinguishing all potential sources from various geological zones and land uses is not possible due to the unreliability of using a single diagnostic property. To solve these problems, the use of composite fingerprinting that incorporates several geochemical properties and mineral magnetic properties will facilitate robust evaluation of the source contributions spatially and quantitatively. This study, which promptly investigated the provenance of the suspended sediments by differentiating and evaluating source types using ^{137}Cs as a tracer, provided a practical approach useful for determining the contributions to reservoir sediment. Also, despite its limitations, this study's result indicating the dominance of channel bank materials is expected to play a role in effective reservoir management with respect to controlling sediment influx.

4.4.4. Summary

To evaluate quantitatively the relative contributions of slope-floor and channel-bank materials to suspended sediment in the Yeongsan River, three time-integrated

suspended-sediment samplers were installed in July 2012 on the upper and middle Yeongsan River (sites S1, S2, and S3), where river flow is almost stagnant after entering the slack water of reservoirs. Reservoir sediment samples from three samplers were obtained at monthly intervals until December 2012 from three samplers, and potential sources of the reservoir sediment were sampled using a soil scraper in the forest floor and channel bank. The radioactivity of ^{137}Cs of the reservoir sediment and possible source materials were measured using gamma detectors. And the relative contributions of forest-floor and bank material were calculated by a simple mixing model and a Monte Carlo simulation based on derived probability distribution functions fit to the detected values of ^{137}Cs at the forest floor and channel bank, respectively.

The results of this study, achieved through the use of numerous iterations, indicated that the dominant source of suspended sediments in the Yeongsan River is channel-bank materials. Previous studies noted that dredging a riverbed and constructing river-crossing facilities commonly affect the river by accelerating channel erosion, but it remains unclear how much the human impacts are influencing channel erosion from this result only because of the absence of pre-interference data on the contributions of forest floor and bank material to reservoir sediment. Further studies using composite fingerprints incorporating several geochemical properties and mineral magnetic properties will facilitate robust evaluation of the source contributions spatially and quantitatively. This study, which quickly investigated the provenance of the suspended sediments by differentiating and evaluating source types using ^{137}Cs as a tracer, has practical significance for effectively managing the reservoir with respect to the control of sediment influx, despite several limitations.

5. Suspended sediment source tracing of the Juksan weir in the Yeongsan River using composite fingerprints

5.1. Research scope

Reservoir sediments of the Juksan weir were obtained from July 2012 to December 2012 at monthly intervals. Especially first (21 Aug 2012) and second (25 Sep 2012) sediment samples reflect the periods of high flow as a result of heavy rainfall events and the typhoons occurring one after another. Because the sediments trapped in November and December 2012 were insufficient for following analysis, composite sample was made to measure the geochemical, physical, and magnetic properties, and activity of radioactive isotopes.

To compare the trapped reservoir sediments with potential sediment sources, surface materials were taken from the cropland topsoils (*n*=15), forest floor topsoils (*n*=15), and channel banks (*n*=17) between August to November 2012 (Table 7).

	crop land	**forest**	**channel banks**	**urban**	**grass land**	**wetland**	**bare ground**	**total**
Area (km^2)	791	1225	60	189	47	22	29	2363
Area (%)	33.5	51.8	2.5	8.0	2.0	0.9	1.2	100.0
Number of samples	15	15	17	-	-	-	-	47

Table 7. Land cover information of the study area (WAMIS, 2006) and the number of source samples for each land cover type.

In total, 47 possible sources of the reservoir sediment were sampled using a soil scraper (0-2 cm depth), considering the spatial distributions for each land use and for each Yeongsan River sub-catchment. Detailed information for each sampling point is listed in Table 8. Channel bank materials were taken from lower part of the riverbank on undercut slope which is more likely to be eroded by flowing rivers. Forest floor topsoil samples were composed of various tree species (coniferous, decideous, and mixed stand forest) and canopy conditions.

Source type	No.	Location	Subcatchment	Underlying rock	Slope angle
Cropland topsoil	C1	N35 03.290 E126 54.635	Jiseokcheon	volcanic	flat
	C2	N34 59.339 E126 59.875	Jiseokcheon	volcanic	″
	C3	N34 51.360 E126 46.185	Middle Yeongsan Riv.	gneiss	″
	C4	N34 56.475 E126 55.986	Jiseokcheon	volcanic	″
	C5	N35 01.787 E126 41.153	Middle Yeongsan Riv.	volcanic	″
	C6	N34 52.497 E127 02.706	Jiseokcheon	gneiss	″
	C7	N35 27.423 E126 47.375	Hwangnyong Riv.	granite	″
	C8	N35 08.326 E126 40.565	Middle Yeongsan Riv.	sedimentary	″
	C9	N35 07.944 E126 57.577	Upper Yeongsan Riv.	volcanic	8°
	C10	N35 03.340 E126 54.642	Jiseokcheon	volcanic	6°
	C11	N35 03.249 E127 01.090	Jiseokcheon	volcanic	0°
	C12	N34 59.344 E126 59.879	Jiseokcheon	volcanic	2°
	C13	N35 22.708 E126 55.693	Hwangnyong Riv.	sedimentary	3°
	C14	N35 01.769 E126 41.137	Middle Yeongsan Riv.	volcanic	0°
	C15	N34 53.165 E126 51.053	Jiseokcheon	volcanic	1°
Forest floor topsoil	F1	N35 12.201 E126 58.922	Upper Yeongsan Riv.	granite	46°
	F2	N35 07.904 E126 57.703	Upper Yeongsan Riv.	volcanic	40°
	F3	N35 17.666 E126 38.226	Hwangnyong Riv.	granite	30°
	F4	N35 17.839 E126 52.649	Upper Yeongsan Riv.	gneiss	12°

Table 8. Detailed information for each sampling point.

Source type	No.	Location	Subcatchment	Underlying rock	Slope angle
Forest floor topsoil	F5	N35 27.422 E126 47.066	Hwangnyong Riv.	granite	32°
	F6	N35 22.685 E126 55.709	Hwangnyong Riv.	sedimentary	23°
	F7	N35 15.885 E127 04.995	Upper Yeongsan Riv.	gneiss	0°
	F8	N35 25.172 E127 00.773	Upper Yeongsan Riv.	sedimentary	38°
	F9	N35 01.760 E126 37.876	Middle Yeongsan Riv.	granite	2°
	F10	N35 05.832 E126 57.859	Upper Yeongsan Riv.	volcanic	48°
	F11	N35 03.296 E127 01.083	Jiseokcheon	volcanic	29°
	F12	N35 15.616 E126 46.930	Upper Yeongsan Riv.	gneiss	10°
	F13	N35 01.755 E126 41.115	Middle Yeongsan Riv.	volcanic	24°
	F14	N34 53.094 E126 51.067	Jiseokcheon	volcanic	32°
	F15	N35 08.309 E126 40.623	Middle Yeongsan Riv.	sedimentary	6°
Channel bank	B1	N35 27.491 E126 50.417	Hwangnyong Riv.	alluvium	58°
	B2	N35 23.741 E126 45.616	Hwangnyong Riv.	alluvium	76°
	B3	N35 10.165 E126 41.040	Hwangnyong Riv.	alluvium	54°
	B4	N35 17.670 E126 38.224	Hwangnyong Riv.	alluvium	58°
	B5	N35 13.409 E126 44.150	Hwangnyong Riv.	alluvium	80°
	B6	N35 13.888 E127 03.025	Upper Yeongsan Riv.	alluvium	44°
	B7	N35 11.177 E126 57.377	Upper Yeongsan Riv.	alluvium	38°
	B8	N35 05.615 E126 48.182	Middle Yeongsan Riv.	alluvium	32°
	B9	N35 14.737 E126 53.336	Upper Yeongsan Riv.	alluvium	86°
	B10	N35 19.513 E126 59.793	Upper Yeongsan Riv.	alluvium	34°
	B11	N35 01.017 E126 38.186	Middle Yeongsan Riv.	alluvium	50°
	B12	N35 19.383 E126 44.428	Hwangnyong Riv.	alluvium	84°
	B13	N35 10.184 E126 50.003	Upper Yeongsan Riv.	alluvium	25°
	B14	N34 50.974 E126 46.241	Middle Yeongsan Riv.	alluvium	88°
	B15	N34 59.011 E126 38.805	Middle Yeongsan Riv.	alluvium	74°
	B16	N35 07.039 E126 41.342	Middle Yeongsan Riv.	alluvium	65°
	B17	N34 52.564 E127 02.774	Jiseokcheon	alluvium	85°

Table 8. *(continued)* Detailed information for each sampling point.

5.2. Data analysis

5.2.1. End-member selection

Before proceeding the sediment source apportionment, appropriate end-members were considered to determine the number of contributing potential end-members and whether they are discrete source or not. Grassland and wetland were excluded from analysis since their limited distribution (about 1 % of the total catchment area, respectively, Table 7) and the low probability that erosion will occur. Using land as pasture which has vegetation cover with weeds or forage species for livestock grazing occurs very seldom in study area. Generally stockbreeding takes place in the cramped barns, and the lands covered with grass and weeds and left fallow were not observed in the field. In addition, signatures of land cover such as fibrous root system which is good for holding the soil in place and for recharging water or ponded condition of wetlands are well known as aids in reducing surface runoff and soil detachment (Dao, 1993; Gyssels and Poesen, 2003).

Though paddy plain requires the water-ponded conditions for rice growing, whereas field does not, combining paddy plain and field into one source type (land use) was determined by following reasons; most of the fields in study area are surrounded by paddy plains (Lim et al., 2014), characterized by field-paddy sequences across the slope toe zone to the floodplain. During sediment-delivery processes, mixing with each other materials was expected, and consequentially, it appears there's no statistically significant difference between the average fingerprint properties of paddy and field. Meanwhile, rice paddy agricultural practices in study area can affect the runoff characteristics; growing season of rice which is indicating hydrologically active period ranges from May to September (or

to early October). After harvest, most of the paddy plains have been drained and left fallow, and it increases the likelihood of erosion for the winter and spring, but very low slope angle makes paddy plain contribute less to reservoir sediments. As going downstream, location, distribution, and slope condition of the paddy and field are clearly categorized, therefore, it is necessary to evaluate at sub-catchment scales and a large sample size.

The forest floor topsoils and channel banks are determined as appropriate end-members, which are representative of surface soil receiving a little human interference and subsurface material, respectively. They have distinctive properties, which are statistically distinguished from other source groups. Fingerprinting property values of the bare ground showed mixed signatures with three end-members, cropland, forest floor, and channel bank materials. In the field, most of the bare ground is usually used as farm roads to carry agricultural machines and vehicles. It is not only the kind of episodic stream, but also extension of forestry or agricultural land use. Farm roads would have contributed a considerable amount of sediment by rill and sheet flows in very heavy rainfall events (Kim et al., 2013), however, the bare ground was excluded from end-members due to their indistinct properties which wasn't statistically distinguished with limited samples. As a result, cropland topsoils (combined source of paddy plain and field), forest floor topsoils, and channel banks were selected as end-members of the Juksan weir sediments.

5.2.2. Sediment source discrimination

First of all, examination of conservative behavior during erosion and transport was carried out to determine whether the property values of the reservoir sediments fall within the observed range of sediment source samples' property values. Tracer properties falling outside the range in source values were excluded from either subsequent statistical analysis or the mixing modeling.

A two-stage statistical procedure including the non-parametric Kruskal–Wallis H-test and multivariate discriminant function analysis (DFA) was used to identify the optimum combination of fingerprint properties, as proposed by Collins et al. (1997b) and Collins and Walling (2002). This approach have been employed in sediment source tracing by many researchers (Collins et al., 1997a; Collins and Walling, 2007; Walling et al., 2008a; Collins et al., 2010a; Collins et al., 2010c; Mukundan et al., 2010; Collins et al., 2012a; Collins et al., 2012b; Haddadchi et al., 2014; Nosrati et al., 2014; Palazón et al., 2014; Lamba et al., 2015; Lin et al., 2015)

In first stage, the Kruskal–Wallis H-test (hereafter designated simply as KW H-test) was applied to screen the individual fingerprint properties that do not exhibit a statistically significant difference between at least two source groups. To decide whether the population distributions of source groups are identical, non-parametric KW H-test was conducted without assuming them to follow the normal distribution. If the *p*-value is less than 0.05, the null hypothesis (H_0; tracer property populations of source groups have the same median, and hence they are identical populations) is rejected by comparing the medians of the three groups of populations. The statistic for the KW H-test are presented in Table 9, and a total of 16 individual properties that marked with asterisks (*) passed the KW H-test, and included in the second process.

Property	H-value	*p*-value
Ta	3.184	0.203
W	5.618	0.060
Mo	1.765	0.414
Zr	19.437	0.000 *
La	9.060	0.011 *
Sc	13.255	0.001 *
Y	16.645	0.000 *
Co	26.752	0.000 *
Cr	17.757	0.000 *
Li	6.058	0.048 *
Ni	14.698	0.001 *
Pb	9.046	0.011 *
Rb	11.514	0.003 *
Sr	10.267	0.006 *
V	24.107	0.000 *
Zn	10.211	0.006 *
MS	3.499	0.174
^{137}Cs	27.682	0.000 *
^{210}Pb	27.776	0.000 *
^{210}Pbex	30.282	0.000 *
^{226}Ra	5.678	0.058

Table 9. Result of applying the Kruskal-Wallis H-test to the fingerprint property.

Non-conservative Nb, Sn, Ba, and Cu were not included in further statistical analysis.

* means statistically significant at p-value < 0.05, critical H-value is 5.92 at α=0.05.

In second step, multivariate discriminant function analysis based on minimizing Wilks' Lambda as a step-wise selection algorithm was carried out to maximally separate the source groups, and to select optimum composite properties. A lambda of 1 occurs when all group means are same, whereas values close to zero indicate

that there is more variation between groups than within the group. At each step, the variable that minimizes the overall Wilks' lambda is entered. A variable is entered into the discriminant equation if its probability of *F* statistic is less than the entry criterion (0.05), and is removed if the significance level is greater than the removal criterion (0.10). Table 10 provides the final result of applying DFA to construct the optimum composite fingerprints for discriminating individual sediment source types.

Step	Fingerprint Property	Wilks' lambda	Cumulative % source type samples classified correctly	% source type samples classified correctly	Tracer discriminatory weighting
1	$^{210}Pb_{ex}$	0.363	76.6	76.6	2.12
2	Zr	0.215	78.7	55.3	1.53
3	V	0.151	89.4	42.6	1.18
4	Pb	0.126	91.5	42.6	1.18
5	Co	0.107	95.7	36.2	1.00

Table 10. Result of the stepwise discriminant function analysis for identifying the optimum composite fingerprints

5.2.3. Sediment source apportionment

The relative contributions of the each potential sediment sources to the reservoir sediments were estimated using multivariate mixing model based on the Collins et al. (2010a, 2010c). The formula $f(E)$ to minimize the sum of the squares of the relative errors between selected tracer concentrations in reservoir sediment sample and the mean tracer concentrations for each sources multiplied by the optimized estimates of relative contributions from the potential sources is as follow:

$$f(E) = \sum_{i=1}^{n} \left\{ \left(C_i - \left(\sum_{s=1}^{m} P_s S_{si} SV_{si} \right) \right) / C_i \right\}^2 W_i \qquad \text{(Eq. 5)}$$

where C_i is the concentration of tracer property (i) in time-integrated reservoir sediment sample; P_s is the optimized contribution from source group (s); S_{si} is the mean concentration of tracer property (i) in source group (s); SV_{si} is weighting representing the within-source variation of tracer property (i); W_i is the tracer discriminatory weighting factor; n is the number of tracer properties comprising the optimum composite set; and m is the number of sediment source groups.

The optimized estimates of relative contributions, P_s, from the each potential source in the mixing model (Eq. 5) must satisfy the following two constraints. To apportion sediment sources, the relative contributions from the each potential source must be between 0 and 1 (Eq. 6), and these contributions sum to unity (Eq. 7):

$$0 \leq P_s \leq 1 \qquad \text{(Eq. 6)}$$

$$\sum_{s=1}^{n} P_s = 1 \qquad \text{(Eq. 7)}$$

The within-source variation weighting, SV_{si}, was included in the numerical mixing model to ensure that the tracer property values with smaller variability in the particular source group exert the greater influence on the optimized solutions. The weighting was calculated using the inverse of the coefficient of variation, equals the standard deviation divided by the mean (Collins et al., 2012a). The tracer discriminatory weighting factor, W_i, was also incorporated to ensure the relative discriminatory efficiency of each individual tracer properties selected by the stepwise DFA (Table 10). This factor was calculated by assigning a weighting of 1.0 to the property that provide the lowest discrimination, based on the percentage of samples that were correctly classified. The weightings for the remainder properties were calculated using the ratio of their discriminatory power to that of the weakest property in optimum composite fingerprints (modified mixing model after Collins et al., 2010c).

5.3. Results and discussion

5.3.1. Discriminating sediment source groups

The fingerprinting properties that passed the initial screening, the Kruskal-Wallis H-test with a critical H-value of 5.92 at a 0.05 significance level, are presented in Table 9. Four properties including Nb, Sn, Ba, and Cu that failed the mass conservation test were excluded from further statistical analysis. Five individual properties, Ta, W, Mo, MS (magnetic susceptibility), and ^{226}Ra, failed the KW H-test. And a total of 16 individual properties that marked with asterisks (*) exhibit a statistically significant difference between source groups with a *p*-value less than 0.05. Most of the tracer properties, such as Zr, Sc, Y, Co, Cr, Ni, Rb, V, ^{137}Cs, ^{210}Pb, $^{210}Pb_{ex}$, showed the *p*-values close to zero.

In second stage, the optimum composite fingerprints capable of classifying 95.7 percent of source type samples correctly are selected by the stepwise DFA (Table 10). Final fingerprints are composed of different characteristics of the properties including one fallout radionuclide ($^{210}Pb_{ex}$) and four trace elements (Zr, V, Pb, and Co). It has been commonly accepted that multiple fingerprint properties based on the wide range of subset, such as geochemistry, radionuclides, or magnetic signatures probably provide better discrimination, owing to tracer properties with differing environmental behavior (Walling et al., 1993; Walling and Woodward, 1995; Foster, 2000).

5.3.2. Contributions of potential source materials to reservoir sediments

The numerical mixing model was applied to the reservoir sediments obtained from July to December 2012 at monthly intervals. Since two samples collected in November and December were insufficient for following analysis, tracer property values of this composite sample were used for numerical mixing model. Figure 16 shows the estimated relative contributions of channel banks, forest topsoils, and cropland topsoils to reservoir sediments. According to the results, channel banks are the dominant source of the reservoir sediment during the entire monitoring period. Contribution from channel banks reached 100 percent especially in the second sample (21 Aug to 25 Sep), with the remainder ranging from 90.4 to 96.8 %. Conversely, relative contributions from forest topsoils varied with seasons; 0 % under high river flows, 9.6 % in winter. In the reservoir sediments collected in November and December, relative contribution from forest topsoils shows marked increase from 2.4 % (third sample) to 9.6 %.

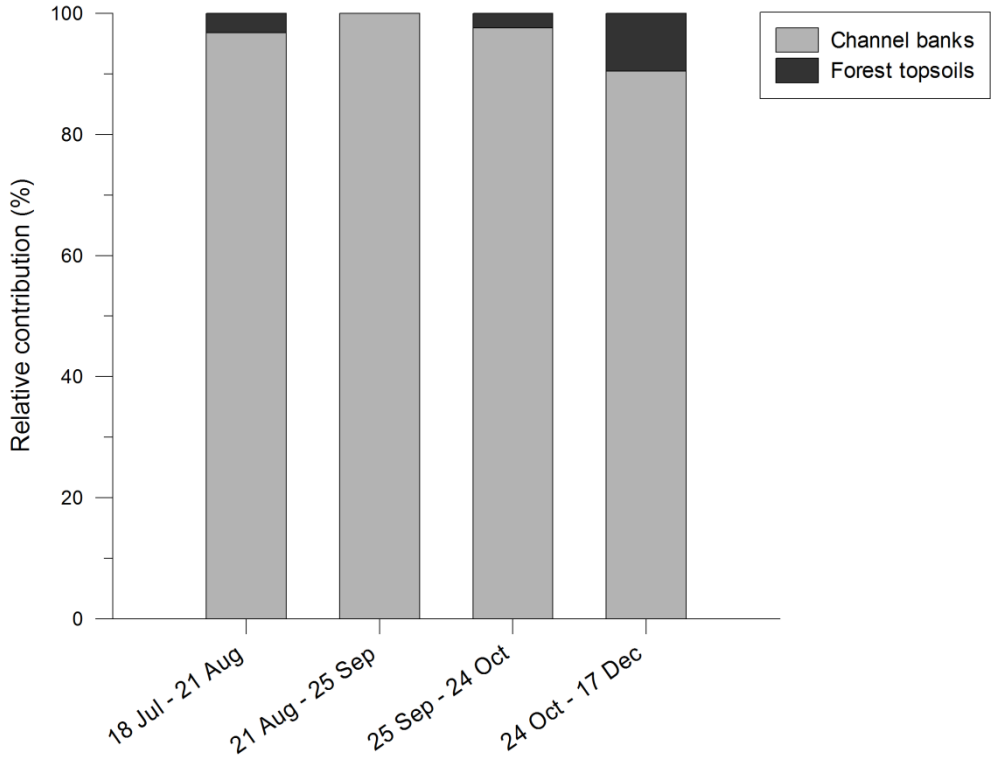

Figure 16. Relative contributions of channel banks and forest topsoils to reservoir sediments

Contributions from each source to its sedimentation rate (kg m^{-2}) were calculated (Figure 17). It should be noted that two figures have very different orders of magnitude (Figure 17a and 17b), and there is remarkable high sedimentation rate during the period from 21 August to 25 September. Estimated range of contribution from channel banks is two orders of magnitude greater than that of contribution from forest topsoils; contribution from channel banks ranged from 2.31 to 141.98 kg m^{-2}, whereas contribution from forest materials ranged from 0 to 0.28 kg m^{-2}. Contribution quantity of forest floor materials during first period is highest, while the lowest contribution to the reservoir sediments appeared in second period. Comparing the third sediment (25 Sep-24 Oct) with the fourth (24 Oct-17 Dec), there is a slight increase in the contribution from forest topsoils, from 0.08 to 0.25 kg m^{-2}.

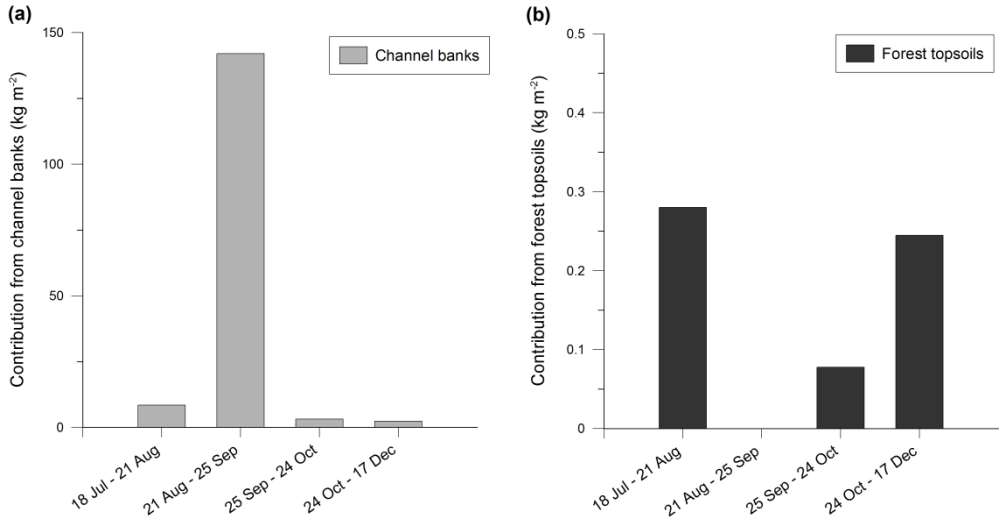

Figure 17. Contributions of each source to its sedimentation rate (kg m^{-2}), (a) from channel banks, and (b) from forest topsoils.

Cropland contributed 0 % of the reservoir sediments, in spite of wide distributions with 33.5 % of the catchment area along the river. In middle course of the Yeongsan river, riparian areas are generally used as agricultural land, especially rice cultivation on the floodplain (Figure 4). Despite its proximity to the river, significant soil erosion and transport would be difficult since agricultural practice requires a water-ponded condition during crop growth season. Even in the bare soil period after harvesting, its very gentle or flat slope and ridges surrounding rice paddy may make it hard for detached materials to contribute to the riverine suspended sediments. While the non-cultivation period, fine materials in ploughed paddy plain (clay and silt) are present as aggregates based on the cohesion of wetted fine particles. Though there occurs soil detachment, aggregates are more likely to be deposited at a short distance.

Limited contributions of catchment slope materials to the reservoir sediment are attributed to the poor connectivity with the channel networks. Several factors

causing conveyance losses, which consequentially influence the sediment connectivity, such as a lot of agricultural dams, check-dams, and embankment were fully discussed in chapter 4.4.1.

5.3.3. Seasonal variations in the contribution of source materials to reservoir sediment

The maximum relative contribution from forest floor materials was obtained in the sample collected in November and December (9.6 %, 24 October to 17 December). It is well-established that capacity to erode and transport sediment is proportional to rainfall intensity and stream power. Contribution of channel banks to 100 % reservoir sediments can be explained by the high flows based on the heavy rainfall and increased discharge in summer season (Figure 16). However in winter, there were no significant precipitation events capable of detaching and transporting slope surface materials, except for 27 October with 29.5mm of daily precipitation. Even in November and December, rainfall that exceeds 1 mm of 60-minute maximum precipitation was totally absent (Korea Meteorological Administration, 2012). It indicates that other variables that cause loosening of slope materials or reduce forces holding the materials in place would be involved in the higher relative contribution from forest topsoils in this period.

There have been many researches that address freeze–thaw effects on soil erosion (Edwards and Burney, 1989; Bajracharya and Lal, 1992; Wang et al., 2009), since soil fluffing from freeze-thaw actions enables soil particles to be detached even by low raindrop impacts (RUSLE; Renard et al., 1997). The studies referenced above found that loosen materials which had experienced repeated freeze–thaw cycles showed higher erodibility during spring. These surface

materials susceptible to (re)mobilization may lead to temporal variations in relative contribution from the each source (Gellis and Noe, 2013; Kim et al., 2013).

During last sampling period (24 Oct to 17 Dec), the number of days on which daily minimum temperature falls below zero was 14 days based on the measurement at the Gwangju weather station (Korea Meteorological Administration, 2012). It can be expected that freeze–thaw process could influence the surface materials on forest floor at its upstream catchment of high altitudes. Increase of relative contribution from forest topsoils in winter was attributed to the freeze-thaw activity and increased soil erodibility (Wall et al., 1988).

5.3.4. Uncertainties and limitations associated with the mixing model

Uncertainty associated with the use of mean (or median) fingerprinting property concentrations of the source and reservoir samples in the mixing model can be evaluated with a Monte Carlo simulation, as applied in chapter 4.

In previous studies, a particle size correction factor and an organic matter content correction factor have been incorporated into the multivariate mixing model (Collins et al., 1997b; Collins et al., 2010b; Collins et al., 2012a), based on their influence upon elemental concentrations in source materials and sediments (Horowitz and Elrick, 1987; Horowitz, 1991). A number of studies have found that high concentrations of major and trace elements are associated with fine-grained sediments owing to their high specific surface area (Horowitz, 1985; Rubio et al., 2000; Bouchez et al., 2011). As to the fallout radionuclides, it has been demonstrated that differences in the particle size could explain the selective adsorption of the radionuclides by the finer fraction of surface mineral soils (He

and Walling, 1996). Also considering selective erosion and transport of the fine sediments, difference in grain size distribution between the reservoir sediment and the source material was taken into account for direct comparison of the mean concentrations in reservoir sediment with those in source materials. The particle size correction factor was usually calculated as the ratio of the mean specific surface area (m^2 g^{-1}) of the reservoir samples to the corresponding mean specific surface area for each source group (e.g. Collins et al., 1998; Smith et al., 2011; Stone et al., 2014). The organic matter content correction factor was also calculated in a similar way using LOI (loss on ignition, wt. %) ratios of sediment to source.

However, Koiter et al. (2013) and Smith and Blake (2014) found that correcting tracer property values for differences in organic matter between the sediment and the source material can cause spurious source apportionments. They strongly suggested that commonly accepted positive relationships between SSA or organic matter content and geochemistry concentrations cannot be generalized to all tracer properties, and involve over-correction risk (Walling et al., 1999).

For this reason, relation between SSA (specific surface area) and organic matter content (LOI) of each source group and the reservoir sediment was examined to determine whether there are significant differences between those of sources and of the reservoir sediments (Figure 18). Even though sample size of the reservoir sediment is very small, it can be identified that SSA or LOI of the reservoir sediment varied with season or dominant contributor, and conspicuous enrichment of SSA or LOI is not found in the reservoir sediment. As pointed out by Smith and Blake (2014), corrections simply based on the SSA or LOI ratios of sediment to source can totally alter or even nullify the inherent differences of tracer property values between source groups.

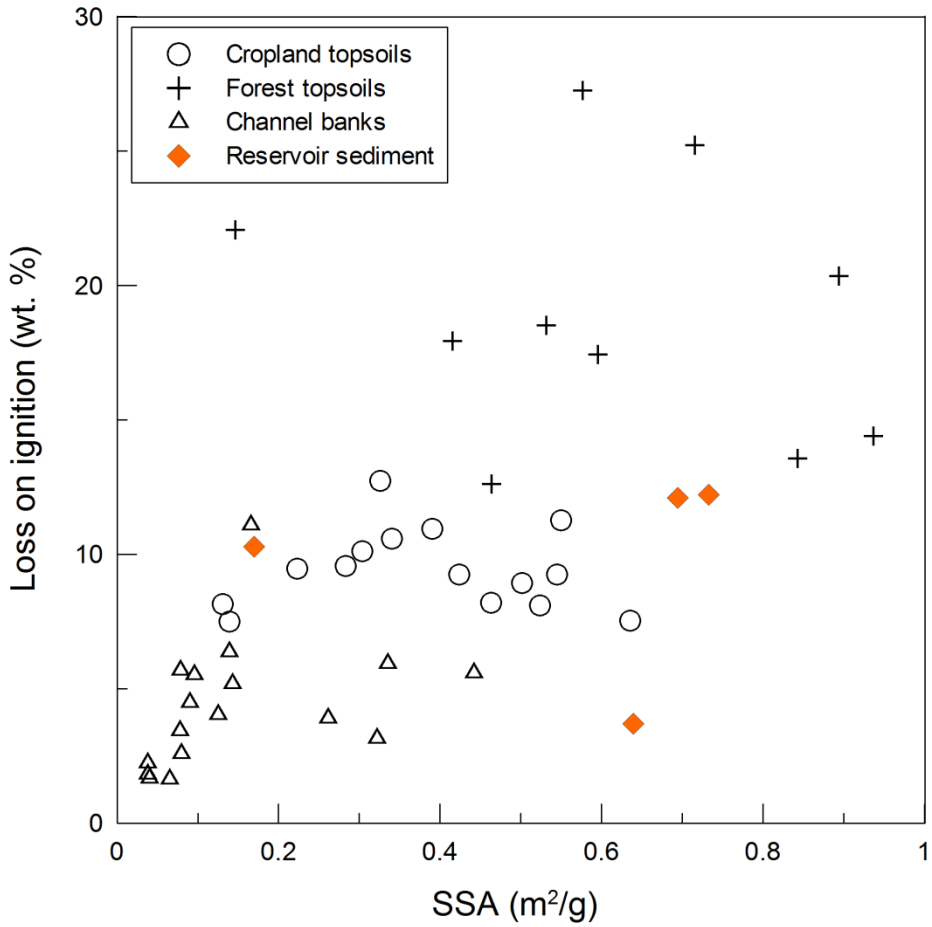

Figure 18. Scatter plot showing relation between SSA (specific surface area, in $m^2 g^{-1}$) and organic matter content (LOI, in wt. %) of each source group and the reservoir sediment

Dependence of element concentrations on SSA or LOI was also investigated using Pearson correlation analysis. Table 11 shows the Pearson's correlation coefficients (*r*) at the 0.05 and 0.01 significance level between element concentrations and specific surface area (SSA) or organic matter content (LOI), respectively. No significant correlations were noted between SSA and concentrations of the trace properties used for discriminating, except for one tracer (Zr) from channel banks group. Correlation coefficients varied from -0.445 to

0.620, and it implies that clear positive relationship between SSA and element concentrations might not exist. In case of correlation with LOI (Table 11b), most of the trace properties exhibited low correlation coefficients ranging from -0.551 to 0.657. Though some tracer properties of channel banks group such as $^{210}Pb_{ex}$ and Zr did show significant positive trends, there is no consistent significant correlation between LOI and element concentration for three source groups. Hence, this study did not take into account the particle size correction and the organic matter content correction.

Recent studies on the inappropriate corrections by Koiter et al. (2013), Smith and Blake (2014), and Pulley et al. (2015) have suggested that applying uniform correction factor to all tracer properties causes unquantified errors that probably exceed errors from the uncorrected data. However, to identify particle size or organic matter effects on tracer concentrations, measuring element concentration for subsamples of each size fraction or mineral fraction apart from organic fraction is time-consuming and very expensive. Therefore, careful application such as using tracer-specific correction factors based on the clear relationship between SSA or LOI and element concentrations combined with uncertainty analysis is needed.

(a) Correlation coefficients between SSA and element concentrations

	Cropland		Forest		Channel banks	
	Pearson's *r*	*p*-value	Pearson's *r*	*p*-value	Pearson's *r*	*p*-value
$^{210}Pb_{ex}$	-0.445	0.10	-0.189	0.50	0.082	0.75
Zr	0.312	0.26	0.262	0.35	0.620 **	0.01
V	-0.212	0.45	0.177	0.53	0.258	0.32
Pb	-0.031	0.91	0.103	0.72	0.210	0.42
Co	-0.223	0.42	-0.068	0.81	0.395	0.12

(b) Correlation coefficients between LOI and element concentrations

	Cropland		Forest		Channel banks	
	Pearson's *r*	*p*-value	Pearson's *r*	*p*-value	Pearson's *r*	*p*-value
$^{210}Pb_{ex}$	0.231	0.41	0.657 **	0.01	0.511 *	0.04
Zr	-0.112	0.69	-0.551 *	0.03	0.655 **	0.00
V	-0.106	0.71	-0.341	0.21	0.378	0.13
Pb	0.051	0.86	0.188	0.50	0.628 **	0.01
Co	-0.110	0.70	-0.253	0.36	0.432	0.08

Table 11. Pearson's *r* correlation coefficients (a) between specific surface area (SSA) and tracer property concentrations used for discriminating of each source group (b) between organic matter content (Loss On Ignition) and tracer property concentrations.

* means that data is significant at 0.05 significance level

** means that data is significant at 0.01 significance level

Based on the monitoring of the reservoir sediments at monthly intervals, sediment source fingerprinting was conducted in order to identify dominant sediment source and its seasonal variations. By applying the Kruskal–Wallis H-test and stepwise discriminant function analysis (DFA), final fingerprints were composed of different characteristics of the properties including $^{210}Pb_{ex}$, Zr, V, Pb, and Co. According to the mixing model result, channel bank materials were the dominant source of reservoir sediment during the entire monitoring period. In winter, there was a slight increase in the contribution from forest topsoils, which can be influenced by the freeze-thaw actions. Examination whether incorporation of the particle size and organic matter content correction factor into the mixing model are appropriate exhibited that there is no consistent significant correlation between element concentration and specific surface area (SSA) or organic matter content (LOI). Careful application of tracer-specific correction factors combined with uncertainty analysis is needed to better estimate source apportionment.

6. Conclusions

Three time-integrated suspended-sediment samplers were installed in July 2012 on the upper and middle Yeongsan River, where river flow is almost stagnant after entering the slack water of reservoirs. Reservoir suspended sediment samples were obtained at monthly intervals until October 2014. Based on field monitoring, geochemical elements, magnetic properties, physical properties including particle size and radioactivity of collected suspended sediments were analyzed.

Seasonal trends of suspended sedimentation rates and particle size distributions were examined based on variations in precipitation and discharge fluctuations. Remarkably high rates of reservoir sedimentation were recorded in summer with increased precipitation and discharge. At the Seungchon weir (YS-S1), coarse silt with medium sand-sized peaks under high flows appeared. At the downstream Juksan weir (YS-S3), most sediments fell within the medium silt size with an increase in the coarser fraction with high flows. At the halfway point between the two weirs (YS-S2), medium to coarse silt-sized particles accounted for 50 % of the sediments, regardless of season, indicating the formation of a lake-like condition by the obstruction from the two weirs upstream and downstream.

Concentrations of the major and trace elements of the collected sediments were analyzed and compared with the chemical composition of the underlying rocks. It was noticeable that easily mobilized elements, such as Ca, Mg, K, and Na, were considerably depleted in the suspended sediments relative to the bedrock of the river basin, indicating weak to moderate degrees of weathering. Trace elements including Ba, Co, Cr, Cu, La, Li, Mo, Nb, Ni, Pb, Rb, Sc, Sn, Sr, Ta, V, W, Y, Zn, and Zr were detected, with an abundance of several elements (e.g. Cu, W, Mo, Ba,

Zn, Li, Cr, Rb, Ni, Co, and Pb) that are more likely to be affected by anthropogenic input.

To quantitatively evaluate the relative contributions of slope-floor and channel-bank materials to suspended sediment in the Yeongsan River, a source fingerprinting approach using ^{137}Cs as a single tracer was applied, based on distinguishing characteristics of ^{137}Cs between surface and subsurface (bank) materials. The radioactivity of ^{137}Cs in the reservoir sediment and possible source materials were measured using gamma detectors; and the relative contributions of forest-floor and bank materials were calculated using a simple mixing model and a Monte Carlo simulation based on derived probability distribution functions fit to the detected values of ^{137}Cs at the forest floor and channel bank, respectively. The results of this study, achieved through the use of numerous iterations, indicated that the dominant source of suspended sediments in the Yeongsan River is channel-bank materials.

To reduce the uncertainty and limitations of the ^{137}Cs methodology, a composite fingerprinting analysis, using fallout radionuclides, geochemical elemental concentrations, and the magnetic properties of each source material combined with a multivariate mixing model, was conducted. Cropland topsoils, forest topsoils, and channel bank materials were selected as end-members. By applying the Kruskal–Wallis H-test and stepwise discriminant function analysis (DFA), final fingerprints were composed of different characteristics of the properties including $^{210}Pb_{ex}$, Zr, V, Pb, and Co. Composite fingerprinting procedures provided the same results as those obtained with ^{137}Cs as a single tracer. The possibility that contributions from the slope floor were underestimated due to the connectivity problem arising from the impediments to sediment movement cannot be excluded. Conveyance losses of

delivered forest floor materials would be expected to occur at hill-foot zones, alluvial fans, and agricultural dams. Embankments largely prevented slope materials from flowing into the channel and consequently influenced sediment connectivity.

There were seasonal variations in the contribution of slope materials to the reservoir. Contributions from the forest floor increased slightly during periods of heavy rainfall. Along with increasing discharge, forest roads act as conduits between hillslope and channel; this may have improved sediment connectivity. In winter, there was a slight increase in the contribution from forest topsoils, which may be influenced by repeated freeze–thaw actions at the upstream catchment at high altitudes.

Previous studies noted that dredging a riverbed and constructing river-crossing facilities commonly affect the river by accelerating channel erosion. However, it remains unclear as to how and to what extent human impact influences channel erosion from the results of this study alone, due to the absence of pre-interference data. The dominance of in-channel suspended sediments (those that are eroded, stored, and remobilized within the channel) implies that contributions of river bed materials as potential sources of downstream suspended sediments must be assessed; this was confirmed by the close correspondence between major element concentrations of suspended sediments and river bed materials.

Despite several limitations, this study, which investigated the provenance of the suspended sediments by discriminating and evaluating potential sources applying a fingerprinting approach, has practical significance for effectively managing the reservoir with respect to the control of sediment influx. Further studies targeting each subcatchment will facilitate robust evaluation of the source contributions

spatially and quantitatively. Careful application of tracer-specific correction factors combined with uncertainty analysis is expected to provide a better estimate of source apportionment.

References

Bajracharya, R.M. and Lal, R., 1992, Seasonal soil loss and erodibility variation on a Miamian silt loam soil, Soil Science Society of America Journal, 56(5), 1560-1565.

Barker, R., Dixon, L. and Hooke, J., 1997, Use of terrestrial photogrammetry for monitoring and measuring bank erosion, Earth Surface Processes and Landforms, 22(13), 1217-1227.

Blake, W.H., Wallbrink, P.J., Wilkinson, S.N., Humphreys, G.S., Doerr, S.H., Shakesby, R.A. and Tomkins, K.M., 2009, Deriving hillslope sediment budgets in wildfire-affected forests using fallout radionuclide tracers, Geomorphology, 104(3–4), 105-116.

Bottrill, L.J., Walling, D.E. and Leeks, G.J.L., 2000, Using recent overbank deposits to investigate contemporary sediment sources in larger river basins, In: Foster, I.D.L. (Ed.), Tracers in geomorphology, John Wiley & Sons, Chichester, England.

Bouchez, J., Gaillardet, J., France-Lanord, C., Maurice, L. and Dutra-Maia, P., 2011, Grain size control of river suspended sediment geochemistry: Clues from Amazon River depth profiles, Geochemistry, Geophysics, Geosystems, 12(3), Q03008.

Bourg, A.C.M., 1983, Role of fresh water/sea water mixing on trace metal adsorption phenomena, In: Wong, C.S., Boyle, E., Bruland, K.W., Burton, J.D., Goldberg, E.D. (Eds.), Trace metals in sea water, Plenum Press, New York.

Bracken, L.J. and Croke, J., 2007, The concept of hydrological connectivity and its contribution to understanding runoff-dominated geomorphic systems, Hydrological Processes, 21(13), 1749-1763.

Brandt, S.A., 2000, Classification of geomorphological effects downstream of dams, Catena, 40(4), 375-401.

Brookes, A., 1988, Channelized rivers: perspectives for environmental management, Wiley Chichester, England.

Caitcheon, G.G., 1993, Sediment source tracing using environmental magnetism: a new approach with examples from Australia, Hydrological processes, 7(4), 349-358.

Caitcheon, G.G., Olley, J.M., Pantus, F., Hancock, G. and Leslie, C., 2012, The dominant erosion processes supplying fine sediment to three major rivers in tropical Australia, the Daly (NT), Mitchell (Qld) and Flinders (Qld) Rivers, Geomorphology, 151-152, 188-195.

Callow, J.N. and Smettem, K.R.J., 2009, The effect of farm dams and constructed banks on hydrologic connectivity and runoff estimation in agricultural landscapes, Environmental Modelling & Software, 24(8), 959-968.

Canfield, D.E., 1997, The geochemistry of river particulates from the continental USA: major elements, Geochimica et Cosmochimica Acta, 61(16), 3349-3365.

Cerdà, A., 1997, Rainfall drop size distribution in the Western Mediterranean basin, València, Spain, Catena, 30(2), 169-182.

Chang, H.H., 1987, Modelling fluvial processes in streams with gravel mining, John Wiley & Sons, New York.

Chester, R. and Stoner, J.H., 1973, Pb in particulates from the lower atmosphere of

the eastern Atlantic, Nature, 245, 27-28.

Church, M., 1995, Geomorphic response to river flow regulation: case studies and time-scales, Regulated Rivers-Research and Management, 11(1), 3-22.

Collins, A.L. and Walling, D.E., 2002, Selecting fingerprint properties for discriminating potential suspended sediment sources in river basins, Journal of Hydrology, 261(1), 218-244.

Collins, A.L. and Walling, D.E., 2007, Sources of fine sediment recovered from the channel bed of lowland groundwater-fed catchments in the UK, Geomorphology, 88(1), 120-138.

Collins, A.L., Walling, D.E. and Leeks, G.J.L., 1997a, Fingerprinting the origin of fluvial suspended sediment in larger river basins: combining assessment of spatial provenance and source type, Geografiska Annaler: Series A, Physical Geography, 79(4), 239-254.

Collins, A.L., Walling, D.E. and Leeks, G.J.L., 1997b, Source type ascription for fluvial suspended sediment based on a quantitative composite fingerprinting technique, Catena, 29(1), 1-27.

Collins, A.L., Walling, D.E. and Leeks, G.J.L., 1997c, Use of the geochemical record preserved in floodplain deposits to reconstruct recent changes in river basin sediment sources, Geomorphology, 19(1), 151-167.

Collins, A.L., Walling, D.E. and Leeks, G.J.L., 1998, Use of composite fingerprints to determine the provenance of the contemporary suspended sediment load transported by rivers, Earth Surface Processes and Landforms, 23(1), 31-52.

Collins, A.L., Walling, D.E., McMellin, G.K., Zhang, Y., Gray, J., McGonigle, D. and Cherrington, R., 2010a, A preliminary investigation of the efficacy of riparian fencing schemes for reducing contributions from eroding channel

banks to the siltation of salmonid spawning gravels across the south west UK, Journal of Environmental Management, 91(6), 1341-1349.

Collins, A.L., Walling, D.E., Stroud, R.W., Robson, M. and Peet, L.M., 2010b, Assessing damaged road verges as a suspended sediment source in the Hampshire Avon catchment, southern United Kingdom, Hydrological Processes, 24(9), 1106-1122.

Collins, A.L., Walling, D.E., Webb, L. and King, P., 2010c, Apportioning catchment scale sediment sources using a modified composite fingerprinting technique incorporating property weightings and prior information, Geoderma, 155(3), 249-261.

Collins, A.L., Zhang, Y., McChesney, D., Walling, D.E., Haley, S.M. and Smith, P., 2012a, Sediment source tracing in a lowland agricultural catchment in southern England using a modified procedure combining statistical analysis and numerical modelling, Science of The Total Environment, 414(0), 301-317.

Collins, A.L., Zhang, Y., Walling, D.E., Grenfell, S.E., Smith, P., Grischeff, J., Locke, A., Sweetapple, A. and Brogden, D., 2012b, Quantifying fine-grained sediment sources in the River Axe catchment, southwest England: application of a Monte Carlo numerical modelling framework incorporating local and genetic algorithm optimisation, Hydrological Processes, 26(13), 1962-1983.

Collins, B.D. and Dunne, T., 1989, Gravel transport, gravel harvesting, and channel-bed degradation in rivers draining the southern Olympic Mountains, Washington, USA, Environmental Geology and Water Sciences, 13(3), 213-224.

Committee on Missouri River Recovery and Associated Sediment Management Issues, 2011, Missouri River Planning: Recognizing and Incorporating Sediment Management, National Research Council of the National Academies, Washington, D.C.

Dao, T.H., 1993, Tillage and winter wheat residue management effects on water infiltration and storage, Soil Science Society of America Journal, 57(6), 1586-1595.

Davis, C.M. and Fox, J.F., 2009, Sediment fingerprinting: review of the method and future improvements for allocating nonpoint source pollution, Journal of Environmental Engineering, 135(7), 490-504.

Davis, R.J. and Gregory, K.J., 1994, A new distinct mechanism of river bank erosion in a forested catchment, Journal of Hydrology, 157(1), 1-11.

de Vente, J., Poesen, J., Arabkhedri, M. and Verstraeten, G., 2007, The sediment delivery problem revisited, Progress in Physical Geography, 31(2), 155-178.

Dearing, J.A., 2000, Natural magnetic tracers in fluvial geomorphology, In: Foster, I.D.L. (Ed.), Tracers in Geomorphology, John Wiley & Sons, Chichester, England.

Dekov, V.M., Komy, Z., Araujo, F., Van Put, A. and Van Grieken, R., 1997, Chemical composition of sediments, suspended matter, river water and ground water of the Nile (Aswan-Sohag traverse), Science of the total environment, 201(3), 195-210.

Devault, D.A., Gérino, M., Laplanche, C., Julien, F., Winterton, P., Merlina, G., Delmas, F., Lim, P., Sánchez-Pérez, J.M. and Pinelli, E., 2009, Herbicide accumulation and evolution in reservoir sediments, Science of the total environment, 407(8), 2659-2665.

Dupré, B., Gaillardet, J., Rousseau, D. and Allègre, C.J., 1996, Major and trace elements of river-borne material: the Congo Basin, Geochimica et Cosmochimica Acta, 60(8), 1301-1321.

Edwards, L.M. and Burney, J.R., 1989, The effect of antecedent freeze-thaw frequency on runoff and soil loss from frozen soil with and without subsoil compaction and ground cover, Canadian Journal of Soil Science, 69(4), 799-811.

Evrard, O., Navratil, O., Ayrault, S., Ahmadi, M., Némery, J., Legout, C., Lefèvre, I., Poirel, A., Bonté, P. and Esteves, M., 2011, Combining suspended sediment monitoring and fingerprinting to determine the spatial origin of fine sediment in a mountainous river catchment, Earth Surface Processes and Landforms, 36(8), 1072-1089.

Förstner, U. and Salomons, W., 1980, Trace metal analysis on polluted sediments: Part I: Assessment of sources and intensities, Environmental Technology, 1(11), 494-505.

Förstner, U. and Wittmann, G.T.W., 1983, Metal pollution in the aquatic environment, Springer-Verlag, New York.

Fitzjohn, C., Ternan, J.L. and Williams, A.G., 1998, Soil moisture variability in a semi-arid gully catchment: implications for runoff and erosion control, Catena, 32(1), 55-70.

Folk, R.L. and Ward, W.C., 1957, Brazos River bar: a study in the significance of grain size parameters, Journal of Sedimentary Research, 27(1), 3-26.

Foster, I.D.L., Lees, J.A., Owens, P.N. and Walling, D.E., 1998, Mineral magnetic characterization of sediment sources from an analysis of lake and floodplain sediments in the catchments of the Old Mill Reservoir and Slapton Ley,

South Devon, UK, Earth Surface Processes and Landforms, 23(8), 685-703.

Foster, I.D.L., 2000, Tracers in geomorphology, John Wiley & Sons, England.

Foster, I.D.L. and Lees, J.A., 2000, Tracers in geomorphology: Theory and applications in tracing fine particulate sediments, In: Foster, I.D.L. (Ed.), Tracers in geomorphology, John Wiley & Sons, Chichester, England.

Fox, J.F. and Papanicolaou, A.N., 2008, Application of the spatial distribution of nitrogen stable isotopes for sediment tracing at the watershed scale, Journal of Hydrology, 358(1), 46-55.

Friedman, J.M., Osterkamp, W.R., Scott, M.L. and Auble, G.T., 1998, Downstream effects of dams on channel geometry and bottomland vegetation: regional patterns in the Great Plains, Wetlands, 18(4), 619-633.

Fryirs, K. and Brierley, G.J., 2001, Variability in sediment delivery and storage along river courses in Bega catchment, NSW, Australia: implications for geomorphic river recovery, Geomorphology, 38(3), 237-265.

Fryirs, K.A., Brierley, G.J., Preston, N.J. and Kasai, M., 2007, Buffers, barriers and blankets: The (dis) connectivity of catchment-scale sediment cascades, Catena, 70(1), 49-67.

Gaillardet, J., Viers, J. and Dupré, B., 2003, Trace elements in river waters, In: Drever, J.I. (Ed.), Treatise on geochemistry: Surface and Ground water, weathering, and soils, Elsevier-Pergamon, Oxford.

Gellis, A.C. and Noe, G.B., 2013, Sediment source analysis in the Linganore Creek watershed, Maryland, USA, using the sediment fingerprinting approach: 2008 to 2010, Journal of Soils and Sediments, 13(10), 1735-1753.

Graf, W.L., 2006, Downstream hydrologic and geomorphic effects of large dams on American rivers, Geomorphology, 79(3), 336-360.

Grousset, F.E., Quetel, C.R., Thomas, B., Donard, O.F.X., Lambert, C.E., Guillard, F. and Monaco, A., 1995, Anthropogenic vs. lithogenic origins of trace elements (As, Cd, Pb, Rb, Sb, Sc, Sn, Zn) in water column particles: northwestern Mediterranean Sea, Marine Chemistry, 48(3), 291-310.

Gyssels, G. and Poesen, J., 2003, The importance of plant root characteristics in controlling concentrated flow erosion rates, Earth Surface Processes and Landforms, 28(4), 371-384.

Haddadchi, A., Nosrati, K. and Ahmadi, F., 2014, Differences between the source contribution of bed material and suspended sediments in a mountainous agricultural catchment of western Iran, CATENA, 116, 105-113.

Hart, B. and Sly, P.G., 1992, Sediment/Water Interactions: Proceedings of the Fifth International Symposium, Kluwer Academic Publishers, Netherlands.

Harvey, A.M., 2002, Effective timescales of coupling within fluvial systems, Geomorphology, 44(3), 175-201.

He, Q. and Walling, D.E., 1996, Interpreting particle size effects in the adsorption of ^{137}Cs and unsupported ^{210}Pb by mineral soils and sediments, Journal of Environmental Radioactivity, 30(2), 117-137.

Hernandez, L., Probst, A., Probst, J.L. and Ulrich, E., 2003, Heavy metal distribution in some French forest soils: evidence for atmospheric contamination, Science of the Total Environment, 312(1), 195-219.

Holland, W.N. and Pickup, G., 1976, Flume study of knickpoint development in stratified sediment, Geological Society of America Bulletin, 87(1), 76-82.

Hooke, J., 2003, Coarse sediment connectivity in river channel systems: a conceptual framework and methodology, Geomorphology, 56(1), 79-94.

Horowitz, A.J., 1985, A primer on trace metal-sediment chemistry, US Geological

Survey Water-Supply Paper 2277.

Horowitz, A.J., 1991, A primer on sediment-trace element chemistry, US Geological Survey; Open-File Reports Reston, VA.

Horowitz, A.J. and Elrick, K.A., 1987, The relation of stream sediment surface area, grain size and composition to trace element chemistry, Applied Geochemistry, 2(4), 437-451.

Howard, A. and Dolan, R., 1981, Geomorphology of the Colorado River in the Grand Canyon, The Journal of Geology, 89(3), 269-298.

Iksan Regional Construction and Management Administration, 1998, River management master plan for Yeongsan river, Ministry of Construction and Transportation, Korea (in Korean).

Irving, H. and Williams, R.J.P., 1948, Order of stability of metal complexes, Nature, 162, 746-747.

Jarvie, H.P., Neal, C. and Withers, P.J.A., 2006, Sewage-effluent phosphorus: a greater risk to river eutrophication than agricultural phosphorus?, Science of the Total Environment, 360(1), 246-253.

Jarvie, H.P., Withers, P.J., Hodgkinson, R., Bates, A., Neal, M., Wickham, H.D., Harman, S.A. and Armstrong, L., 2008, Influence of rural land use on streamwater nutrients and their ecological significance, Journal of Hydrology, 350(3), 166-186.

Jayawardena, A.W. and Rezaur, R.B., 2000, Drop size distribution and kinetic energy load of rainstorms in Hong Kong, Hydrological Processes, 14(6), 1069-1082.

Jia, G. and Jia, J., 2012, Determination of radium isotopes in environmental samples by gamma spectrometry, liquid scintillation counting and alpha

spectrometry: a review of analytical methodology, Journal of environmental radioactivity, 106, 98-119.

Jung, K.-H., Sonn, Y.-K., Hong, S.-Y., Hur, S.-O. and Ha, S.-K., 2005, Assessment of national soil loss and potential erosion area using the digital detailed soil maps, Korean Society of Soil Science and Fertilizer, 38(2), 59-65 (in Korean with English abstract).

Kabata-Pendias, A. and Pendias, H., 2001, Trace elements in soils and plants. Third edition ed, CRC press, Washington.

Kim, J.-H., Kim, K.-T. and Lee, H.-J., 2009, Analysis of Korea soil loss and hazard zone, The Journal of GIS Association of Korea, 17(3), 261-268 (in Korean with English abstract).

Kim, J.K., Onda, Y., Yang, D.Y. and Kim, M.S., 2013, Temporal variations of reservoir sediment sources in a small mountainous catchment in Korea, Earth Surface Processes and Landforms, 38(12), 1380-1392.

Kim, J.K. and Park, Y.S., 2005, Geochemical study on geological groups of stream sediments in the Gwangju Area, Economic and Environmental Geology, 38(4), 481-492 (in Korean with English abstract).

Kim, J.S., Oh, S.Y. and Oh, K.Y., 2006, Nutrient runoff from a Korean rice paddy watershed during multiple storm events in the growing season, Journal of Hydrology, 327(1), 128-139.

Kim, J.Y., 2009, Discharged characteristics of non-point pollutants source by soil loss and sediment (Masters thesis), Department of Environmental Engineering, Graduate School of Cheongju University, Cheongju, Korea.

Kim, Y.-J., Lee, C.-S., Kim, H.-N., Park, J.-B. and Lee, H.-G., 1998, Geochemistry on igneous rocks in eastern region of the Jangsung area, Chonnam, Journal

of the Korean earth science society, 19(2), 154-170 (in Korean with English abstract).

Koiter, A.J., Owens, P.N., Petticrew, E.L. and Lobb, D.A., 2013, The behavioural characteristics of sediment properties and their implications for sediment fingerprinting as an approach for identifying sediment sources in river basins, Earth-Science Reviews, 125, 24-42.

Korea Meteorological Administration, 2008-2012, Annual climatological report, Korea Meteorological Administration, Seoul, Korea (in Korean).

Korea Meteorological Administration, 2011, Annual climatological report, Korea Meteorological Administration, Seoul, Korea, 1-314 (in Korean).

Korea Meteorological Administration, 2012, Annual climatological report, Korea Meteorological Administration, Seoul, Korea, 1-311 (in Korean).

Lamba, J., Karthikeyan, K.G. and Thompson, A.M., 2015, Apportionment of suspended sediment sources in an agricultural watershed using sediment fingerprinting, Geoderma, 239, 25-33.

Lantzy, R.J. and Mackenzie, F.T., 1979, Atmospheric trace metals: global cycles and assessment of man's impact, Geochimica et Cosmochimica Acta, 43(4), 511-525.

Lawler, D.M. and Leeks, G.J.L., 1992, River bank erosion events on the Upper Severn detected by the Photo-Electronic Erosion Pin (PEEP) system, Erosion and sediment transport monitoring programmes in river basins: Proceedings of the Oslo Symposium, August 1992, IAHS Publication, 210, 95-105.

Lee, B.J., Kim, J.C., Kim, Y.B., Cho, D.L., Choi, H.I., Jeon, H.Y. and Kim, B.C., 1997, Explanatory note of the 1:250,000 Geological Map of Gwangju sheet,

Korea Institute of Geoscience and Mineral Resources, 1-82 (in Korean).

Lee, S., Moon, J.-W. and Moon, H.-S., 2003, Heavy metals in the bed and suspended sediments of Anyang River, Korea: Implications for water quality, Environmental geochemistry and health, 25(4), 433-452.

Lim, Y.S., Kim, J.K., Kim, J.W. and Hong, S.S., 2014, Evaluation of suspended-sediment sources in the Yeongsan River using Cs-137 after major human impacts, Quaternary International, 344, 64-74.

Lin, J., Huang, Y., Wang, M.-k., Jiang, F., Zhang, X. and Ge, H., 2015, Assessing the sources of sediment transported in gully systems using a fingerprinting approach: An example from South-east China, CATENA, 129, 9-17.

Logan, T.J., 1987, Diffuse (non-point) source loading of chemicals to Lake Erie, Journal of Great Lakes Research, 13(4), 649-658.

Logan, T.J., Oloya, T.O. and Yaksich, S.M., 1979, Phosphate characteristics and bioavailability of suspended sediments from streams draining into Lake Erie, Journal of Great Lakes Research, 5(2), 112-123.

Ludwig, J.A., Tongway, D.J., Eager, R.W., Williams, R.J. and Cook, G.D., 1999, Fine-scale vegetation patches decline in size and cover with increasing rainfall in Australian savannas, Landscape Ecology, 14(6), 557-566.

Mainstone, C.P. and Parr, W., 2002, Phosphorus in rivers—ecology and management, Science of the Total Environment, 282, 25-47.

Martin, J.-M. and Meybeck, M., 1979, Elemental mass-balance of material carried by major world rivers, Marine chemistry, 7(3), 173-206.

Meybeck, M., 2003, Global occurrence of major elements in rivers, In: Drever, J.I. (Ed.), Treatise on geochemistry.

Ministry of Construction and Transportation, 2000, Report on development of

water resources management methods: Design of probable precipitation, vol. 1, Korea Institute of Construction Technology, 1-292, (in Korean).

Mizugaki, S., Onda, Y., Fukuyama, T., Koga, S., Asai, H. and Hiramatsu, S., 2008, Estimation of suspended sediment sources using ^{137}Cs and $^{210}Pb_{ex}$ in unmanaged Japanese cypress plantation watersheds in southern Japan, Hydrological Processes, 22(23), 4519-4531.

Motha, J.A., Wallbrink, P.J., Hairsine, P.B. and Grayson, R.B., 2003, Determining the sources of suspended sediment in a forested catchment in southeastern Australia, Water Resources Research, 39(3), 1056.

Mukundan, R., Radcliffe, D.E., Ritchie, J.C., Risse, L.M. and McKinley, R.A., 2010, Sediment fingerprinting to determine the source of suspended sediment in a southern Piedmont stream, Journal of environmental quality, 39(4), 1328-1337.

Murray, A., Marten, R., Johnston, A. and Martin, P., 1987, Analysis for naturally occuring radionuclides at environmental concentrations by gamma spectrometry, Journal of Radioanalytical and Nuclear Chemistry, 115(2), 263-288.

N'guessan, Y.M., Probst, J.-L., Bur, T. and Probst, A., 2009, Trace elements in stream bed sediments from agricultural catchments (Gascogne region, SW France): where do they come from?, Science of the total environment, 407(8), 2939-2952.

Nagle, G.N., Fahey, T.J., Ritchie, J.C. and Woodbury, P.B., 2007, Variations in sediment sources and yields in the Finger Lakes and Catskills regions of New York, Hydrological Processes, 21(6), 828-838.

Neal, C., Jarvie, H.P., Whitton, B.A. and Gemmell, J., 2000, The water quality of

the River Wear, north-east England, Science of the Total Environment, 251, 153-172.

Neal, C., Robson, A., Harrow, M., Hill, L., Wickham, H., Bhardwaj, C., Tindall, C., Ryland, G., Leach, D. and Johnson, R., 1997, Major, minor, trace element and suspended sediment variations in the River Tweed: results from the LOIS core monitoring programme, Science of the total environment, 194, 193-205.

Neller, R., 1988, A comparison of channel erosion in small urban and rural catchments, Armidale, New South Wales, Earth Surface Processes and Landforms, 13(1), 1-7.

Nesbitt, H.W. and Markovics, G., 1980, Chemical processes affecting alkalis and alkaline earths during continental weathering, Geochimica et Cosmochimica Acta, 44(11), 1659-1666.

Nesbitt, H.W. and Young, G.M., 1982, Early Proterozoic climates and plate motions inferred from major element chemistry of lutites, Nature, 299(5885), 715-717.

Nesbitt, H.W. and Young, G.M., 1984, Prediction of some weathering trends of plutonic and volcanic rocks based on thermodynamic and kinetic considerations, Geochimica et Cosmochimica Acta, 48(7), 1523-1534.

Nesbitt, H.W. and Young, G.M., 1989, Formation and diagenesis of weathering profiles, The Journal of Geology, 129-147.

Nesbitt, H.W. and Young, G.M., 1996, Petrogenesis of sediments in the absence of chemical weathering: effects of abrasion and sorting on bulk composition and mineralogy, Sedimentology, 43(2), 341-358.

Nesbitt, H.W., Young, G.M., McLennan, S.M. and Keays, R.R., 1996, Effects of

chemical weathering and sorting on the petrogenesis of siliciclastic sediments, with implications for provenance studies, The Journal of Geology, 525-542.

Nosrati, K., Govers, G., Semmens, B.X. and Ward, E.J., 2014, A mixing model to incorporate uncertainty in sediment fingerprinting, Geoderma, 217, 173-180.

Oh, K.-H., Kim, J.-Y., Koh, Y.-K., Youn, S.-T., Shin, S.-E., Park, B.-Y., Moon, B.-C. and Kim, H.-G., 2003, Geochemical characteristics and contamination of surface sediments in streams of Gwangju city, Journal of the Korean Earth Science Society, 24(4), 346-360 (in Korean with English abstract).

Oldfield, F., Rummery, T.A., Thompson, R. and Walling, D.E., 1979, Identification of suspended sediment sources by means of magnetic measurements: some preliminary results, Water Resources Research, 15(2), 211-218.

Olley, J., Burton, J., Smolders, K., Pantus, F. and Pietsch, T., 2012, The application of fallout radionuclides to determine the dominant erosion process in water supply catchments of subtropical South-east Queensland, Australia, Hydrological Processes, 27(6), 885-895.

Owens, P., Batalla, R., Collins, A., Gomez, B., Hicks, D., Horowitz, A., Kondolf, G., Marden, M., Page, M. and Peacock, D., 2005a, Fine-grained sediment in river systems: environmental significance and management issues, River Research and Applications, 21(7), 693-717.

Owens, P.N., Batalla, R.J., Collins, A.J., Gomez, B., Hicks, D.M., Horowitz, A.J., Kondolf, G.M., Marden, M., Page, M.J., Peacock, D.H., Petticrew, E.L., Salomons, W. and Trustrum, N.A., 2005b, Fine-grained sediment in river systems: environmental significance and management issues, River Research and Applications, 21(7), 693-717.

Owens, P.N., Walling, D.E. and Leeks, G.J.L., 2000, Tracing fluvial suspended sediment sources in the catchment of the River Tweed, Scotland, using composite fingerprints and a numerical mixing model, In: Foster, I.D.L. (Ed.), Tracers in geomorphology, John Wiley & Sons.

Palazón, L., Gaspar, L., Latorre, B., Blake, W. and Navas, A., 2014, Evaluating the importance of surface soil contributions to reservoir sediment in alpine environments: a combined modelling and fingerprinting approach in the Posets-Maladeta Natural Park, Solid Earth Discussions, 6(1), 1155-1190.

Park, B.-K., 2003, Petrochemical Study on the volcanic rocks in the Mt. Mudeung area (Masters thesis), Department of Earth System and Environmental Science, Chonnam National University, Graduate School.

Park, C.C., 1977, Man-induced changes in stream channel capacity, In: Gregory, K.J. (Ed.), River channel changes, John Wiley & Sons, Chichester.

Park, Y.-S., Noh, Y.-B. and Lee, C.-S., 1995, Rb-Sr isotopic study of granitoid rocks in the Gwangju-Naju area, Korea, Journal of the Korean Earth Science Society, 16(3), 247-261 (in Korean with English abstract).

Park, Y.S., Kim, J.K. and Jung, Y.H., 2006, Geochemical characteristics of stream sediments based on bed rocks in the Naju area, Korea, Journal of the Korean earth science society, 27(1), 49-60 (in Korean with English abstract).

Parsons, A.J. and Foster, I.D.L., 2011, What can we learn about soil erosion from the use of Cs-137?, Earth-Science Reviews, 108(1), 101-113.

Peart, M.R. and Walling, D.E., 1986, Fingerprinting sediment source: the example of a drainage basin in Devon, UK, Drainage basin sediment delivery: proceedings of a symposium held in New Mexico, August 1986, IAHS Publication, 159, 41-55.

Petts, G.E., 1979, Complex response of river channel morphology subsequent to reservoir construction, Progress in Physical Geography, 3(3), 329-362.

Petts, G.E., 1984, Sedimentation within a regulated river, Earth Surface Processes and Landforms, 9(2), 125-134.

Petts, G.E. and Gurnell, A.M., 2005, Dams and geomorphology: research progress and future directions, Geomorphology, 71(1), 27-47.

Phillips, J.D., Slattery, M.C. and Musselman, Z.A., 2005, Channel adjustments of the lower Trinity River, Texas, downstream of Livingston Dam, Earth Surface Processes and Landforms, 30(11), 1419-1439.

Phillips, J.M., Russell, M.A. and Walling, D.E., 2000, Time-integrated sampling of fluvial suspended sediment: a simple methodology for small catchments, Hydrological processes, 14(14), 2589-2602.

Pulley, S., Foster, I. and Antunes, P., 2015, The uncertainties associated with sediment fingerprinting suspended and recently deposited fluvial sediment in the Nene river basin, Geomorphology, 228, 303-319.

Reimann, C. and de Caritat, P., 2000, Intrinsic flaws of element enrichment factors (EFs) in environmental geochemistry, Environmental Science & Technology, 34(24), 5084-5091.

Reimann, C. and de Caritat, P., 2005, Distinguishing between natural and anthropogenic sources for elements in the environment: regional geochemical surveys versus enrichment factors, Science of the Total Environment, 337(1), 91-107.

Renard, K.G., Foster, G.R., Weesies, G.A., McCool, D. and Yoder, D., 1997, Predicting soil erosion by water: a guide to conservation planning with the revised universal soil loss equation (RUSLE), United States Department of

Agriculture (USDA), Washington, DC.

Rhoads, B.L., 1991, Impact of agricultural development on regional drainage in the lower Santa Cruz valley, Arizona, USA, Environmental Geology and Water Sciences, 18(2), 119-135.

Rinaldi, M. and Simon, A., 1998, Bed-level adjustments in the Arno River, central Italy, Geomorphology, 22(1), 57-71.

Robinson, G.D., 1981, Adsorption of Cu, Zn and Pb near sulfide deposits by hydrous manganese—Iron oxide coatings on stream alluvium, Chemical Geology, 33(1), 65-79.

Rubio, B., Nombela, M.A. and Vilas, F., 2000, Geochemistry of major and trace elements in sediments of the Ria de Vigo (NW Spain): an assessment of metal pollution, Marine Pollution Bulletin, 40(11), 968-980.

Russell, M.A., Walling, D.E. and Hodgkinson, R.A., 2000, Appraisal of a simple sampling device for collecting time-integrated fluvial suspended sediment samples, IAHS Publication, 263, 119-127.

Sánchez-Chardi, A. and López-Fuster, M.J., 2009, Metal and metalloid accumulation in shrews (Soricomorpha, Mammalia) from two protected Mediterranean coastal sites, Environmental pollution, 157(4), 1243-1248.

Schäfer, J. and Blanc, G., 2002, Relationship between ore deposits in river catchments and geochemistry of suspended particulate matter from six rivers in southwest France, Science of the Total Environment, 298(1), 103-118.

Schumm, S.A., 1969, River metamorphosis, Journal of Hydraulics Division, 95(HY1), 255-273.

Schumm, S.A., Harvey, M.D. and Watson, C.C., 1984, Incised channels:

morphology, dynamics, and control, Water Resources Publications, Littleton, Colorado.

Sidle, R.C., Sasaki, S., Otsuki, M., Noguchi, S. and Rahim Nik, A., 2004, Sediment pathways in a tropical forest: effects of logging roads and skid trails, Hydrological Processes, 18(4), 703-720.

Simon, A., 1989, A model of channel response in disturbed alluvial channels, Earth Surface Processes and Landforms, 14(1), 11-26.

Simon, A., 1994, Gradation processes and channel evolution in modified West Tennessee streams: process, response, and form, U.S. Geological Survey professional paper: 1470, US Government Printing Office Denver, CO.

Sly, P.G. and Hart, B.T., 1989, Sediment/water interactions: proceedings of the fourth international symposium, Kluwer Academic Publishers, Netherlands.

Smith, H.G. and Blake, W.H., 2014, Sediment fingerprinting in agricultural catchments: A critical re-examination of source discrimination and data corrections, Geomorphology, 204, 177-191.

Smith, H.G., Sheridan, G.J., Lane, P.N.J., Noske, P.J. and Heijnis, H., 2011, Changes to sediment sources following wildfire in a forested upland catchment, southeastern Australia, Hydrological Processes, 25(18), 2878-2889.

Stone, M., Collins, A.L., Silins, U., Emelko, M.B. and Zhang, Y.S., 2014, The use of composite fingerprints to quantify sediment sources in a wildfire impacted landscape, Alberta, Canada, Science of The Total Environment, 473, 642-650.

Stumm, W., 1987, Aquatic surface chemistry: Chemical processes at the particle-water interface, John Wiley & Sons, US.

Sutherland, R.A., 2000, Bed sediment-associated trace metals in an urban stream, Oahu, Hawaii, Environmental Geology, 39(6), 611-627.

Tamtam, F., Mercier, F., Le Bot, B., Eurin, J., Dinh, Q.T., Clément, M. and Chevreuil, M., 2008, Occurrence and fate of antibiotics in the Seine River in various hydrological conditions, Science of the Total Environment, 393(1), 84-95.

Taylor, S.R. and McLennan, S.M., 1985, The continental crust: its composition and evolution, Blackwell Scientific Publications, Oxford ; London

The Four Major Rivers Restoration Project Headquarters, 2009, Master plan of the four major rivers restoration project Ministry of Land, Transport and Maritime Affairs, Korea, 1-61 (in Korean).

Thornton, I., 1983, Applied environmental geochemistry, Academic Press, London.

Viers, J., Dupré, B. and Gaillardet, J., 2009, Chemical composition of suspended sediments in World Rivers: new insights from a new database, Science of the total Environment, 407(2), 853-868.

Wall, G.J., Dickinson, W.T., Rudra, R.P. and Coote, D.R., 1988, Seasonal soil erodibility variation in southwestern Ontario, Canadian Journal of Soil Science, 68(2), 417-424.

Wallbrink, P.J. and Murray, A.S., 1993, Use of fallout radionuclides as indicators of erosion processes, Hydrological Processes, 7(3), 297-304.

Wallbrink, P.J., Murray, A.S., Olley, J.M. and Olive, L.J., 1998, Determining sources and transit times of suspended sediment in the Murrumbidgee River, New South Wales, Australia, using fallout 137Cs and 210Pb, Water Resources Research, 34(4), 879-887.

Wallbrink, P.J., Olley, J.M., Murray, A.S. and Olive, L.J., 1996, The contribution of

subsoil to sediment yield in the Murrumbidgee River basin, New South Wales, Australia, IAHS Publication, 236, 347-355.

Walling, D.E., 1983, The sediment delivery problem, Journal of Hydrology, 65(1–3), 209-237.

Walling, D.E., 2006, Tracing versus monitoring: New challenges and opportunities in erosion and sediment delivery research, In: Owens, P.N., Collins, A.J. (Eds.), Soil erosion and sediment redistribution in river catchments: measurement, modelling and management, CABI, UK.

Walling, D.E. and Collins, A.L., 2008, The catchment sediment budget as a management tool, environmental science & policy, 11(2), 136-143.

Walling, D.E., Collins, A.L. and Stroud, R.W., 2008a, Tracing suspended sediment and particulate phosphorus sources in catchments, Journal of Hydrology, 350(3), 274-289.

Walling, D.E., Collins, A.L. and Stroud, R.W., 2008b, Tracing suspended sediment and particulate phosphorus sources in catchments, Journal of Hydrology, 350(3-4), 274-289.

Walling, D.E., He, Q. and Blake, W., 1999, Use of ^{7}Be and ^{137}Cs measurements to document short- and medium-term rates of water-induced soil erosion on agricultural land, Water Resources Research, 35(12), 3865-3874.

Walling, D.E. and Quine, T.A., 1992, The use of caesium-137 measurements in soil erosion surveys, IAHS Publication, 210, 143-152.

Walling, D.E. and Woodward, J.C., 1992, Use of radiometric fingerprints to derive information on suspended sediment sources, IAHS Publication, 210, 153-164.

Walling, D.E. and Woodward, J.C., 1995, Tracing sources of suspended sediment

in river basins: a case study of the River Culm, Devon, UK, Marine and Freshwater Research, 46(1), 327-336.

Walling, D.E., Woodward, J.C. and Nicholas, A.P., 1993, A multi-parameter approach to fingerprinting suspended-sediment sources, Tracers in Hydrology (Proceedings of the Yokohama Symposium, July 1993), IAHS Publication, 215, 329-338.

WAMIS, 2013a, Current condition of agricultural dam (2009) by the Korea Rural Community Corporation and visiting research of local government, http://www.wamis.go.kr/main/usrdt_src.aspx, Ministry of Land, Infrastructure, and Transport (5 December 2013) (in Korean).

WAMIS, 2013b, WAMIS (Water Resources Management Information System), http://www.wamis.go.kr/main/usrdt_src.aspx, Ministry of Land, Infrastructure, and Transport (5 December 2013) (in Korean).

Wang, G., Hu, H. and Li, T., 2009, The influence of freeze–thaw cycles of active soil layer on surface runoff in a permafrost watershed, Journal of Hydrology, 375(3), 438-449.

Wildi, W., Dominik, J., Loizeau, J.L., Thomas, R.L., Favarger, P.Y., Haller, L., Perroud, A. and Peytremann, C., 2004, River, reservoir and lake sediment contamination by heavy metals downstream from urban areas of Switzerland, Lakes & Reservoirs: Research & Management, 9(1), 75-87.

Williams, G.P. and Wolman, M.G., 1984, Downstream effects of dams on alluvial rivers, U.S. Geological survey professional paper: 1286, US Government Printing Office Washington, DC, USA.

Wilson, P., Clark, R., McAdam, J.H. and Cooper, E.A., 1993, Soil erosion in the Falkland Islands: an assessment, Applied Geography, 13(4), 329-352.

Wolman, M.G., 1967, A cycle of sedimentation and erosion in urban river channels, Geografiska Annaler. Series A, Physical Geography, 49(2/4), 385-395.

Yang, S.L., Milliman, J.D., Li, P. and Xu, K., 2011, 50,000 dams later: erosion of the Yangtze River and its delta, Global and Planetary Change, 75(1), 14-20.

Yang, S.L., Zhang, J. and Xu, X.J., 2007, Influence of the Three Gorges Dam on downstream delivery of sediment and its environmental implications, Yangtze River, Geophysical research letters, 34(10), L10401, 1-5.

Yang, S.L., Zhang, J., Zhu, J., Smith, J.P., Dai, S.B., Gao, A. and Li, P., 2005, Impact of dams on Yangtze River sediment supply to the sea and delta intertidal wetland response, Journal of Geophysical Research: Earth Surface (2003–2012), 110, F03006, 1-12.

Yu, L. and Oldfield, F., 1989, A multivariate mixing model for identifying sediment source from magnetic measurements, Quaternary Research, 32(2), 168-181.

Yu, L. and Oldfield, F., 1993, Quantitative sediment source ascription using magnetic measurements in a reservoir-catchment system near Nijar, SE Spain, Earth Surface Processes and Landforms, 18(5), 441-454.

Yun, H.-S., Lee, J.-Y., Hong, S.-S., Yang, D.-Y., Kim, J.-Y. and Cho, D.-L., 2013, GIS-based areal distribution ratios and characteristics of constituent rocks with geologic ages and rock types in Jeonnam and Gwangju areas, The Journal of the Petrological Society of Korea, 22(2), 153-177 (in Korean with English abstract).

Zoller, W.H., Gladney, E.S. and Duce, R.A., 1974, Atmospheric concentrations and sources of trace metals at the South Pole, Science, 183(4121), 198-200.

국문초록

영산강 부유토사의 기원지 평가

임영신

사범대학 사회교육과 지리전공

서울대학교 대학원

4대강 사업 이후, 영산강 유역에서 최근 두부침식 및 보(洑)의 안정성과 관련된 사항들에 대한 관심이 높다. 보로 인한 퇴적물의 트랩효과 및 대규모 준설 등으로 인한 퇴적물 수지 변화로 인해 하류에서의 침식현상이 예상되는 상황에서 하도의 안정 및 하천 시설물의 지속적인 유지관리를 위해서는 현 상황에서의 퇴적물 수지에 대한 이해가 필요하다. 토사 관련 문제들에 대한 적절한 대책을 수립하기 위해서는 현재 하천에서 이동되는 부유토사의 물리적, 지화학적 특성을 이해하고 나아가 부유토사의 기원을 파악하는 것이 매우 중요하다. 따라서 본 연구의 목적은 첫째, 영산강 부유토사의 물리적, 지화학적 특성을 파악하고 둘째, ^{137}Cs을 추적자로 이용하여 현재 하천에서 이동되는 퇴적물에 유역사면의 침식작용과 하천에 의한 침식작용이 얼마만큼 기여했는지를 정량적으로 평가하며, 셋째, 다변량 믹싱 모델과 결합된 composite fingerprinting 방법을 적용하여 죽산보 부유토사의 기원지를 평가하는 것이다.

이를 위해 본 연구는 영산강 중·상류를 대상으로 하여 승촌보, 영산포 수변공원, 죽산보 세 지점에 시간누적형 부유토사 샘플러를 설치하고 (YS-S1, S2, S3), 2012년 7월부터 2014년 10월까지 한달 간격으로 정기적인 모니터링를 실시하였다. 강수가 집중되는 여름 동안 다른 시기와 비교할 수 없을 정도로 높은 보 퇴적률이 기록되었다. 보 퇴적물의 입도는 중립에서 조립 실트 크기의 입자가 지배적으로 나타났으며, 유량변동이 큰 시기에 조립의 피크가 성장하면서 음의 왜도(skewness)가 나타났다. 부유토사의 주원소 분석결과, Ca, Mg, K, Na 같이 풍화과정에서 보다 쉽게 이동하는 원소들이 유역의 기반암보다 낮은 농도를 보였고 이는 약하거나 중간 정도의 풍화단계를 지시한다. 미량원소는 Ba, Co, Cr, Cu, La, Li, Mo, Nb, Ni, Pb, Rb, Sc, Sn, Sr, Ta, V, W, Y, Zn, Zr이 검출되었고, Cu, W, Mo, Ba, Zn, Li, Cr, Rb, Ni, Co, Pb 같이 인간활동에 의해 발생할 가능성이 높은 원소들의 농도가 높게 나타났다.

두 번째로, 퇴적물 기원의 유형을 밝히고자 한 연구목적에 따라 잠재적 기원지 유형을 하안과 유역사면 시료로 크게 구분하였으며, 유역의 공간 분포를 고려하여 산사면과 하안에서 각각 잠재적 기원 물질을 채취하였다. 기원지 핑거프린팅은 지표와 지표하 물질의 구분이 가능한 ^{137}Cs 값을 추적자 속성으로 이용하였다. 채취된 보 퇴적물과 잠재적 기원지 시료를 대상으로 방사성동위원소분석을 실시하였고, 검출된 ^{137}Cs 값의 분포에 가장 적합한 확률분포모형을 구축하였다. 이에 몬테카를로 시뮬레이션이라는 무작위 추출기법을 적용하여 무한대에 가깝게 반복 계산한 결과, 영산강의 보 일대에 퇴적된 퇴적물은 주로 하천침식에 의해 기원한 것으로 추정된다. 이러한 결과에는 사면과 하천의 (비)연결성, 즉 사면침식으로부터 기원한

물질이 운송되는 과정에서 손실되거나 다양한 형태의 지형적 장애물에 일시적 혹은 장기적으로 저장될 가능성 및 양안을 따라 건설된 하천 제방으로 인해 하천으로 유입되기 힘든 환경 등이 작용했을 것으로 보인다. 반면, 하안 물질은 하천 내에서 침식되고 흐르는 물에 직접적으로 전달될 수 있다는 측면에서 운송 손실이 적을 수 있다. 볼라벤을 비롯한 큰 규모의 태풍 3개가 연달아 한반도에 상륙하면서 많은 강수가 기록된 시기 동안에 예외적으로 사면 물질 기여도의 증가가 나타났다. 이러한 강우사상은 활발한 토양침식을 유발하여 더 많은 양의 사면 물질을 발생시킬 수 있고, 유량의 증가와 함께 임도(forest road)가 일시적인 유로 역할을 함으로써 사면과 하천의 연결성이 증대될 가능성이 있다. 한편, 선행연구를 통해 하상 준설 및 하천을 가로지르는 시설물 건설이라는 인간간섭의 충격으로 하천 침식이 가속화된 것이라는 추측은 가능하지만, 간섭 이전의 사면 침식 및 하천침식의 기여도 평가 자료가 없으므로 인간간섭의 영향이 어느 정도인가에 대해서는 본 연구결과만으로는 알 수 없다.

^{137}Cs을 이용한 기원지 평가의 불확실성과 한계를 보완하고자 물질의 지화학적, 자기적 특성 및 여러 방사성동위원소를 결합한 composite finger-printing을 수행하였다. 농경지 표토, 산사면 표토, 하안물질을 각각 부유토사 기원지 엔드멤버로 선정하였다. Kruskal-Wallis H-test와 다변량 판별분석을 적용하여 $^{210}Pb_{ex}$, Zr, V, Pb, Co으로 구성된 최종 fingerprints를 구축하였다. 이를 대상으로 죽산보 부유토사의 농도 값과 기원물질의 농도 값 차이를 비교하면서 상대오차를 최소로 하는 최적의 기여율을 구하는 믹싱 모델을 적용한 결과, 죽산보의 부유토사는 대부분 하안물질에서 기원한 것으로 추정되었다. 겨울에 산사면 물질의 기여가 약간 증가한

것으로 나타났는데 이는 반복된 동결융해작용에 영향을 받은 것으로 보인다. 입도보정계수와 유기물 보정계수를 믹싱 모델에 결합하는 것이 적절한지에 대한 검토가 이루어졌으며, 비표면적 또는 유기물 함량과 원소 농도 사이에 유의미한 상관관계가 없는 것으로 나타났다. 보다 나은 기원지 추정을 위해서는 추적자 각각을 대상으로 한 보정 계수의 적용 및 불확실성 분석과의 결합이 요구된다. 하안물질과 더불어 하상물질 역시 하천 내에서 침식, 저장, (재)이동되는 물질이므로, 추후 부유토사의 잠재적 기원물질로써 하상물질이 얼마만큼 기여하는지에 대한 평가가 보완되어야 할 것이다. 여러 한계에도 불구하고 본 연구는 효율적인 보 토사관리를 위한 가장 기본적인 기원지 평가를 수행했다는 점에서 의의가 있으며, 유역 내 퇴적물 조절에 대한 계획 수립 및 실행에 유용한 정보를 제공할 것으로 기대된다.

주요어: 부유토사, 퇴적물 기원 핑거프린팅, 방사성동위원소, 믹싱 모델, 인간간섭, 영산강

학번: 2012-30398